The Petrology and Geochemistry of the Port Mouton Migmatites

by

Douglas Merrett

Submitted in partial fullfillment of an
Honours Bachelor of Science degree, April 16, 1987.

DALHOUSIE UNIVERSITY
Department of Geology
Halifax, N.S. Canada B3H 3J5 Telephone (902) 424-2358 Telex: 019-21863

DALHOUSIE UNIVERSITY, DEPARTMENT OF GEOLOGY

B.Sc. HONOURS THESIS

Author: Douglas Merrett

Title: The Petrology & Geochemistry of the Port Mouton Migmatites

Date: June 24 1987

Distribution License

DalSpace requires agreement to this non-exclusive distribution license before your item can appear on DalSpace.

NON-EXCLUSIVE DISTRIBUTION LICENSE

You (the author(s) or copyright owner) grant to Dalhousie University the non-exclusive right to reproduce and distribute your submission worldwide in any medium.

You agree that Dalhousie University may, without changing the content, reformat the submission for the purpose of preservation.

You also agree that Dalhousie University may keep more than one copy of this submission for purposes of security, back-up and preservation.

You agree that the submission is your original work, and that you have the right to grant the rights contained in this license. You also agree that your submission does not, to the best of your knowledge, infringe upon anyone's copyright.

If the submission contains material for which you do not hold copyright, you agree that you have obtained the unrestricted permission of the copyright owner to grant Dalhousie University the rights required by this license, and that such third-party owned material is clearly identified and acknowledged within the text or content of the submission.

If the submission is based upon work that has been sponsored or supported by an agency or organization other than Dalhousie University, you assert that you have fulfilled any right of review or other obligations required by such contract or agreement.

Dalhousie University will clearly identify your name(s) as the author(s) or owner(s) of the submission, and will not make any alteration to the content of the files that you have submitted.

If you have questions regarding this license please contact the repository manager at dalspace@dal.ca.

Grant the distribution license by signing and dating below.

_____ _____

Name of signatory Date

Acknowledgements

Many friends in geology helped me out in ways big and small. I especially thank Dr. D.B. Clarke for the many discussions and guidance, Dr. Becky Jameison for answering my "hypothetical questions" and Bob Mackay for helping me out of many sticky situations with the Department's second-most ornery machine. I thank Kevin DesRoches for helping draft my map at 3:00 am, Heather Avison for her comments (good and bad), Steve Dudka for the company and terrible music, and Jill Marcotte for a lot of little things. My parents get thanked too, of course, plus all those who influenced my life but are reluctant to admit it in public. I wish to thank P.D.Q. Bach for being there during the midnight probe sessions and finally my very special friend M.C. who cared and understood me, even when I did not.

Table of Contents

List of Figures:

List of Photographs

Abstract: This study is centered on the migmatites found along certain portions of the contact between the Port Mouton pluton of Shelburne and Queens counties, Nova Scotia, and the local host lithology. The field relations, petrology and chemistry of samples taken were studied to determine the genetic processes and the geochemical nature of the migmatites.

The Goldenville Formation (host lithology) consists of two units, the competent quartz-rich psammite showing little melting or distortion, and the aluminous, semi-pelitic schist, the metamorphosed equivalent of semipelitic interbeds in the psammite. This has been intruded by the Port Mouton pluton and is cut in the thesis locality by pegmatitic, aplitic, tonalitic and granodioritic dykes originating from the pluton. These semipelitic interbeds were more ductile during emplacement and tended to be intruded preferentially by granitic phases. The semipelites are almost always strongly folded and contorted, appearing to mix with the intruding dykes in places.

Chemical and petrographic evidence suggests that most leucosomes have hybrid compositions due to melt mixing between the injections and partial melts in the host. There is an indication of at least local equilibration between the granite and psammite lithologies.

Chapter 1 - Introduction

Location: The thesis locality (Figure 1) is about a two-hour drive from Halifax, and the three study areas are spread about the contact of the pluton. The major series of outcrops (A-001 to A-009) are found along about 0.5 km of shoreline between Summerville Center and Hunts Point. Two more outcrops are located about four kilometers to the north-east at White Point (C-001 and C-002). Finally, there is a large xenolith of Goldenville within the pluton, north of Forbes Cove and ~13 kilometers west of Hunts Point (D-001 to D-003).

General geology: The local lithologies consist of the Goldenville Formation, which is a thickly bedded psammite locally containing calc-silicate nodules and semipelitic schistose interbeds. Minor slate and conglomerate, reported by Hope and Woodend (1986), were not observed in the study areas.

The Port Mouton pluton is a Devono-Carboniferous complex intrusive body consisting of at least nine distinct cross-cutting units. The pluton was radiometrically dated using both Rb/Sr and Ar-40/Ar-39 methods, giving ages of approximately 340-349 Ma (cited by Hope & Woodend, 1986).

Previous work: Geological maps of the area were published by Gesner (1836), Bailey (1896), Faribault (1915) and Taylor (1967). De Albuquerque (1977) studied the geochemistry and evolution of the various southern plutons, including that of Port Mouton. Current work in this area includes Masters' theses by

Figure 1: Field area

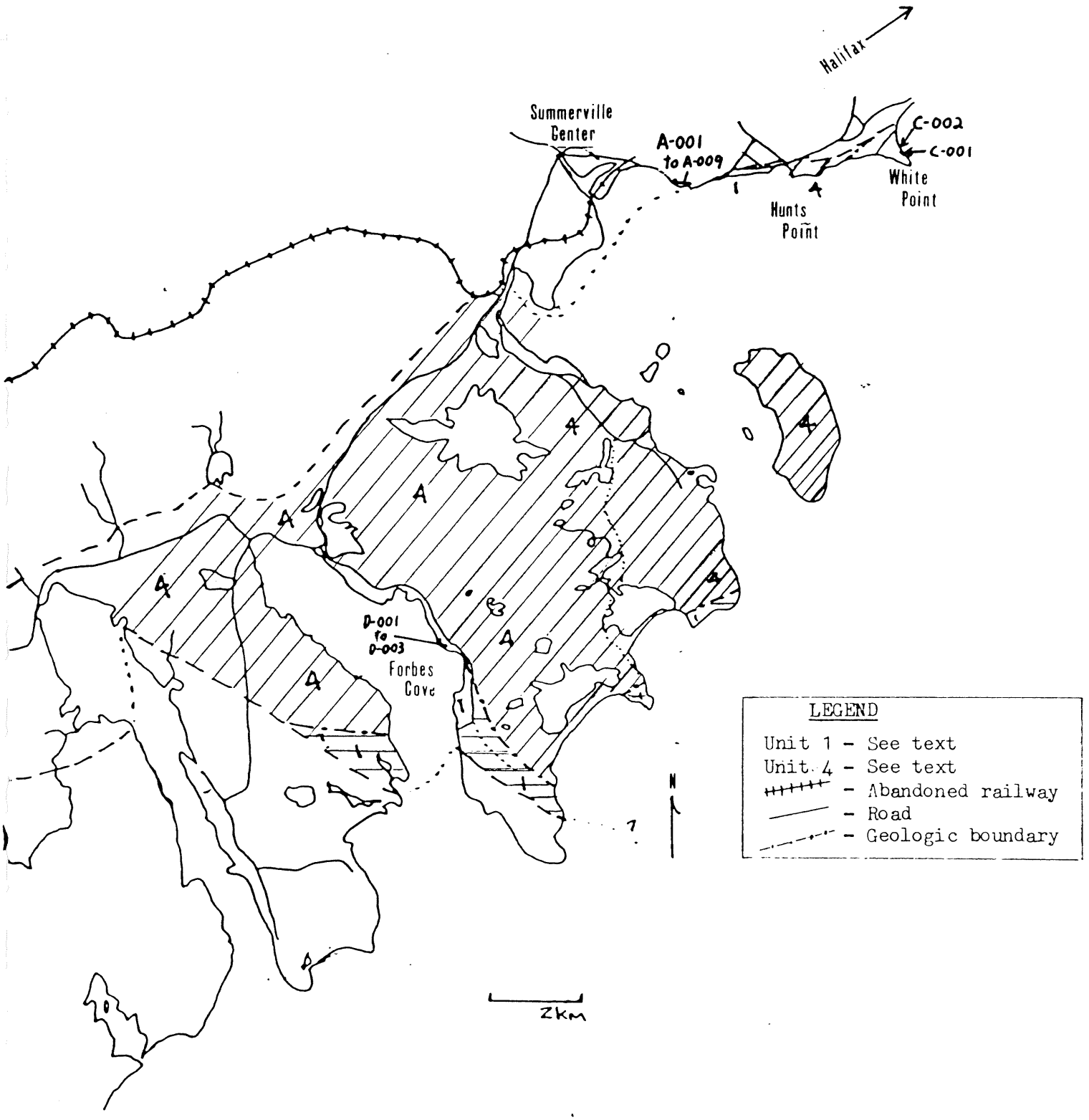

Stephanie Douma (Woodend) of Dalhousie who is studying the pluton, and by Tracy Hope of Acadia University who is studying the surrounding local Meguma metasediments. Except for being noted, the migmatites have not been studied to any degree. This thesis attempts to address the problem of their genesis.

Introduction to migmatites: Generically, migmatites are rocks that have both "light" and "dark" components (see Photo #1). This is usually expressed by a leucosome of felsic minerals such as quartz, plagioclase and potassium feldspar, and a melanosome of mostly mafic minerals such as biotite. Johannes (1983), working from Mehnert's original definition, states:

> "Migmatites are composite rocks consisting partly of gneiss or schist and partly of portions having a plutonic appearance."

Migmatites are composite, heterogeneous rocks with a mafic component (often foliated and contorted) mingled with a leucocratic (light-coloured) portion. These components are usually in the form of planar to folded and contorted layers, cross-cutting veins and irregular pods. Mingling of the different components is common, suggesting very ductile conditions.

In order to better describe migmatites, a few textural and structural terms must be defined:

Leucosome: The light-coloured portion of the migmatite, predominantly feldspathic or quartzo-feldspathic.

Melanosome: The dark-coloured lithology present in many migmatites. It is often complementary to the leucosome.

Photo 1: (A-009) Typical neosomes. Blue arrow points to leucosome Red arrow points to melanosome (mafic rim).

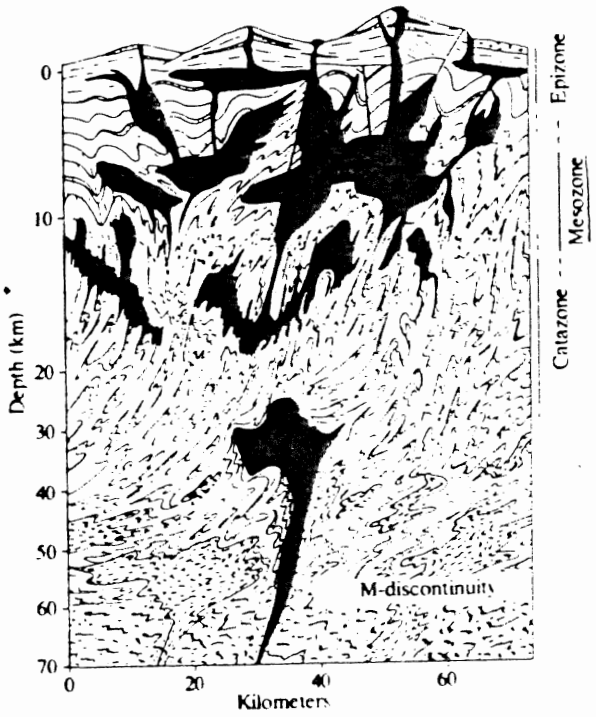

Figure 2: Relative depths of emplacement for the different 'zones' of pluton. From Best 1982 (fig. 4-31, p. 130)

Neosome: The leucosome and melanosome when described together as one co-existing unit.

Stromatic: A layered form of migmatite, often irregular.

Anatexis: Partial melting.

Genesis of Migmatites: The first models proposed to explain the formation of migmatites originated with such workers as Michel-Levy and Sederholm in the late nineteenth and early twentieth centuries. They believed that migmatites were the result of injection or intrusion of magmas into gneisses or schists. It was pointed out by later workers that while this might explain local occurrences, more widespread, regional-scale migmatites could not have originated in this manner (cited in Johannes, 1983). Work by Winkler and von Platen (1961) and Mehnert (1951-1968) proposed that partial melting of the host rock was responsible for the development of migmatites.

Much of the following discussion is based on the excellent introduction given by Ashworth (1985, pp. 1-31). Generally migmatites can be formed in two different geological terranes. Locally they may occur at the margins of mostly mesozonal plutonic bodies (see Figure 2) as a result of the influx of thermal energy and volatiles, both of which may produce partial melting. Alternatively, migmatites can form in a regional setting associated with deep metamorphic zones of mostly upper amphibolite to granulite facies (Ashworth, 1985). Under these conditions they are characteristically far more voluminous than

the first group and usually stromatic or regularly layered with less complex folding and contortion.

Although originally a textural term, the modern interpretation of migmatitic rocks is that they should involve a separation of components from an originally homogenous source. This separation could involve either sub-solidus segregation or partial melting. Partial melting is currently thought to be responsible for the formation of **most** migmatites, although genesis through solid-state metamorphic processes has been demonstrated.

Theoretically, a leucosome formed under conditions of partial melting should have a composition near the pressure-dependant eutectic in the Qz-Ab-Or ternary system. This is the point at which a rock of predominantly quartz-(Qz), albite-(Ab) and orthoclase-(Or) composition will form its first melt, as is commonly seen in the petrogenesis of granites (see Figure 3). However, leucosomes rarely have this composition due to a number of complications, including that of a significant calcic (anorthite) component and/or incomplete segregation of melt. The presence of the An component in the plagioclase raises the solidus temperature of the system (see Figure 4). Other complications arise from advanced melting, where one or more of the residual phases are eliminated, causing the melt to evolve away from the 'granitic minimum'.

The Or content of the 'granitic minimum' is approximately 25-30%, but commonly there are leucosomes with far less Or, being

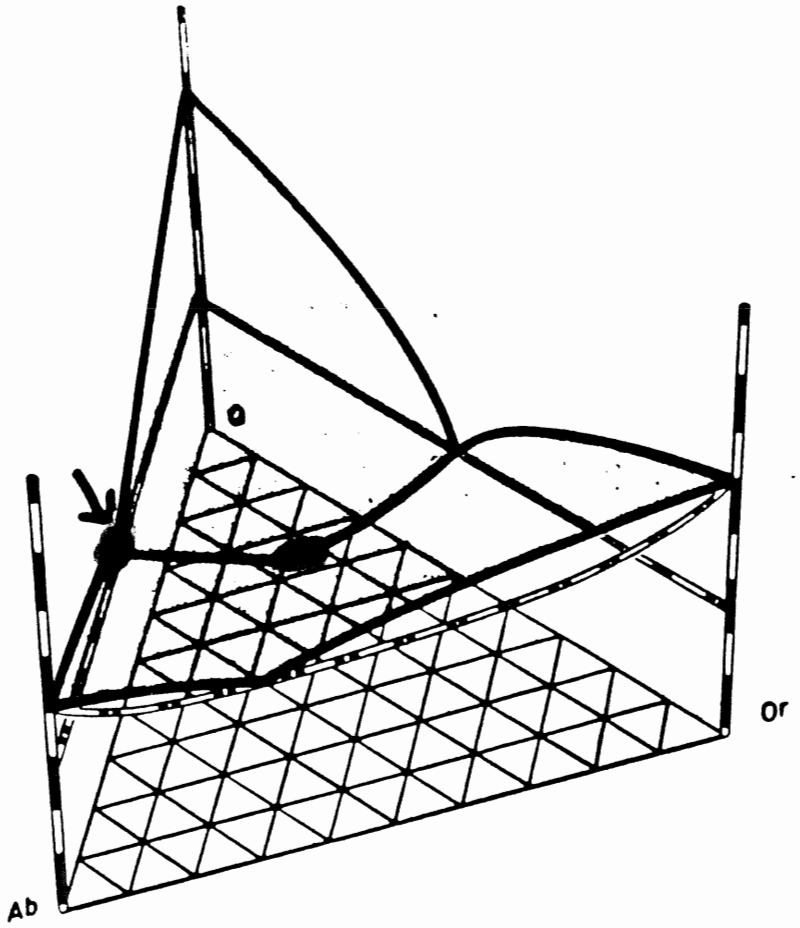

Figure 3: Three dimensional plot of the Qz-Ab-Or-H_2O system at p_{H2O}=1kbar and H_2O in excess. Relative temperatures are plotted on the y-axis.

Yellow = 'Granite minimum'

Green = Peritectic, low T of Tonalite system

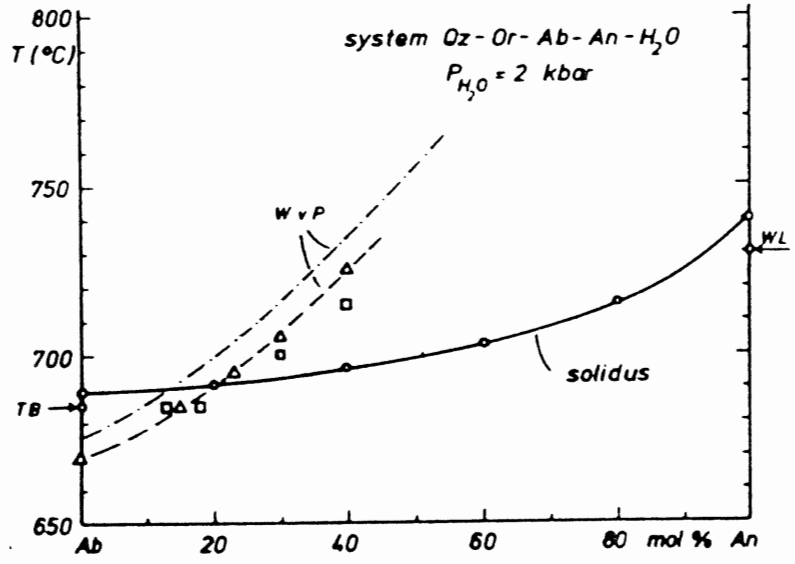

Figure 4: Increase in solidus temperature as a function of An mol. % (from Ashworth, 1985) at P=2 kbars. Heavy line labelled 'solidus' is from Johannes (1984), TB=Tuttle and Bowen (1958), WL=Winkler and Lindemann (1972). Dashed-dotted curve; composition of plagioclase coexisting with cotectic melts (Winkler and V. Platen, 1961).

primarily composed of quartz and plagioclase. These 'tonalitic' or 'plagiogranite' leucosomes require much higher temperatures in order to form, as can be seen by examination of Figure 3 and point B, the binary eutectic for Qz-Ab.

Realistically, for either system to work there must also be an excess of water in the system to lower the solidus enough for partial melting to occur. Dry rocks have considerably higher solidi and are thus less likely to melt. Also, intruding granites are commonly at their liquidus with some suspended crystals. So a source of water is needed in order to precipitate partial melting in the host. The dehydration reaction of muscovite could provide this, through the reaction

muscovite + quartz = sillimanite + microcline + H_2O

which is initiated by increasing temperature in argillaceous rocks (p. 348, Nockolds et al., 1978).

From the experiments of Bowen (1913), it is expected that the composition of plagioclase in the melt would be more sodic than the plagioclase in the residuum. So if the leucosome forms by crystallization of a partial melt, its plagioclase should be more Na-rich than that in the melanosome.

In addition to partial melting, another feasible process of migmatite formation is lit-par-lit injection. This involves the infiltration of plutonic material into its host lithology along planes of weakness, such as fractures, cleavage, or less competent sedimentary interbeds. In order to produce a mafic

rim, however, some sort of segregation process (i.e. chemical reaction, physical separation) must also take place.

This leaves us with a number of possible processes of migmatite formation: Sub-solidus segregation, anatexis, and lit-par-lit injection.

Chapter 2 - Field Observations

Introduction: A number of weekends during the months of July and August (1986) were used to study the three areas listed in Chapter 1. A fourth area (B-000) located at Hunts Point, was composed entirely of granitic outcrop, however the local breakwater contained excellent migmatite-bearing boulders. These boulders had been quarried locally to provide material for the breakwater and attempts were made to determine their source. Their origin could not be ascertained definitively, however, and so this group was abandoned. The host lithology found in the study area is the Goldenville Formation, which may be subdivided into the main psammite and minor semipelitic horizons. The intruding Port Mouton pluton is composed of at least nine mappable units, but only Units 1 and 4 (following the labelling system of S. Douma [Woodend]) occur widely in the study areas. The general compositions of the lithologies are taken from Hope and Woodend (1986) and Hope and Woodend (1985).

Goldenville

i. Psammite: Primarily a fine grained (< 1mm), metamorphosed (andalusite/staurolite/cordierite facies) blue to grey psammite which still has relict sedimentary features visible in some areas. The beds range in thickness from 1 cm to 10 m but are mostly > 2 m thick in the thesis areas. In thin section they are typically recrystallized quartz and plagioclase (0.05 to 0.1 mm diameter) with intergranular biotite and muscovite. The quartz is often stretched and sutured but some grains have been

recrystallized, producing polygonal grain boundaries. Plagioclase is often partly altered to sericite. Muscovite is generally smaller than biotite and together they form a weak foliation. Common accessories are apatite, epidote, sphene, magnetite and pyrite. It should be noted that while in general the psammites in the study area followed this description from Hope and Woodend (1986), they do deviate at certain points. The grain size of quartz and plagioclase is often greater (0.25 to 0.5 mm) and polygonal grain boundaries are common. Muscovite is generally irregular, larger than biotite and randomly oriented rather than following the weak foliation defined by the biotite.

Calc-silicate nodules occur in this unit, normally oriented parallel to the bedding, although they appear to be affected by deformation associated with migmatite development. The nodules range in size from 3 cm to 2 m in diameter.

ii. Semipelite: These occur as beds of semipelitic schists, commonly intruded and contorted by the plutonic emplacement. They range from 4 cm to 3 m in thickness and are thought to have an aluminous shale or siltstone protolith. In thin section the semipelitic schists commonly contain one or more of biotite, garnet, staurolite, cordierite, and andalusite as porphyroblast phases in a quartz-plagioclase-biotite matrix. The garnet is distributed throughout individual samples and does not appear to be confined to any particular sedimentary layers. Near the contact with the Port Joli pluton (part of Port Mouton complex) the biotite is coarser grained (0.4 to 0.5 mm) and

occurs as interlocking aggregates with some muscovite. In the thesis locales the semipelite has a somewhat different character. No garnet was found in any of the samples, nor were staurolite, cordierite or andalusite seen. Biotite is the predominant phase and occurs both as a finer grained (0.25 to 0.5 mm) matrix component, and as interlocking aggregates of crystals associated with muscovite. Relict sedimentary features were reported as being rarely preserved in the semipelitic horizons by Hope and Woodend (1986), but none was found in the semipelites of the thesis locales.

Port Mouton pluton: De Albuquerque (1977) predicted the pressure and temperature for what he calls the 'granite' phase of the Port Mouton pluton from comparison of extrapolated experimental work as 4.5-5.5 kbars and 675-705 C, respectively. This 'granite' most likely refers to Douma's [Woodend] Unit 4. Tonalitic intrusions, also found in the study area, would necessarily have a higher temperature of formation (see Figure 3, quartz-albite tie line).

Granite Unit 1: Douma (1987) describes this as a coarse-grained mafic biotite tonalite to coarse-grained mesocratic biotite-muscovite granodiorite. It is equigranular and locally subporphyritic, containing inclusions of country rock of varying abundance and degree of assimilation.

Granite Unit 4: Douma (1987) labels this unit as a medium-grained, mesocratic biotite-muscovite granitoid to a medium-

grained mafic biotite granitoid. This is the predominant lithology in the Port Mouton pluton.

Outcrop descriptions: The first series of outcrops (A-001 to A-009) occur between Summerville Beach and Hunts Point, starting at 64 48' 4.08" W, 43 57' 1.17" N (outcrop A-001) and ending at A-009, which is tied to the Hydrographic survey system as point 2131 1954. In general they are isolated outcrops separated from each other by beaches of rounded cobbles to boulders. The common beach size rock is about 10 cm to 50 cm in diameter and is composed mostly of the local country rock, granites and migmatites (see Photo 2). Some outcrops have abundant rubble or boulders on them, making determinations of extent difficult in places (Photo 3). All outcrops have pegmatites ranging in width from a couple of centimeters to a meter. They cut all lithologies and are usually straight although they sometimes join into networks.

A-001: This outcrop is about 10 m long, 3 m wide, smooth, somewhat weathered, and inter-tidal. It has a set of poorly-developed joints oriented ~045/80 S. Granite is seen outcropping on the south side although it is difficult to tell whether this is a large, local intrusion or the main body of the pluton. Poorly-developed neosomes occur along one face of the country rock.

A-002: This outcrop is about 25 by 50 m. The lithologies present are more complex than the last outcrop with certain portions intensely intruded by a magmatic dyke complex from the

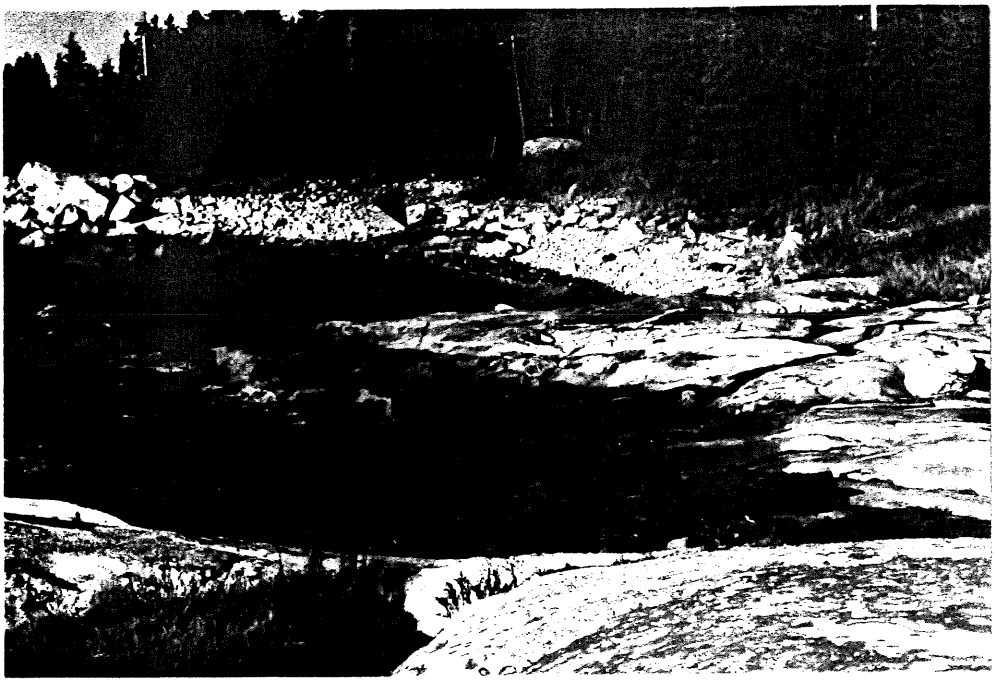

Photo 2: (A-009 & A-008) Typical beach and outcrop exposure along the A-series, between Summerville Center and Hunts Point. The immediate foreground is part of A-009, the small outcrop pointed to by the red arrow is A-008.

Photo 3: (A-009) 'Float' and outcrop-derived rubble, typically found on larger outcrops or covering smaller ones.

pluton. The Goldenville Formation also shows greater ductility along the semipelite beds, as demonstrated by Photo 4. In the upper portion of the photo is the psammite, while the lower half is semipelite. The southern end of the outcrop is mostly semipelitic and contains some thin (~1 cm) ptygmatically folded quartz veins and isolated quartz "blebs". These blebs have a pegmatitic texture, are more resistant to erosion than the host semipelite, as indicated by their relief, and are generally surrounded by mafic rims. The dyke complex contains angular xenoliths of country material from 1 to 20 cm in diameter. Some of the narrower granitic veins have mafic rims.

A-003: This is approximately the same size as A-002, with a row of boulders lying along the shore side, concealing part of the outcrop. A one meter wide, straight pegmatite cuts (173/dip unknown) the outcrop. A "fabric" is visible in the rock, apparently defined by the general alignment of granitic injections and mica orientations. A number of aplite dykes intrude this outcrop, having unusual mafic associates generally occurring as thick (>1 cm) rims. These rims are primarily composed of copasetic, linear aggregates of needle-like biotite in a fine-grained matrix of highly birefringent minerals with additional biotite phenocrysts.

A-004: A long (60-70 m) outcrop bordering directly on the sea with large (~2m^3) boulders covering the shore side of the outcrop. The semipelitic beds show an increased degree of deformation with respect to the first three outcrops and are

Photo 4: (A-002) Dissipation structure in Goldenville. Upper bluish lithology is psammite, lower greyish-brown lithology is semipelite. The ductility contrast is illustrated by the structure of the intruding dyke. The green arrow marks the contact between the two lithologies.

being preferentially penetrated by the granite. The south-east side is a contact between the Goldenville and granite, with the intermediate region showing a great deal of fracturing or stoping when the granite injected the host. The neosomes occur in elongate structures that run parallel to the contact of the igneous body. Calc-silicate nodules are common and are generally oriented sub-parallel to the "fabric", with one local group sub-perpendicular to it.

The Goldenville Formation in one zone displays a relict sedimentary feature resembling "fish-scales" (see Photo 5) which may be deformed trough cross-beds or slump features. As can also be seen in the photo, ptygmatic folds occur in the area, although the "fish-scales" themselves appear to be more competent, structurally, with the folding disappearing as the vein cuts through them.

A-005: No igneous contact was visible in this small outcrop (~5 m by 20 m) which is surrounded by rubble and has some boulders concealing portions of it. No host/pluton contact is visible but a large granitic dyke passes through it. The outcrop is primarily psammite and no neosomes were noted.

A-006 and A-007 are only survey points, needed to tie in the last two outcrops with the first five.

A-008: This is a small outcrop, approximately 7 m wide and 30 m long. There is no granitic contact but a number of veins and dykes cut through the semipelitic horizons and neosomes. The

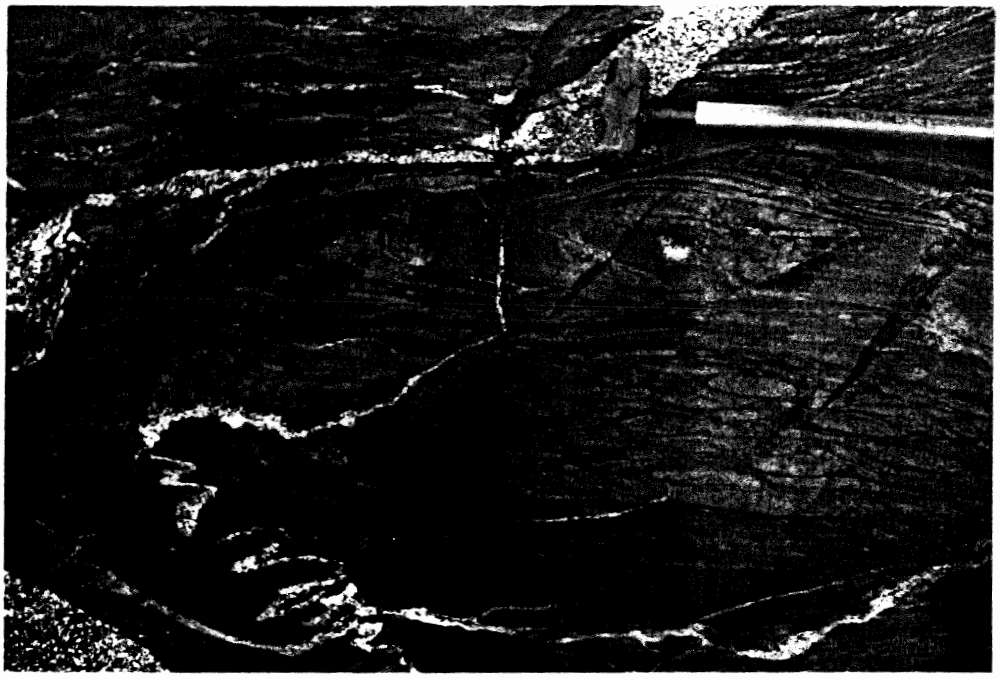

Photo 5: (A-004) "Fish scale" modified sedimentary features. Possibly folded or deformed cross-beds. Note ptygmatic vein cutting the psammite.

Photo 6: (A-008) Sample location A-008-2. Vein pointed to by blue arrow can be traced contiguously into larger granite bodies, implying it is an injection. Note: Difficult to see, but has a mafic rim.

rimmed leucosomes can be traced along in areas (i.e. sample A-008-2, see photo 6) as granitic injections, however, the mafic rims imply segregation of some sort has occurred. The calc-silicate nodules here have round, pinkish-purple spots, generally 1 to 5 mm in diameter. Some nodules also show spotty rust discoloration concentrated in the centers, gradually decreasing outwards.

A-009: This is the largest outcrop of the three study areas (~ 80m long by 35 m wide) and consists of a granite plug intruding, and flanked on both sides by Goldenville Formation (see Outcrop Map 1). Xenoliths are common along the edges and some vein and dyke infiltration into the country rock is observed. The migmatitic "fabric" follows along the margin of the pluton. In one zone where semipelite is in contact with the plutonic body, contorted leucosome "vienlets" can be seen (see Photos 7 and 8). There also appear to be two subtly different granite units present. Leucosomes in the semipelites commonly have distinct rims of an intergrown network of biotite and muscovite crystals (see photo 7). The psammites appear unaltered, although granitic veins cutting through often have rims (see photo 9).

The next pair of outcrops lies along White Point (C-001 and C-002), approximately 10 km north-east of Hunts Point.

C-001: This outcrop can be found along the north-east side of White Point. Except for the two outcrops mapped here, White Point is completely surrounded by cobble beach. This outcrop is

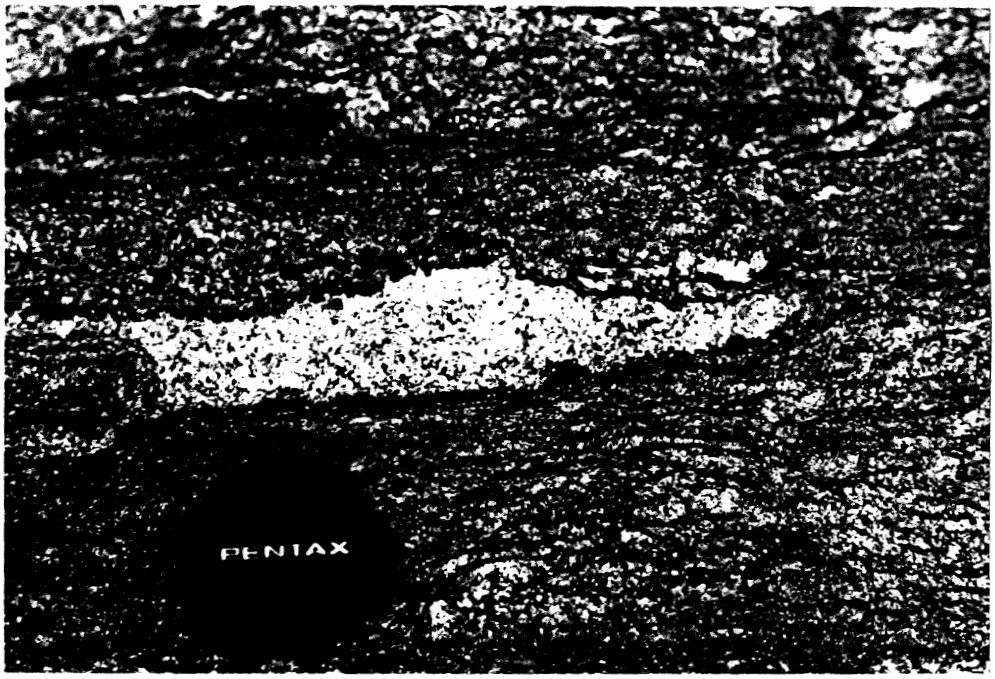

Photo 7: (A-009) A leucosome in semi-pelitic schist, similar to the sample of A-009-1A. It is adjacent to a small (15m X 65 m) plutonic body (not in field of view).

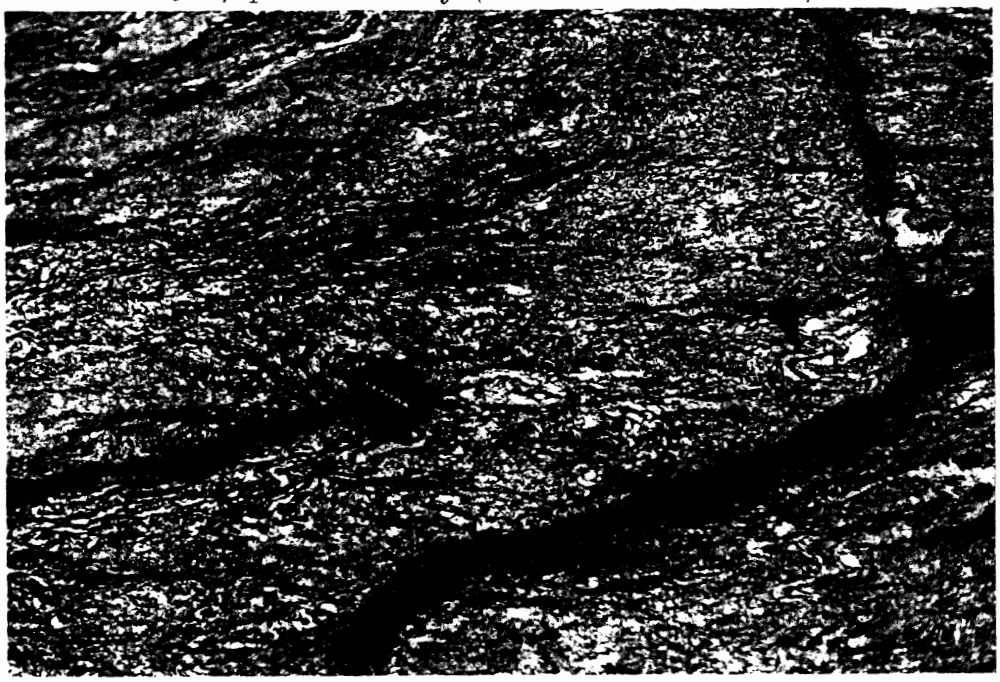

Photo 8: (A-009) Contorted and segregated semi-pelitic schist adjacent to A-009-1. Note leucocratic veinlets (blue arrow), result of partial melting, plutonic injection or both?

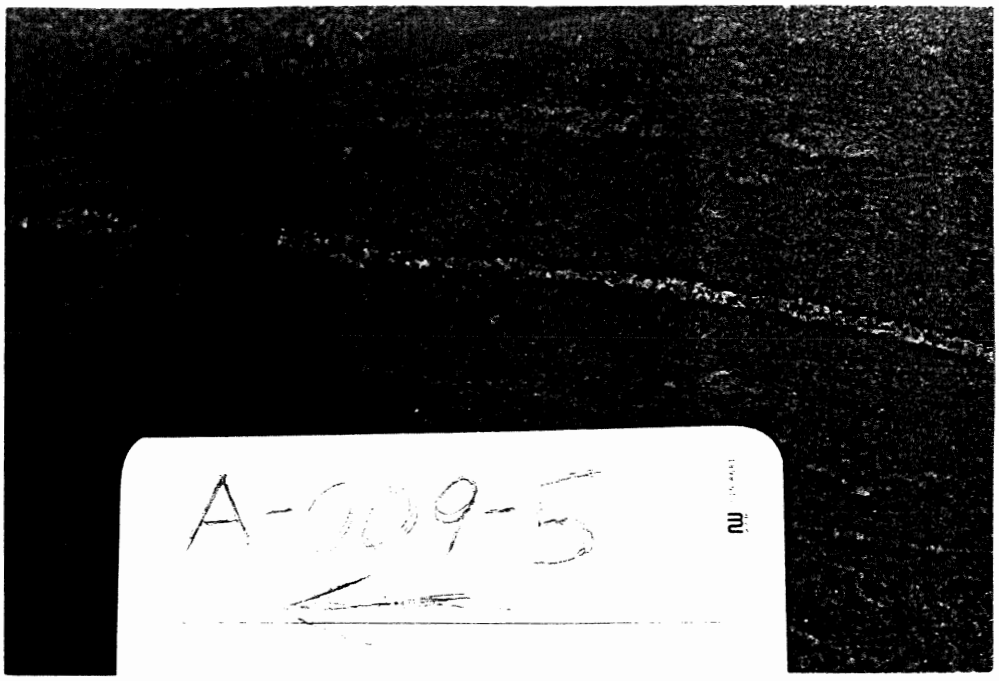

Photo 9: (A-009) Intruding granitic vein with mafic rim, cutting through psammite.

Photo 10: (C-001) General character of outcrop C-001. Note highly foliated texture with little noticeable folding or contortion. Arrow points to layered unit of Photo 11.

about 20 m² and appears to display different conditions of formation than those of the A series (see photo 10 and photo 11). The metasedimentary host rock shows a finer-grain and little of the contorted layering that characterized the first sequence of outcrops. The semipelitic beds are very planar and often show granitic injection (photo 11) along the edge, plus a parallel fabric in the bed itself. This is not the only form the semipelitic beds can take however. The layer below that shown in photo 11 (see photo 12) displays quartzo-feldspathic "blebs" that appear to have grown out of the bands. The layering could be a sign of intense deformation, supported by the nature of the local calc-silicate nodules, which are elongate and oriented precisely along the trend of the deformation (~124 degrees). The granitic unit along White Point is predominantly tonalitic in composition (Douma [Woodend] personal communication), implying high temperatures during emplacement.

C-002: This outcrop, while only ~85 m north-west of C-001, displays a markedly different character. It is larger than the last, ~50 m² and contains two "zones" of different texture. Photo 13 shows the nature of the first zone, a highly contorted series of associated leucosomes and melanosomes, unlike those seen in the A series in that the melanosomes do not occur as rims around the leucosomes. The second zone, which is on the side closest to C-001, displays a somewhat "linear" texture (see photo 14), defined by numerous small (~5 cm X ~20 cm) semipelitic interbeds. The calc-silicate nodules found here are mostly round

Photo 11: (C-001) Close up of layered bed (semipelite). The granitic vein (yellow arrow) appears to have intruded along the contact, which is presumably a plane of weakness. The layers display an unusual cross-cutting texture, pointed to by the side arrows and the red arrow.

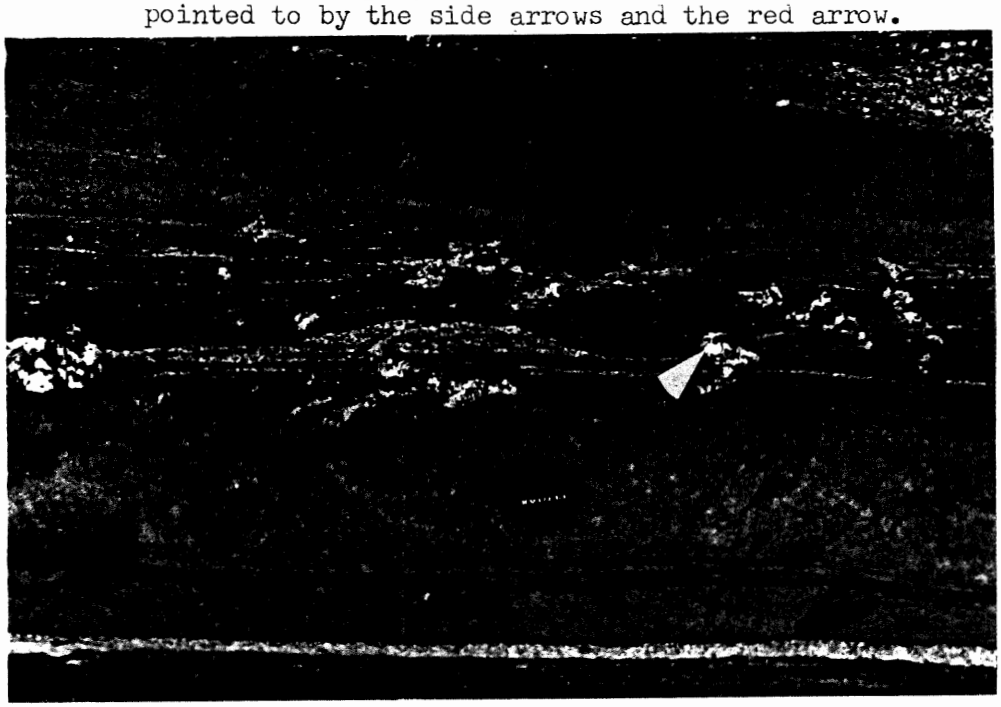

Photo 12: (C-001) Quartzo-feldspathic blebs in another layered semipelite. Note the sequence from photo 11 visible at the bottom. This example is more contorted than the last. Could the blebs be nucleations of partial melting?

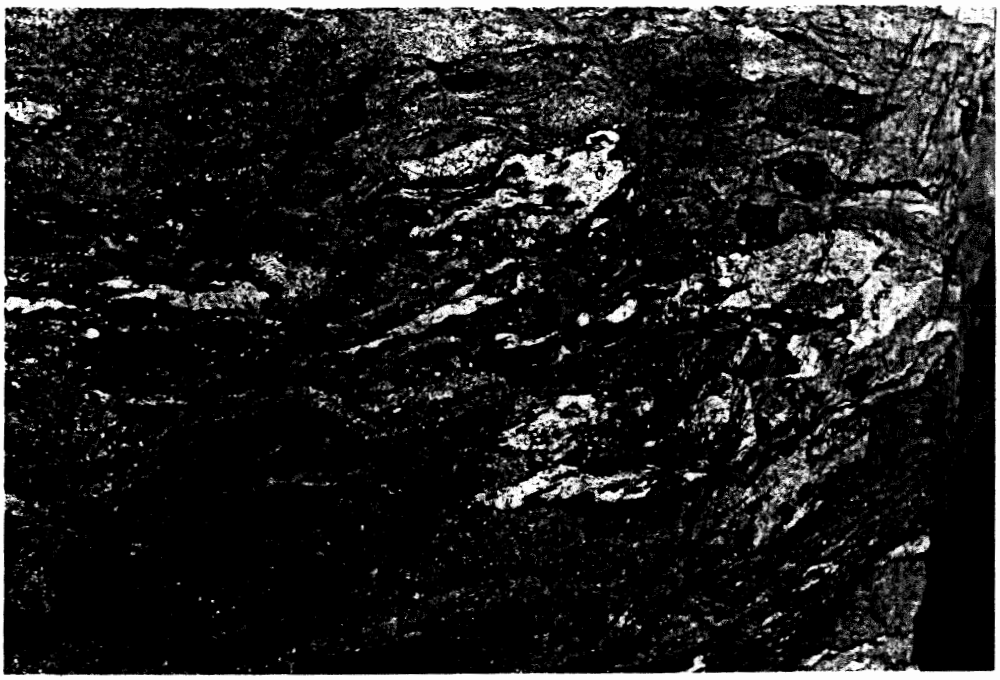

Photo **13** : (C-002) Part of the highly contorted zone, with associated leucosomes and melanosomes.

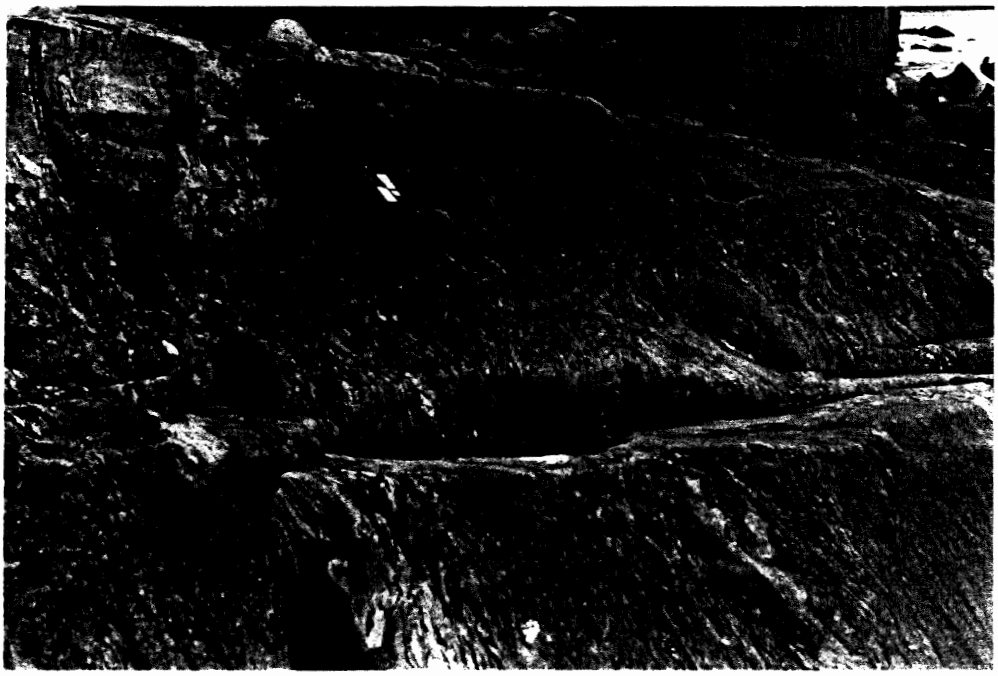

Photo **14** : (C-002) Second zone. More foliated, mostly defined by narrow, elongate pelitic interbeds.

or square and thus difficult to measure for orientation. The strike of the foliation is approximately 118 while that of the cross-cutting pegmatites is about 080 .

The third study area is along a secluded stretch of shoreline on the western shore of the Port Joli peninsula. This continuous exposure on the northern end of Forbes Cove (see Figure 1) defines the shoreline from about 50 m before the xenolith to at least 2 km past its furthest extent. The three survey points delineate the extent of the migmatites which are bounded on both ends by granite. The shore-face of D is topographically higher than the xenolith and is composed of granite, with the migmatite-bearing unit forming a terrace adjacent to and about a meter above the water. There is very poor exposure inland, but a few highly weathered outcrops were found up to 100 m in from the bay, all consisting of granite, indicating that the D series is bounded on at least three sides by the pluton. The xenolith is approximately 60 m long, 5 to 15 m wide and is inundated with dykes and veins from the surrounding granite. From cross-cutting relationships it would appear that there was more than one episode of intrusion (excluding the pegmatites/aplites). A coarse-grained, undeformed granite (Unit 4) and a finer-grained, intensely deformed (i.e. ptygmatically folded, complex contortions) intrusion (Unit 1) are evident, indicating deformation occurred during or after one stage of intrusion but before the next. The granite units in this region are equal proportions of Unit 1 and Unit 4 compositions (Douma

[Woodend] personal communication), with Unit 1 having intruded first. From point D-002 and onwards toward D-003 the texture of the rock becomes very deformed and contorted with much mixing between a presumably thick semipelitic horizon and the granite. This folding and contortion occurs along the pelitic beds (oriented almost due north), presumably parallel to the relict bedding planes. Towards D-003 the Goldenville is increasingly intruded by the pluton until finally only granite with small, elliptical xenoliths (oriented ~220) remains. An unusual segregated dyke runs through the highly deformed region north of D-002 consisting of a very micaceous inner dyke with a thick (~1-2 cm) felsic "rim".

Samples were taken from each of the outcrop areas (A, C and D), with 32 thin sections studied petrographically and 20 of these polished for probe work. The sample and thin section descriptions can be found in Appendix A.

Chapter 3 - General Petrology

Introduction: This section deals with the general characteristics of the samples taken from the three study areas. Detailed petrographic descriptions may be found in Appendix A.

The group of polished sections consisted of those samples which had the best-defined neosomes, as well as contacts between important lithologies. General characteristics of the various units as well as important distinctions between them are covered in this chapter.

The following list documents the different mineralogical suites found. All of them can be discriminated from one another on the basis of petrology with the exception of the two psammite types.

Leucosome type-A.....Leucosome type-B
Melanosomes
Granite type-A.....Granite type-B
Psammite type-A.....Psammite type-B
Pelite
Calc-silicate nodules
Aplite/Pegmatite dykes (post-migmatization)

Petrographically, the distinction between type-A and type-B is similar for granite and leucosome and is based on the presence of microcline. The psammite biotite compositions also display a bimodal distribution; however, they can only be discriminated by chemical analysis.

Leucosome: Leucosomes in the study area occur as: A) leucocratic veins or lenses rimmed with mafic minerals; B) leucocratic patches with associated melanosomes; and C) independent leucocratic patches separated from the melanosome.

Time constraints forced the concentration of this study on primarily one of these types, the segregated dykelets/lenses.

The segregated vein/lenses have one thing in common which distinguishes them from the other leucosomes - a rim of micaceous minerals. In order to keep a generic name for this type, mainly because it is difficult to determine whether a lens is a vein in the more structurally complex areas, the term rimmed leucosome will be used to apply to both. The sample from A-009-1 is a good example. It is a well segregated and concordantly folded lens (see photos 1, 7 and photo 15) occurring with other folded lenses. But are these partial melts or 'pinched' veins? There are clearly traceable granitic dykelets that have formed rims as well as dykelets that have not. There are also "detached" leucosomes, which do not have a rim but are adjacent to, or associated with, a melanosome. One example of this is A-009-4B, which may be a "paired" neosome where the leucosome and melanosome are adjacent but occur as separate units rather than as a rimmed leucosome. The problem with this sort of association is that it is difficult to show that the two are genetically related. Finally there are independent leucosomes which have no obvious adjacent melanosome, (i.e. A-004-5, photo 16). This sample contains a contact between the psammite and semipelitic schist with the leucosome occurring just within the semipelite. The leucosome has noticeably less biotite and is more coarser grained than the two Goldenville Formation lithologies. Petrographic study of the leucosomes in general reveals a texture

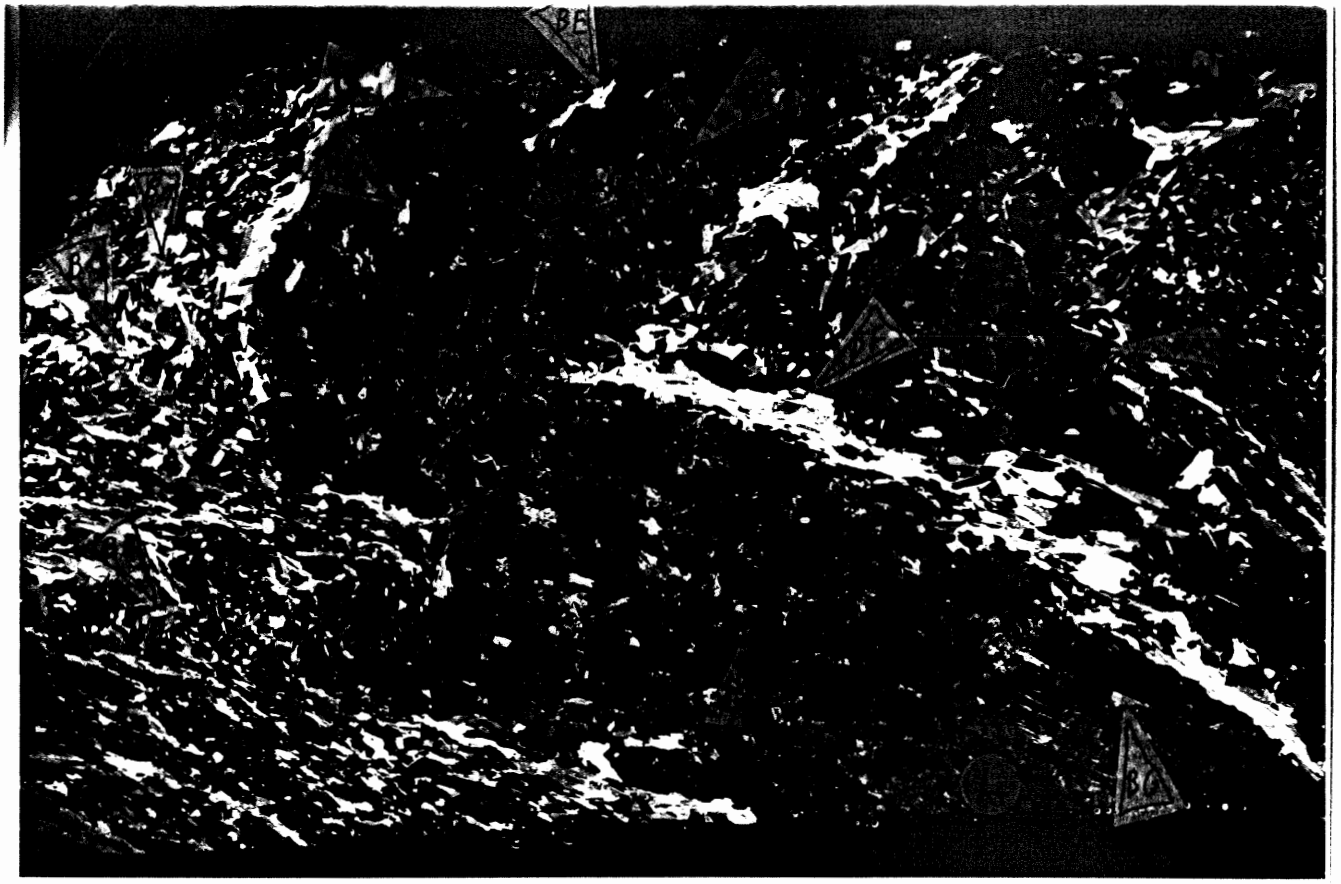

Photo 15: (A-009-1A) Red circle marks the leucosome (see also drawing below). White rim surrounding it is biotite (negative image). Arrows indicate probed grains, P=Plag., B=Biotite and M=Muscovite. The second letter simply defines the grain from the others.

(PPL)
0.25 mm

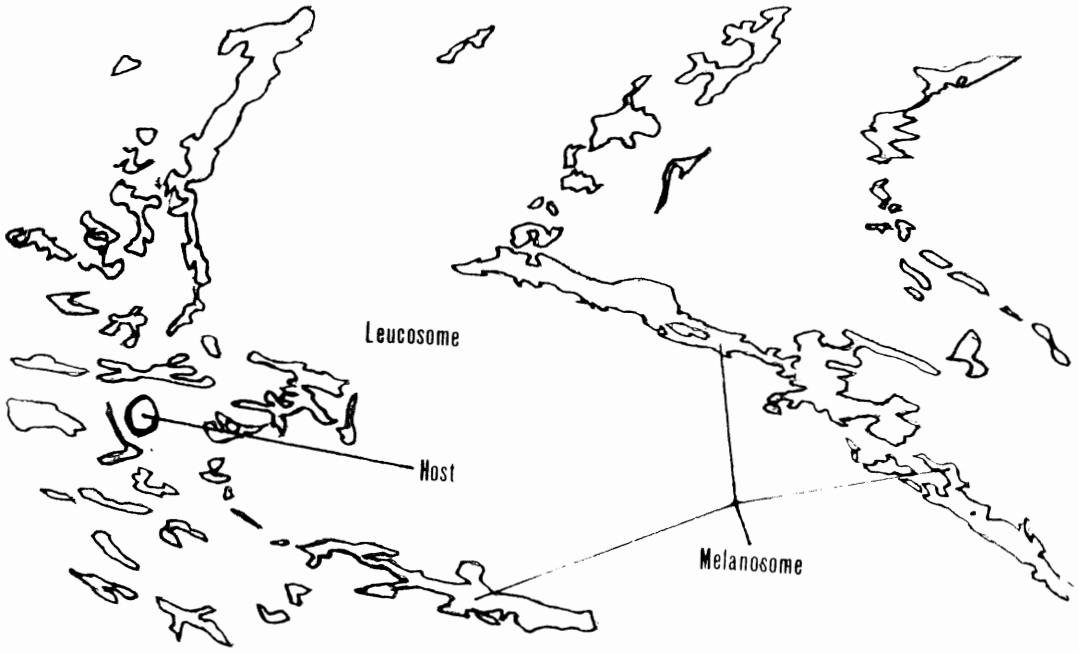

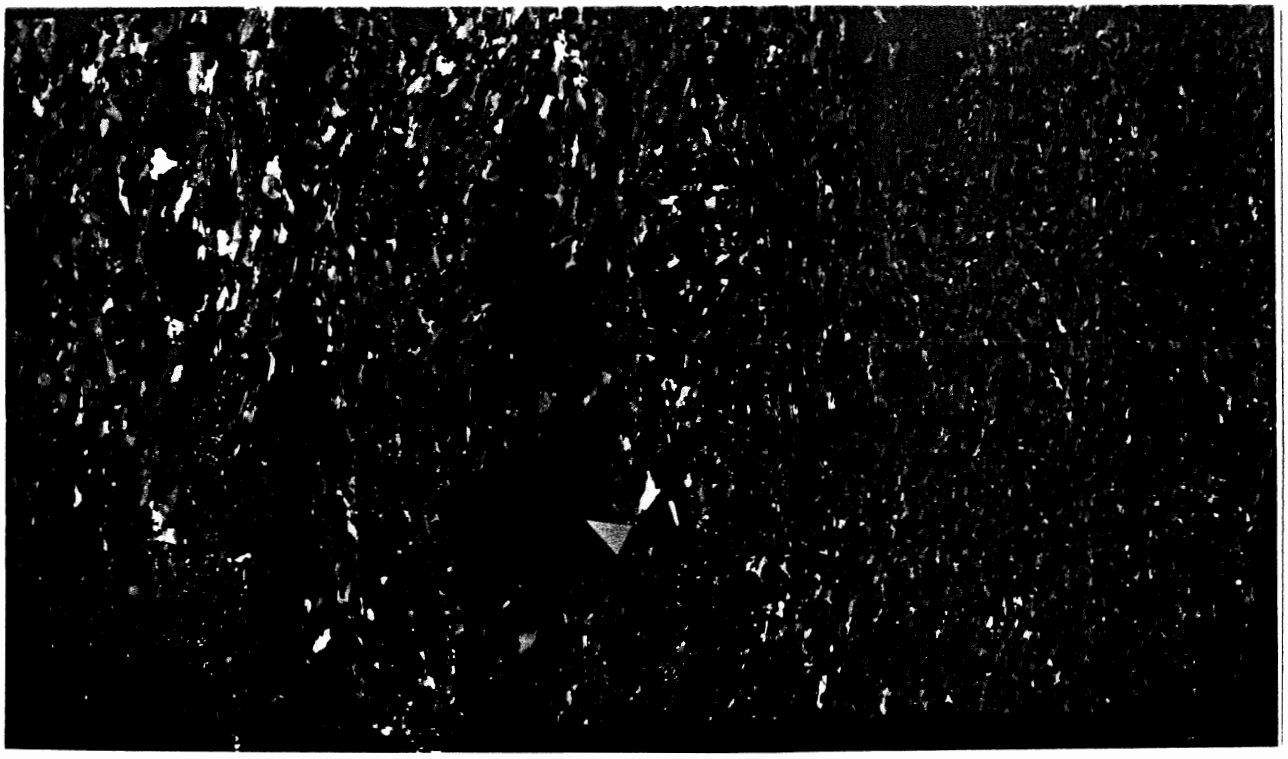

Photo **16:** (A-004-5) Independant leucosome without obvious, associated melanosome. Arrow points to leucosome. (negative image)

(PPL)
0.25 cm

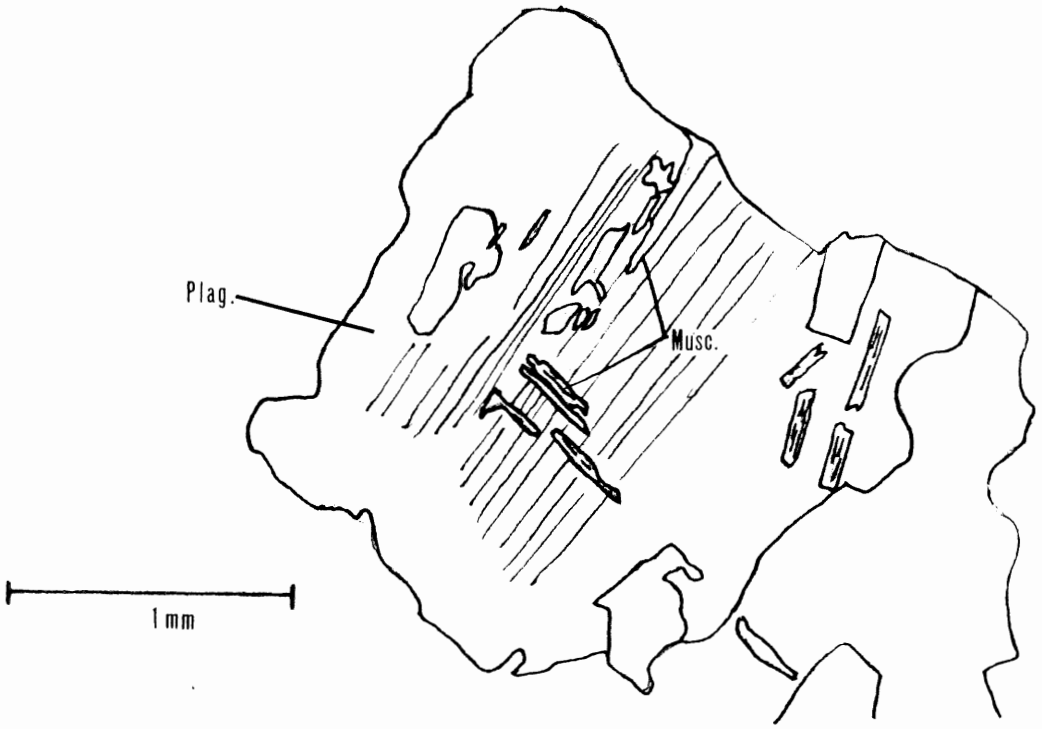

Photo **17:** (D-002-2B) Drawing from photograph, shows secondary muscovite growing within cleavage of plag. grain.

and mineralogy very similar to that of the granites. This similarity is to be expected, however, whether they formed through partial melting, granitic injection or a combination of both, since similar processes are at work.

The mineralogy of the average leucosome is simple, quartz - plagioclase - K-spar - (biotite) - (muscovite), the micas generally being minor phases (<5%) when present. Quartz may show a range from uniform extinction to sub-grain development, sometimes within the same leucosome. Plagioclase tends to alter the most, ranging from clear, subhedral crystals to strongly sericitized grains with secondary muscovite intergrowths along cleavage planes (see photo 17). Plagioclase can also be zoned and in two samples (A-008-3A/1 [neosome + host, sample contains two leocosomes] and D-002-2B [rimless leucosome in psammite] there are hypidiomorphically zoned grains. The potassium feldspar is consistently less altered than the plagioclase and usually has a wavy extinction. Perthitic exsolution was noted in some slides (i.e. D-001-3A). The biotites are generally small, "ragged" and in disequilibrium with their surroundings (i.e. oxidizing rims, altering to chlorite). Muscovite occurs either associated with biotite or as large, well-formed crystals displaying good cleavage and fairly regular outlines. This phase also occurs as secondary intergrowths along the cleavage of highly altered plagioclase grains.

Petrographically, the difference between the two leucosome groups is that both microcline and orthoclase are present in

type-A while only orthoclase is present in type-B. The distinction between type-A and type-B also extends into the chemistry as will be demonstrated in the next chapter. The following is a list of leucosome-bearing samples subdivided by type.

Table 3.1 - The two leucosome groups, with those samples analysed underlined.

type-A (microcline)	type-B (no microcline)
A-008-3A/1	A-009-1A
D-001-3A	A-009-1B
A-009-4A	A-008-3A/2
A-009-4B	D-001-2
D-001-3B	A-004-5
A-009-4B	A-002-1
	A-009-5A

Note: The last letter present in some sample descriptions does not refer to the leucosome group, but identifies it as a different slide made of the same sample, since many of the samples were very heterogeneous and required more than one slide to cover all the interesting features.

Melanosome: This unit is not always as obvious, texturally or mineralogically, as the leucosome. It often grades into the host lithology, and its texture can vary as a function of mica content. The mafic rim around A-009-1A is entirely made up of an interlocking network of biotite and muscovite with no other phases present (see photo 15). It is only about 1 mm thick, however, with very sharp boundaries defined by the grain contacts. Other rims display a more gradational change (e.g. A-009-5A; photo 18), in which the percentage of biotite and muscovite increases in the direction of the leucosome. Interlocking rims, such as those occurring around A-009-1A, generally consist of fairly large (>1 mm), tabular biotite and

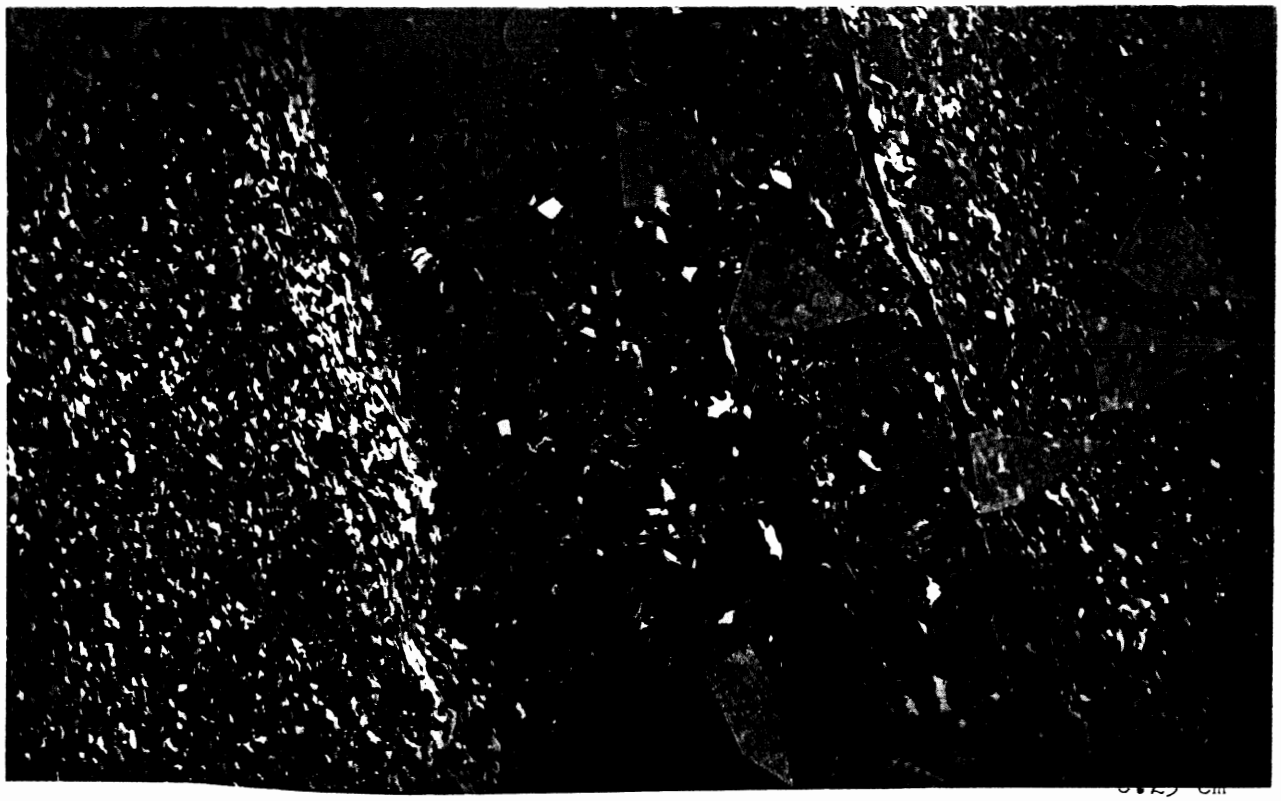

Photo 18: (A-009-5A) An example of a gradational mafic rim (particularly to the left of the leucosome). (Negative image, PPL)

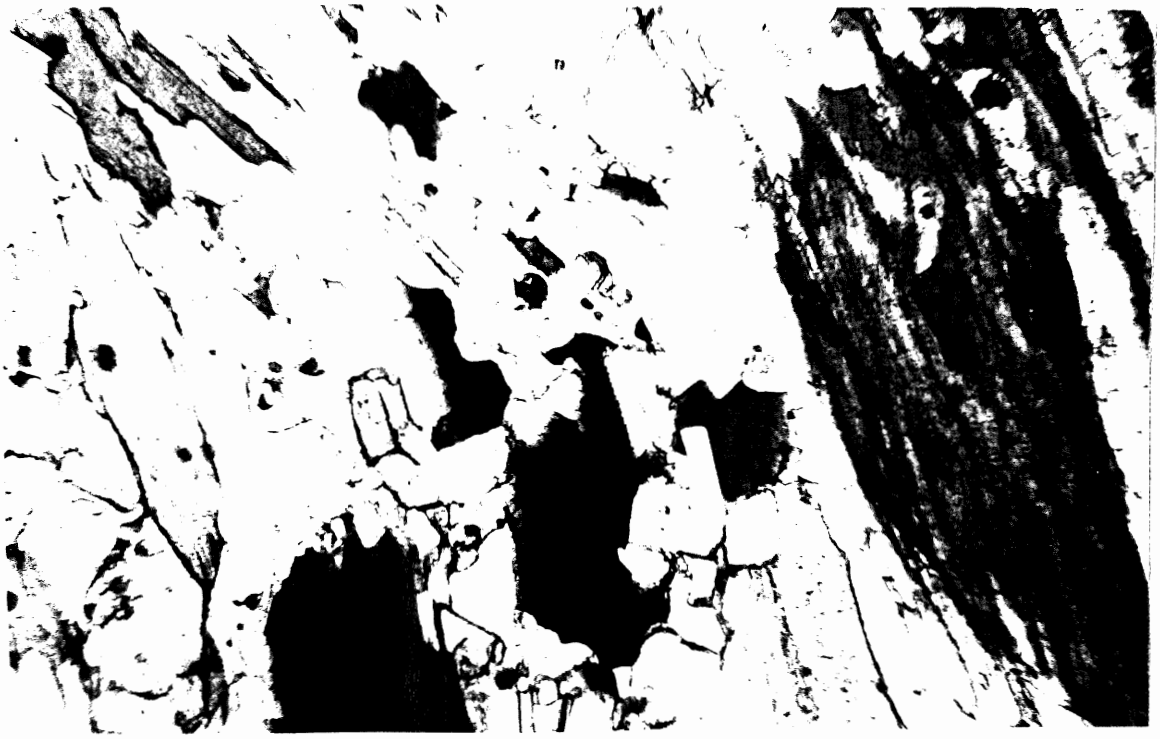

Photo 19: (A-002-4) Both well-formed biotite grains and fine, pleochroic brown tufts that also appear to be biotite. Signs of shearing and secondary biotite growth?

muscovite grains. The biotites are usually unaltered and strongly pleochroic, with rare chlorite alteration and oxidation along rims in some cases. The long axis of the micas is always parallel to the contact with the leucosome. Inclusions of zircon, with pleochroic haloes, occur in many grains, with the percentage varying from slide to slide.

Granite: All samples labelled as granite were either clearly associated with a plutonic body or were from within an unsegregated dyke that could be traced directly to a plutonic body. Mineralogically they are very similar to the leucosomes, although there tends to be less alteration of plagioclase and more mica. Locally, around contacts with semipelite, the plagioclase present in the granites is strongly altered. This alteration normally occurs along the cleavage traces and is not as pervasive as in the leucosomes. Although the mineralogy and textures are similar to those found in the leucosomes, one noticeable difference is the percentage of biotite and muscovite. Leucosomes rarely have more than 5% biotite, and those biotites that do occur in leucosomes are also often very small and altered. In the granite samples studied, however, biotite is commonly present in quantities exceeding 5% and the grains are often larger (0.5-1 mm) and less altered with better cleavage and stronger pleochroism. Occasionally, zonation is noted in the plagioclases of either unit.

As with the leucosomes, granite type-A can be distinguished from type-B by the presence of microcline, and through certain

chemical characteristics which will be covered in the next chapter.

Psammite: This unit could be distinguished from the others by its grain size and a general consistency in its texture. There is little evidence for any but solid-state processes affecting the psammite. Generally the grain size is <0.5 mm and fairly constant between the different phases present. The mineralogy is quartz-plagioclase-biotite-(muscovite) with potassium feldspar present, but relatively unaltered and difficult to estimate relative abundance. Quartz seems to be the most common phase and it usually occurs in a granoblastic matrix. The plagioclase often displays weak to moderate interstitial alteration and the biotites, usually defining a weak foliation, are evenly distributed, rather than concentrated in layers. This layering is, however, a characteristic of the mesosomes, which often resemble psammites in other respects. The muscovite is usually a minor constituent and appears to be secondary and associated with biotite or altered feldspars.

Pelite: This unit displays a wide range of textures and a somewhat variable mineralogy. The semipelite exhibits a more ductile nature than the psammite (photo 4). This picture shows an intruding vein penetrating from the psammite (upper half) into the semipelite (lower half). The dyke dissipates into the semipelitic lithology, indicating very ductile conditions in that unit. Inspection of the photo also reveals that the "plume" appeared to have encountered some sort of flow from left to

right.

The characteristic which best defines this unit is the large, elongate aggregates of biotite and muscovite which commonly form a strong foliation. The micas are usually tabular with good pleochroism. The exception to this is A-002-4 which has both tabular grains as well as very fine-grained, elongate "mats" of mica (photo 19). The semipelites almost always show a strong foliation, although not necessarily a planar one. Contortions and folds are common, as are large grains of both biotite and muscovite defining the foliation. The micas are generally unaltered although they may have oxidized rims and zircon inclusions with pleochroic haloes. Generally the semipelites constitute the host unit, however, on the scale of a thin section the material immediately surrounding the neosomes may be modified. Because of this, the host lithology (immediate surroundings) are dealt with as a separate unit from the semipelites.

Calc-silicate nodules: These nodules occur in the psammite and range from a couple of centimeters to over a meter in diameter. Purves (1974) interpreted them to have originated as diagenetic calcite concretions in the original sediments.

Their general mineralogy is as follows: quartz-calcite-garnet-biotite-potassium feldspar-amphibole. The only phases that always occur are quartz, feldspar and biotite (to a greater or lesser degree). At least one of the other phases is also present, but the number and type of phases vary from one nodule

to another and often from core to rim within a single nodule. Purves (1974) noted that the mineralogy changes depending on the metamorphic grade, which might account for the differences. All the nodules showed a seriate, semi-granoblastic texture and signs of being in disequilibrium. For example, the garnets were almost without exception small and rounded or relict grains. Biotite was either strongly altered or formed poikiloblastic grains around small equant quartz crystals (slide A-008-1).

Aplite/Pegmatite: Aplite and pegmatite dykes are commonly associated with each other, both resulting from the final cooling and degassing of a plutonic body. A mafic unit was often found associated with the aplites (see photo 20). One sample of aplite with a co-existing mafic unit was analysed and the results are shown in the following chapter. It does not appear to be related to the local migmatization around Port Mouton and will not be discussed in detail. The aplite is quart and feldspar rich, much like the leucosomes, but without the granoblastic texture. The mafic unit is a ombination of fine-grained mica aggregates and coarse, elongate biotites, all defining a strong foliation parallel to the aplite.

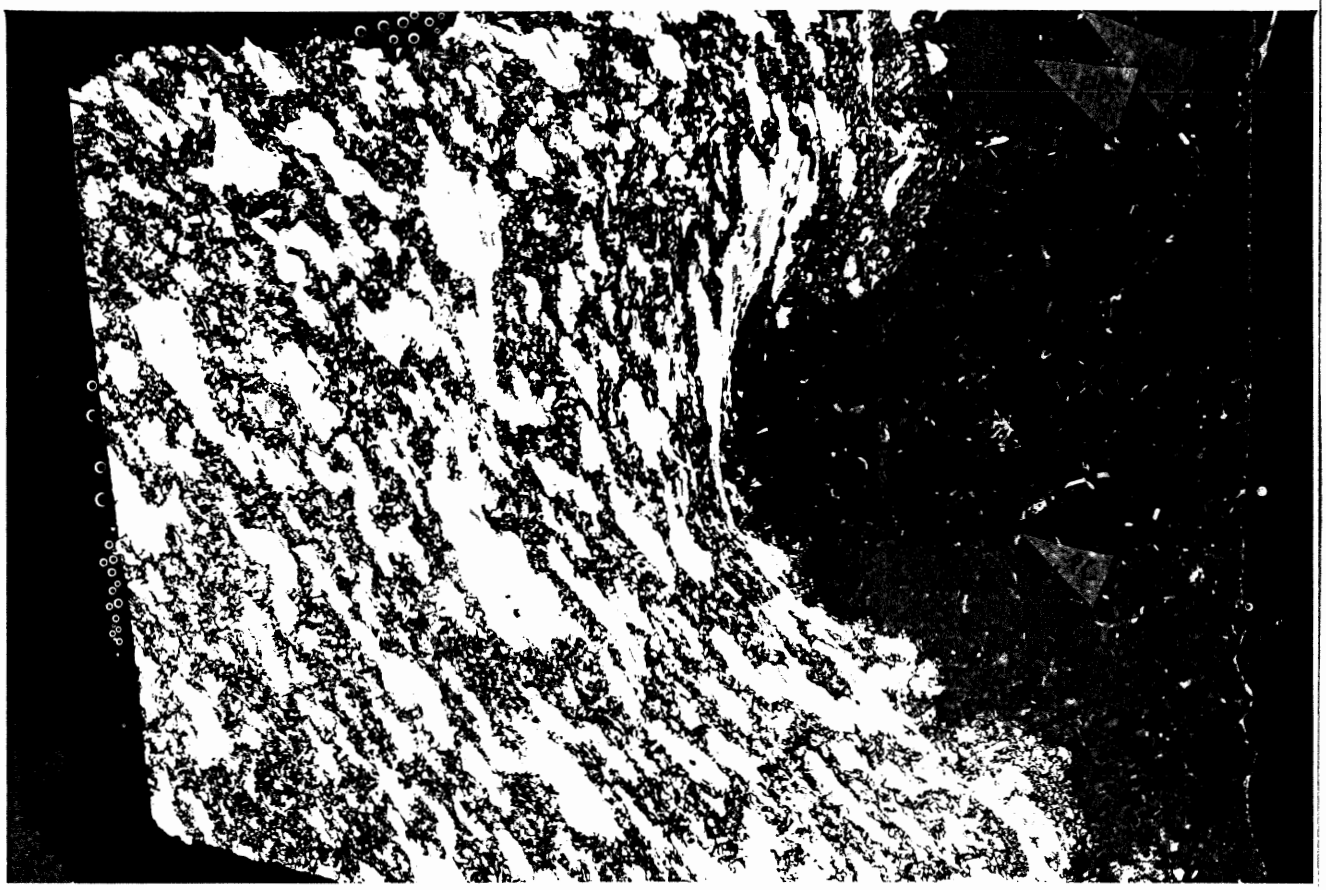

Photo 20: (A-003-1A) Aplite sample with associated mafic unit (left side). (negative image)
Light areas to left are biotite.

(PPL)
0.25 cm

Chapter 4 - Mineral Chemistry

Introduction: Of the 32 thin sections studied in detail, 15 were analysed for plagioclase, 10 of these for biotite and 9 for muscovite. Rims and cores were analyzed for all the plagioclase grains, with no distinct trend noted. Some had higher An in the core, others in the rim and there were grains with no difference greater than the analytical error. A number of grains were analysed repeatedly in order to determine the accuracy of analysis for each phase and each oxide. A summary of these results is presented in Table C.1 and the analytical procedure is discussed in Appendix C. The microprobe analyses were also averaged for each unit per slide (i.e. the plagioclase leucosome analyses for slide A-009-1A were averaged) and the results are presented in Appendix B. The chemistry of the various phases was studied, and the results are presented in this chapter along with some discussion. In the next chapter these data are interpreted with regard to the petrogenesis of the migmatites.

Study of these units reveals that the presence of microcline is not the only method of discriminating type-A from type-B lithologies. Figure 5 shows FeO/MgO versus Al_2O_3 for biotites in the granite and psammite units. The bimodal distribution, when tied into the petrography, indicates that those granites bearing microcline (type-A) all plot in the low-Al_2O_3 field and the non-microcline bearing slides are in the high-Al_2O_3 field. While there are no readily discernible differences in the petrology of the various psammites, they also form bimodal plots. Microcline

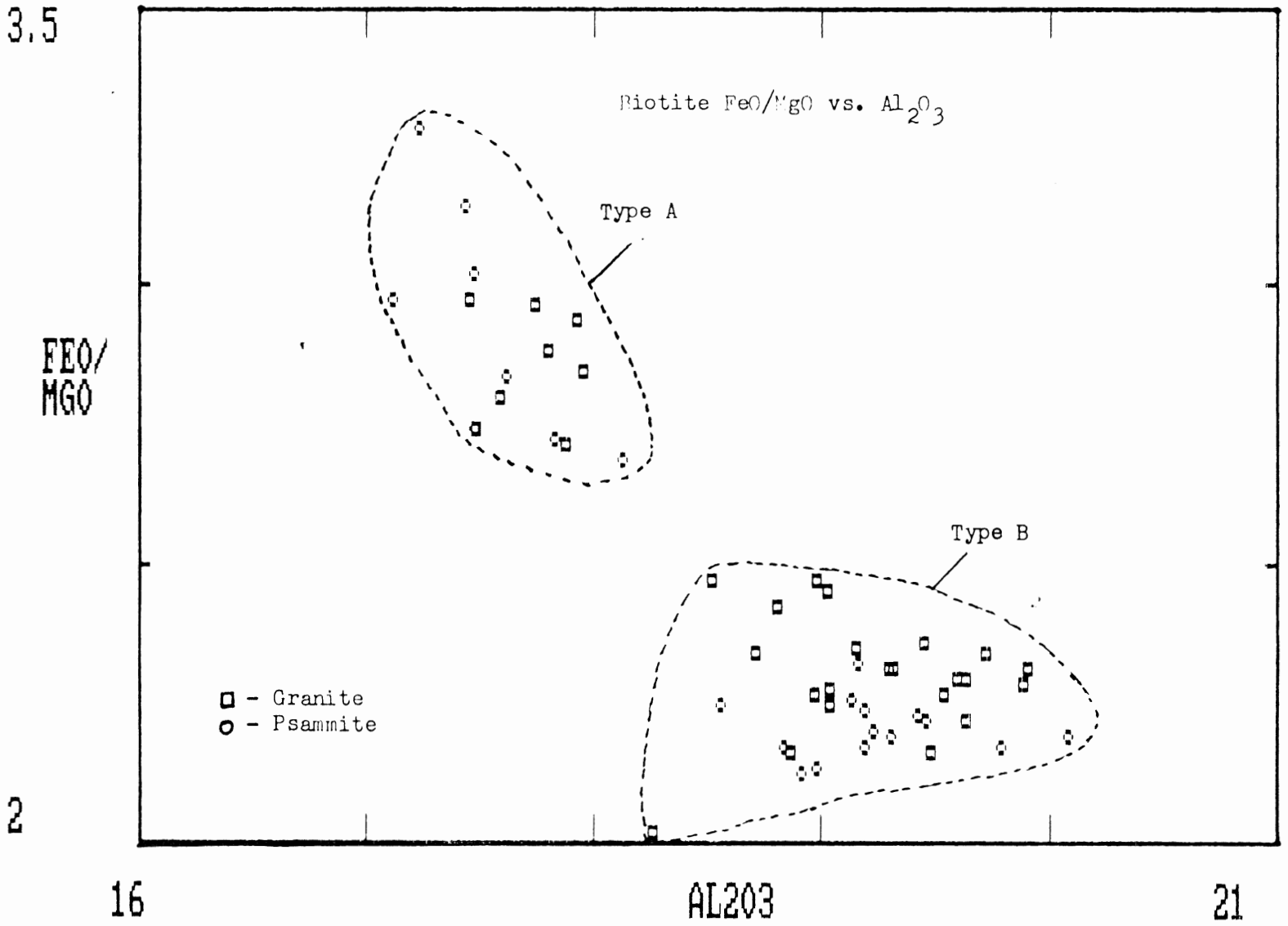

Figure 5: Plot showing Type A and Type B fields of the granite and psammite units.

is present in one psammite sample (A-009-4D, psammite with adjacent microcline-bearing granite unit) but no chemistry is available for this slide. Other psammite samples plotting in the type A field (determined from FeO/MgO ratios, see Figure 5) have no microcline present. The FeO/MgO ratio appears to best define the difference in type for the two units, with ratios above 2.5 being type-A and below 2.5, type-B.

The leucosome biotites, which also show a similar difference in microcline content, plot in one large field (Figure 6). This one field can be split into two overlapping subfields when the type-A and type-B leucosomes are discriminated by microcline content. However, the distinction between the groups is not clear when FeO/MgO and Al_2O_3 content is considered.

Relative to the other units, the average aplite plagioclase has higher An content, placing it in the labradorite field as opposed to andesine (see Figure 7).

The semipelites, in general, seem to plot within a very restricted field relative to the other units. This might be due to unique chemical characteristics, but is more likely a result of the limited number of semipelite analyses available.

Inspection of the average muscovite TiO_2 plot (Figure 8) reveals that most of the muscovites have >0.6 % TiO_2. The raw data for leucosome muscovite TiO_2 % (Appendix B) reveal that there is usually at least one grain with > 1.0 % TiO_2 in each sample. Miller et al. (1981) suggest that magmatic muscovite should have more than 0.4-0.6 % TiO_2, at least for peraluminous

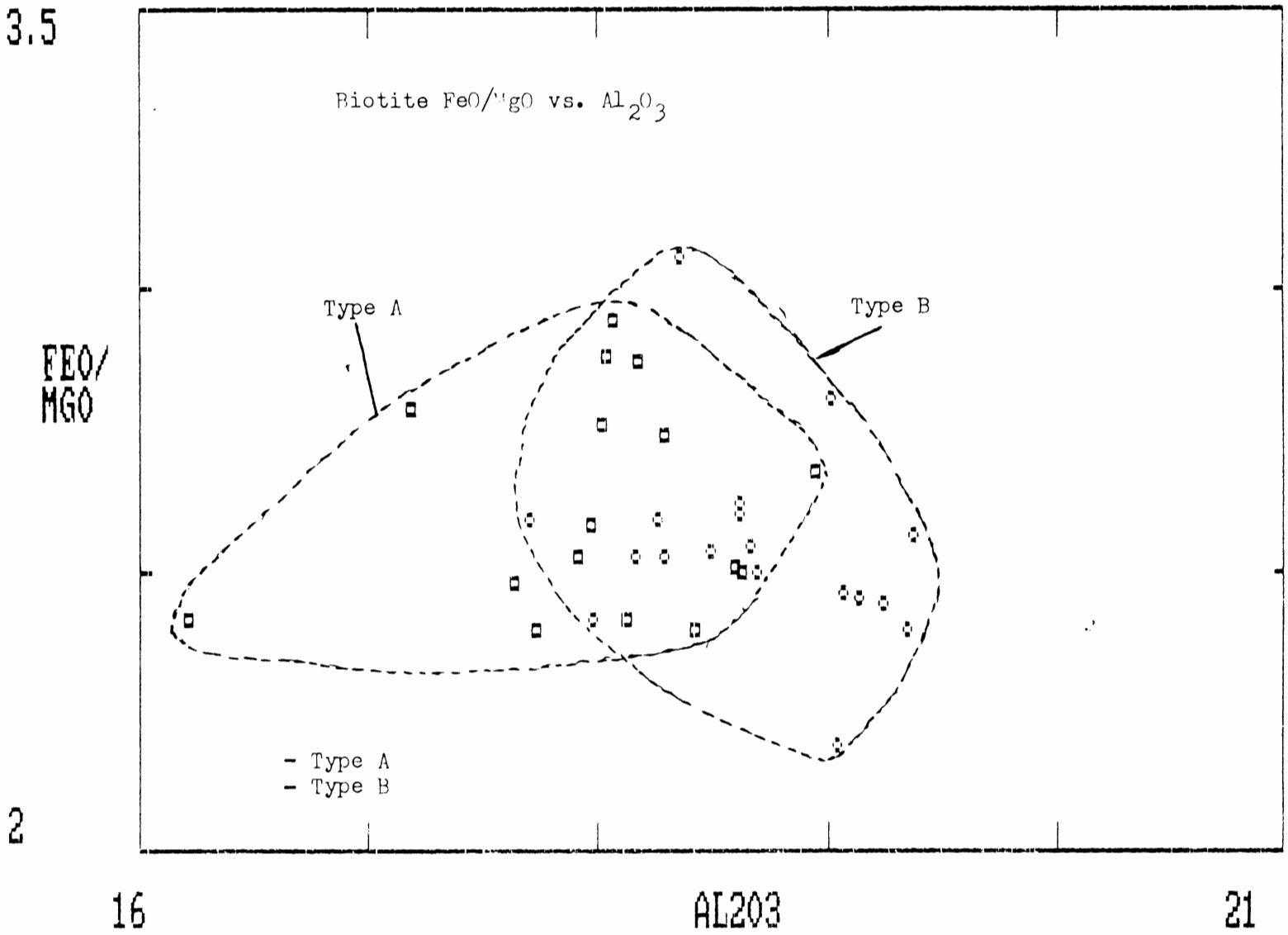

Figure 6: Plot showing Type A and Type B fields for the leucosomes. Note there is a great deal of overlap.

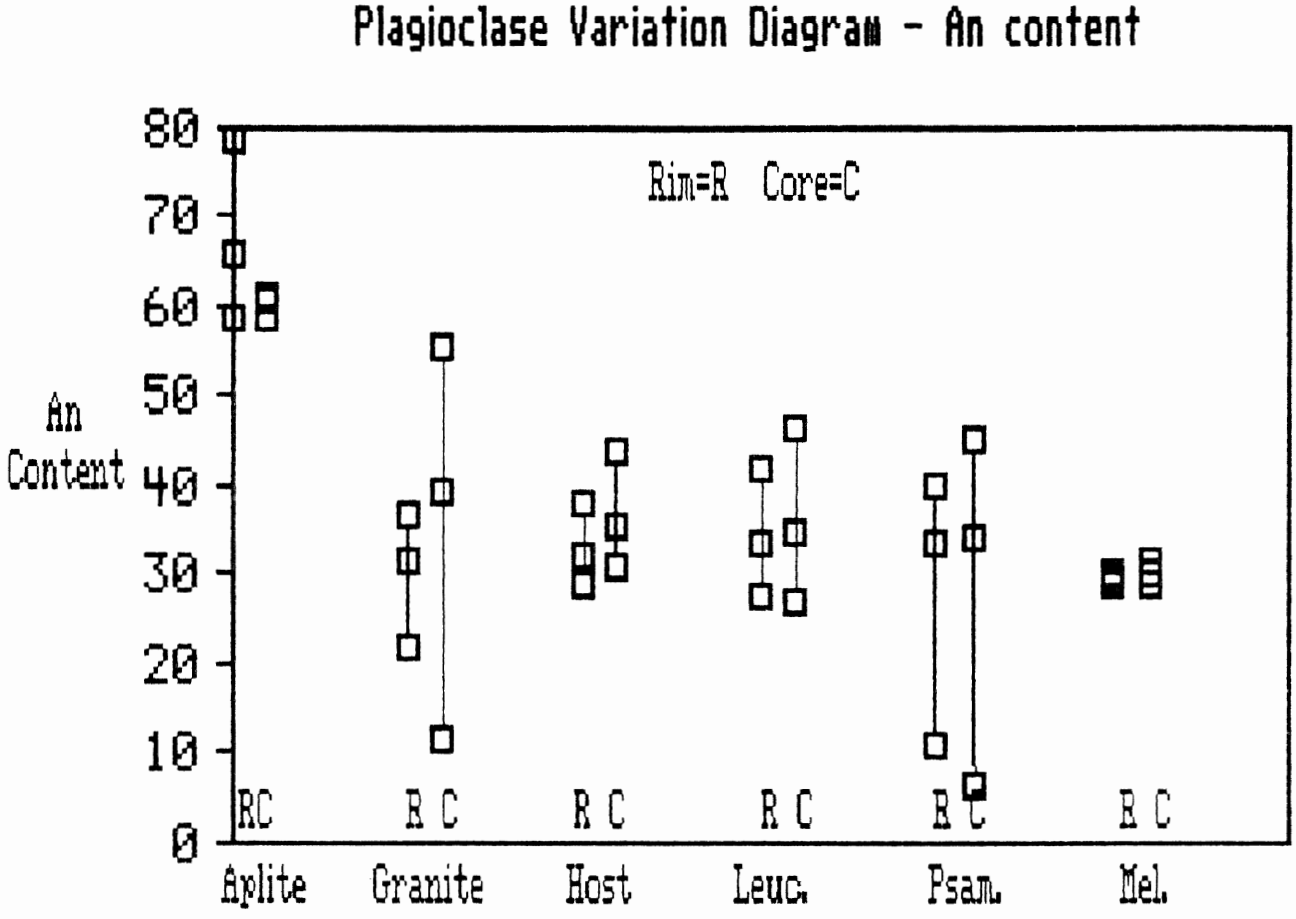

Figure 7: Plot of maximum, average and minimum An contents for the plagioclase analyses of the various units. Note the aplite has a distinct composition.

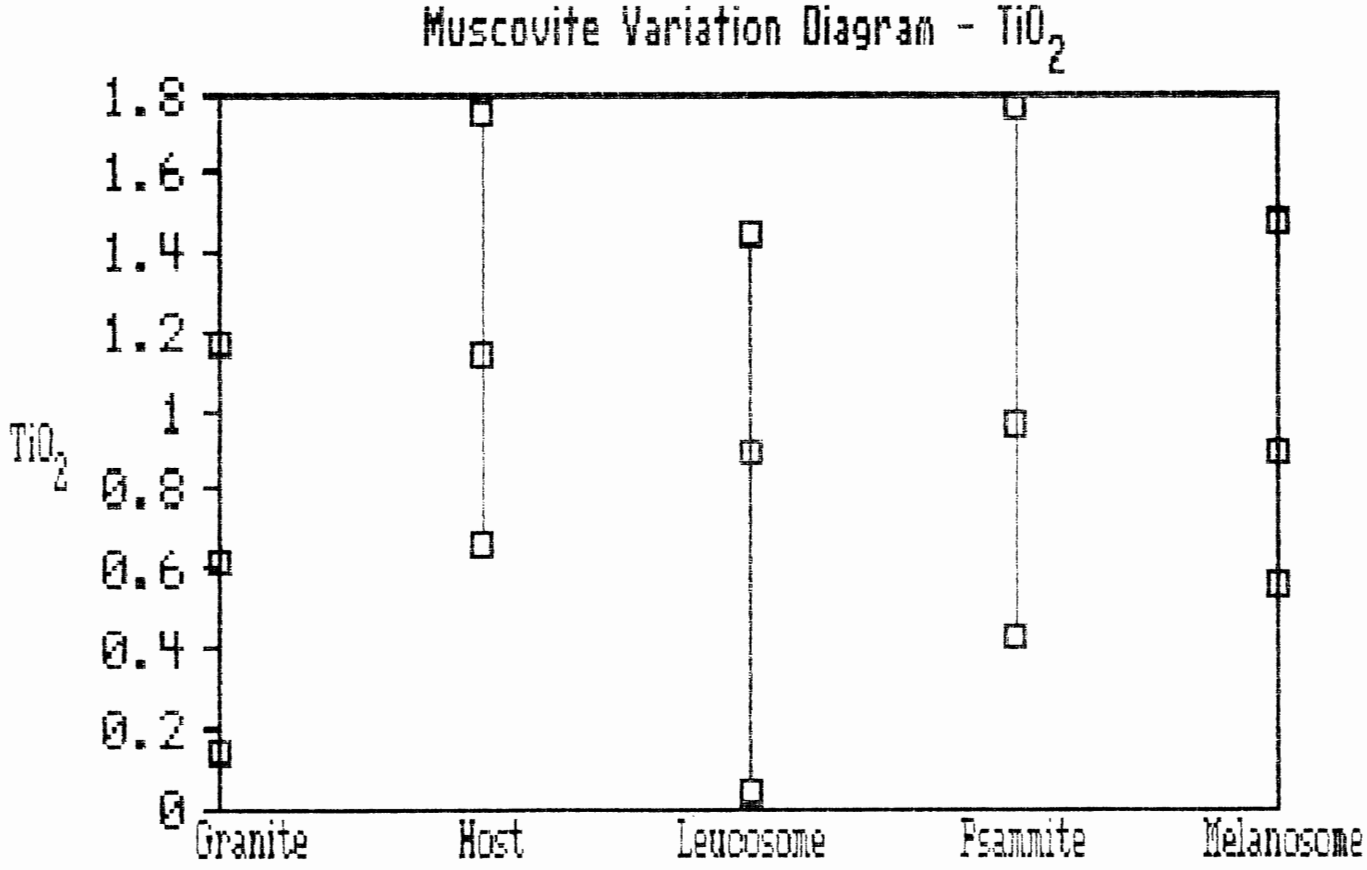

Figure 8: Plot of max., average and min. TiO_2 values for the different units having muscovite analyses.

granites and in the presence of a Ti buffering phase. If these same criteria can be applied to the leucosomes, which appear genetically related to the granites, at least in part, it could be an indication of a magmatic origin for the muscovite present, and thus the leucosome.

A number of lithological contacts were analysed and the results plotted with respect to their X position on the slide, to determine whether any detectable chemical gradients were present. Figure 9a shows the results of a traverse across slide A-004-2B [psammite/granite contact], looking specifically at muscovite TiO_2. The plot shows disequilibrium between the two units with respect to this oxide. Sample C-002-1 [xenolith/granite contact] displays an approximately increasing FeO weight percent across the boundary (see Figure 10), with all xenolith analyses <19.3 % FeO and all granite analyses >19.3 %.

Figure 11 displays FeO vs. MgO for the slide unit averages (with a unit defined as granite, psammite, leucosome, melanosome, host, pelite or aplite). With increasing degrees of fractionation of a melt, the biotite FeO should increase and the MgO decrease. This implies that the B granites may have fractionated from the A granites. Aplite, which is commonly extruded late in the cooling history as a result of degassing, usually originates from the remaining melt, which would logically be expected to be very fractionated. This would result in a very fractionated aplite, but its biotite suggests it has a very primitive composition relative to the other units.

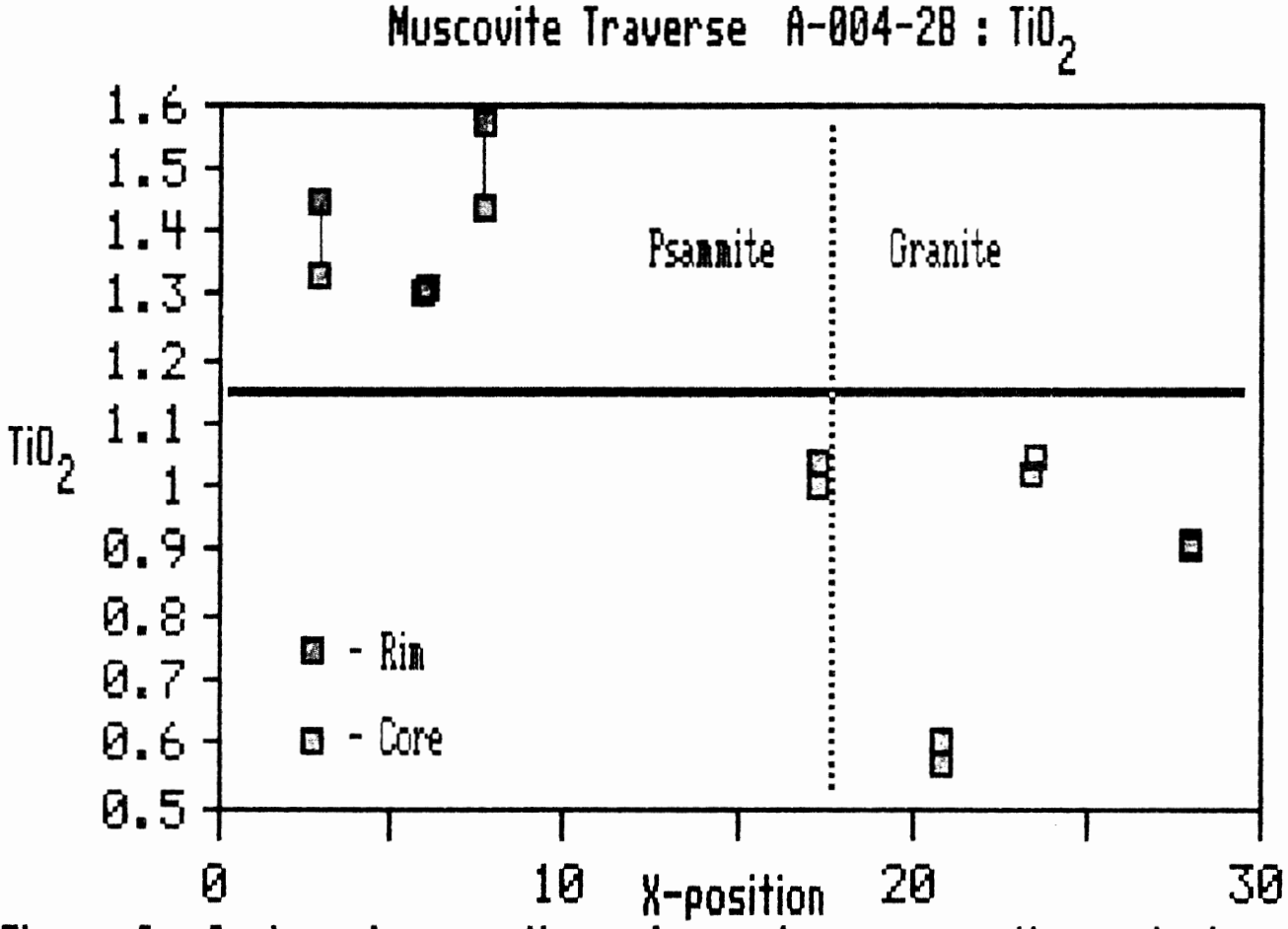

Figure 9a: Series of muscovite analyses done across the contact psammite and granite.

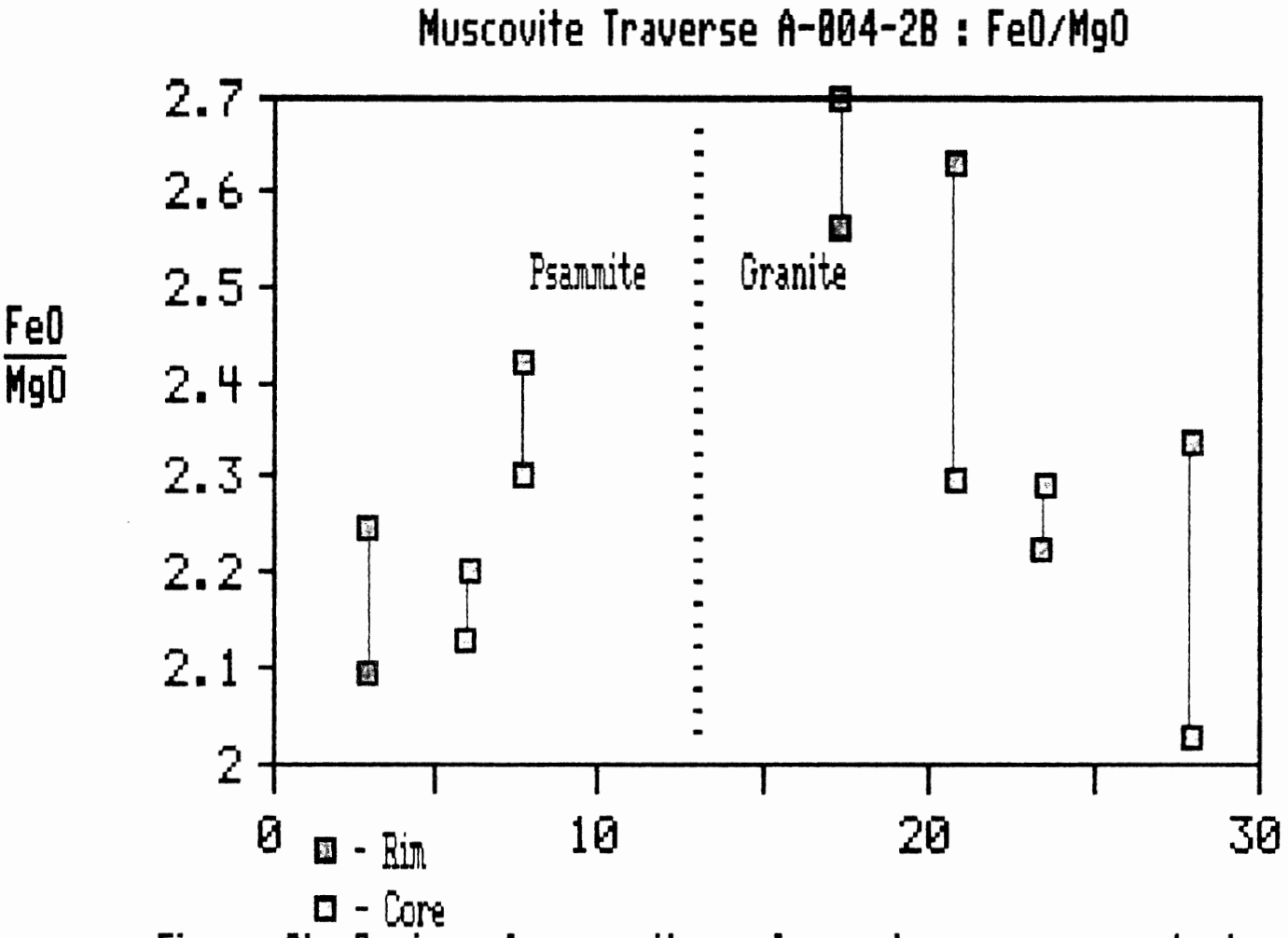

Figure 9b: Series of muscovite analyses done across contact between granite and psammite.

Figure 10:(C-002-1) Biotite traverse plot of FeO

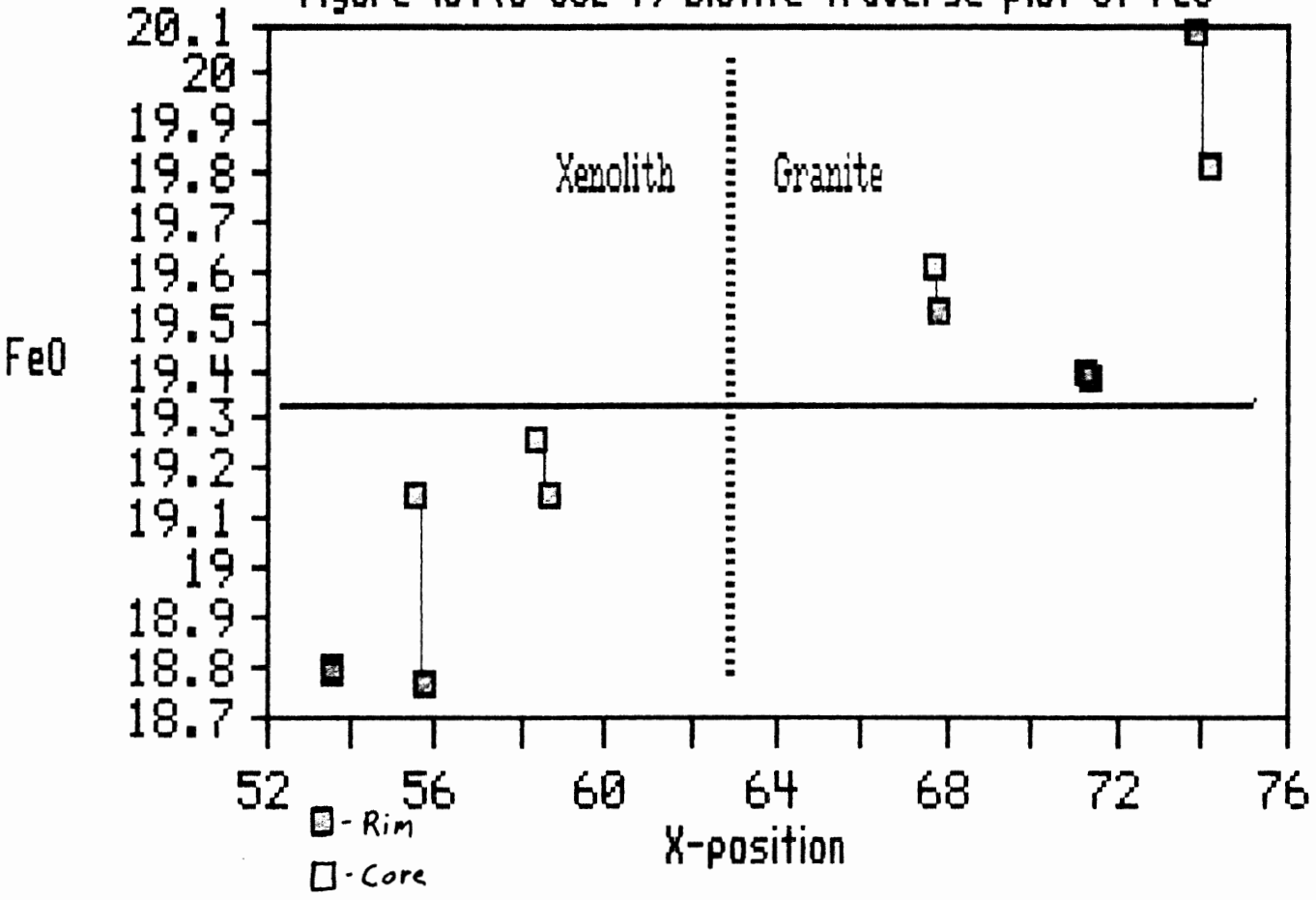

Figure 11a: Biotite Averages - FeO vs. MgO

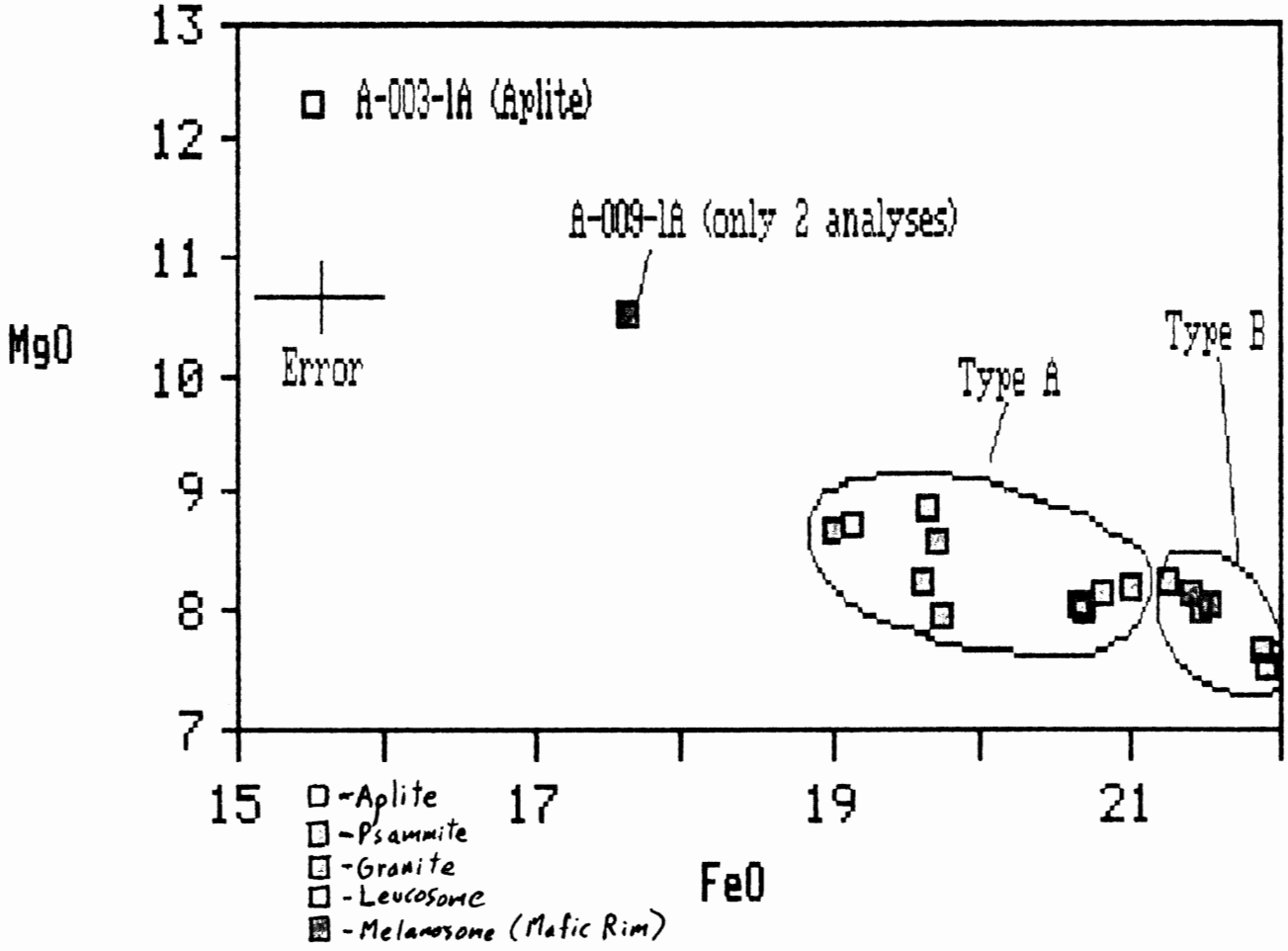

Chapter 5 - Discussion

Problem: The basic question being addressed is that of migmatite genesis. The processes that could be responsible are either magmatic or non-magmatic (i.e. solid-state). Magmatic processes include granitic injection and partial melting, while non-magmatic processes include sub-solidus segregation and other, primarily metamorphic processes occurring in the solid state. A general approach to the solution of this problem comes from the nature of the field region. Given that the migmatites are confined to the margin of the Port Mouton pluton, and are not found elsewhere in the country rock (Hope, 1987), then regional metamorphic processes would appear to be ruled out. Given the proximity of the migmatites to the pluton, it seems very likely that they are the direct or indirect result of the pluton. This would suggest magmatic processes, especially given the plethora of intruding dykes and dykelets noted in most of the study areas. In addition, the presence of hypidiomorphic zonation in the plagioclases of some leucosomes would suggest that they formed in an isotropic medium (i.e. magma). This then raises the question of which magmatic processes are responsible, and a further treatment of the evidence is required to render a conclusion.

Argument for injection: Granitic dykelets were identified by their large lateral extent (>1m), because they could be traced to a portion of the pluton, or because they cut other lithologies. The dykelets tended to inject preferentially along the semipelitic beds which display a high degree of ductility

compared to the psammite (see Photo 4). Many dykelets of plutonic origin displayed mafic rims (see Photo 9), which fits the definition of a neosome and indicates that some form of segregation took place.

Argument for partial melting: The occurrence of leucocratic "lenses" with mafic rims (i.e. A-009-1A [neosome + host], see Photos 1, 7 and 15) but not obviously joined in any manner to the pluton, suggests partial melting took place. Miller (1981) suggested that one method of determining whether muscovite is magmatic or secondary is through TiO2 content. If there is more than 0.4-0.6 weight percent TiO_2, then the muscovite is probably magmatic. Muscovite TiO_2 content for A-009-5A, A-008-3A and D-001-3A ([samples of neosome + host] see Appendix B) show muscovites often have >0.6 % TiO_2, suggesting a magmatic origin for them and thus for their leucosome host. Slide A-008-4B [neosome + host] shows TiO_2 <0.8 % for not only the leucosome but also the host and melanosome, suggesting those muscovites are secondary. Further evidence comes from samples A-008-3A/1 [type-A leucosome in pelite] and D-002-2B [rimless leucosome in psammite], both of which contain hypidiomorphically zoned plagioclase grains (see photo 21). This implies growth in an isotropic medium (i.e. magma or hydrothermal solution channel) where the crystal could grow, unimpeded by other grain boundaries (Ashworth and McLellan, 1985).

Discussion of evidence: Granitic injections forming rimmed veins are observed in many regions of the study area. The rimmed

Photo **21:** (D-002-2R) Example of idiomorphic zoning in plagioclase.

injections can often be traced for meters through the host rock to the pluton, or can be observed cutting across the foliation of the host (i.e. Photo 9). However, the role of partial melting as an important genetic process can still be questioned. In order to address this problem, each piece of evidence given for partial melting will be discussed in turn.

Hypidiomorphic zonation in plagioclase: As stated previously, an isotropic medium is implied for hypidiomorphic zonation. However, it was only noted in two leucosomes, one of which was in psammite, and the other a rimless leucosome which could be an injection (difficult to determine due to contortion of the pelite in which it occurs). None of the other leucosomes displayed hypidiomorphic zonation.

Problems with partial melting: Logically, there should be a simple relationship between host, leucosome, and melanosome if the genetic process at work is partial melting. In any mineral system the Mg end-member composition has a higher melting point than the Fe end-member. As shown in Figure 12 (the actual case may not be this simple), melting bulk composition A will result in a residual composition R and melt composition M, with M being closer to the Fe end member. Thus, the melt biotites should be enriched in Fe and depleted in Mg with respect to the residuum. The result would be high FeO/MgO ratios in the melt phase (i.e. leucosome formed from partial melting), an intermediate ratio in the host lithology and a low ratio in the residual phase (i.e. melanosome depleted during partial melting). However, this

Figure 12: Model binary phase diagram. M=melt, B=bulk comp. and R=residual

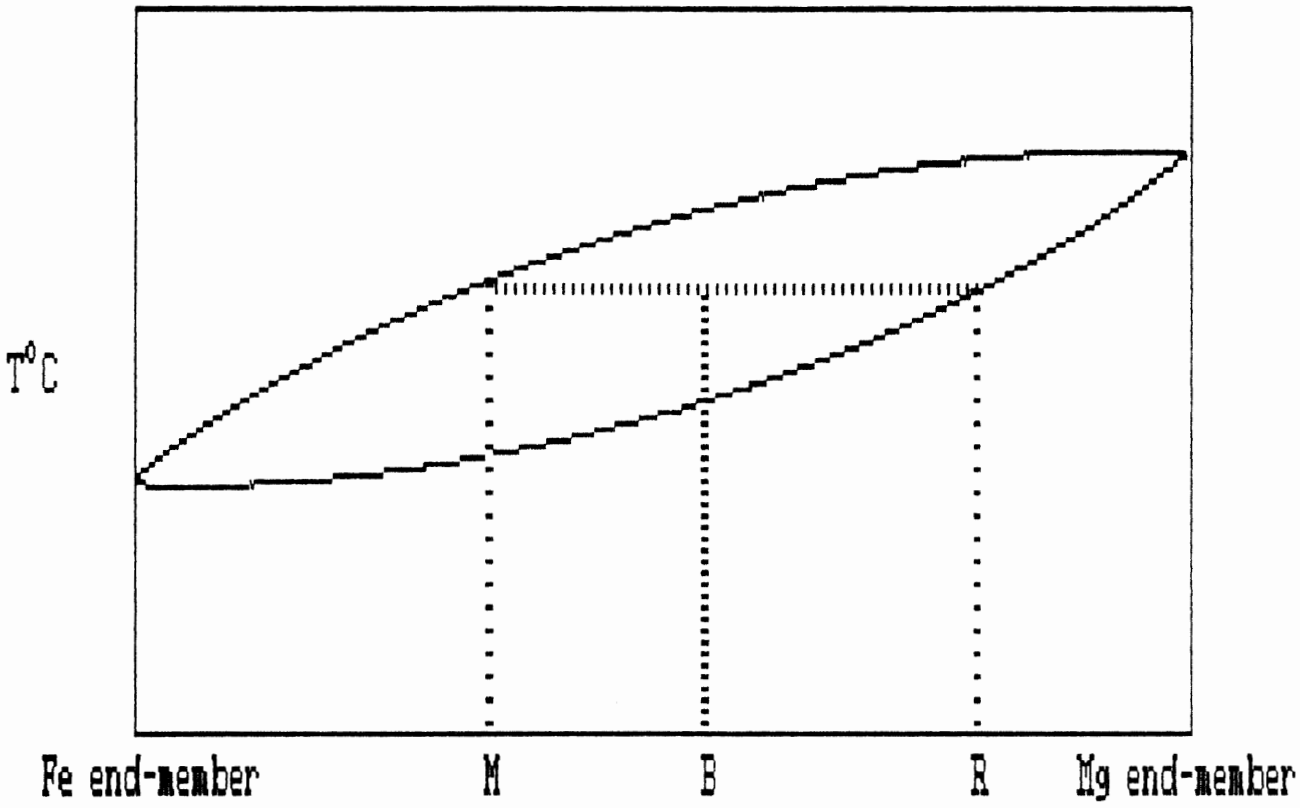

simple relationship is not generally observed in the chemistry of the neosome/host plots. One of the leucosomes (from sample A-009-1A [neosome + host]) does display a pattern of FeO/MgO in the biotite roughly decreasing from leucosome to host to melanosome (see Figure 13). However, the trend is not strong and is close to the level of analytical error. There are probably other factors at work as well, such as a) instrument sensitivity, i.e. the probe may not be sensitive enough to clearly discriminate trends in FeO/MgO accurately; b) there may have been some re-equilibration, blurring the relationship for these samples or c) there may have been mixing with another melt phase, resulting in a hybrid composition. In the case of c, this would mean mixing with granitic injections from the pluton, with the consequent exchange of components. In the case of granitic injections, A-009-1A is less than 3 meters from the large granitoid body outcropping at A-009 and the semipelite bed is in contact with that lithology (see Outcrop map 1). This indicates that A-009-1A is in a position to have experienced a large thermal influx, both to produce partial melting and to have mixed with some component of the pluton. The other leucosomes: A-008-4B, A-009-5A, A-009-1B, D-001-3A and A-008-3A do not show any clear relationships with regard to FeO/MgO ratio.

The problem of equilibration is relevant to the FeO/MgO ratios. If the leucosomes did form from partial melts, but equilibrated with large masses of granite, the leucosomes would reflect granitic compositions. Also, if the leucosomes formed

Figure 13

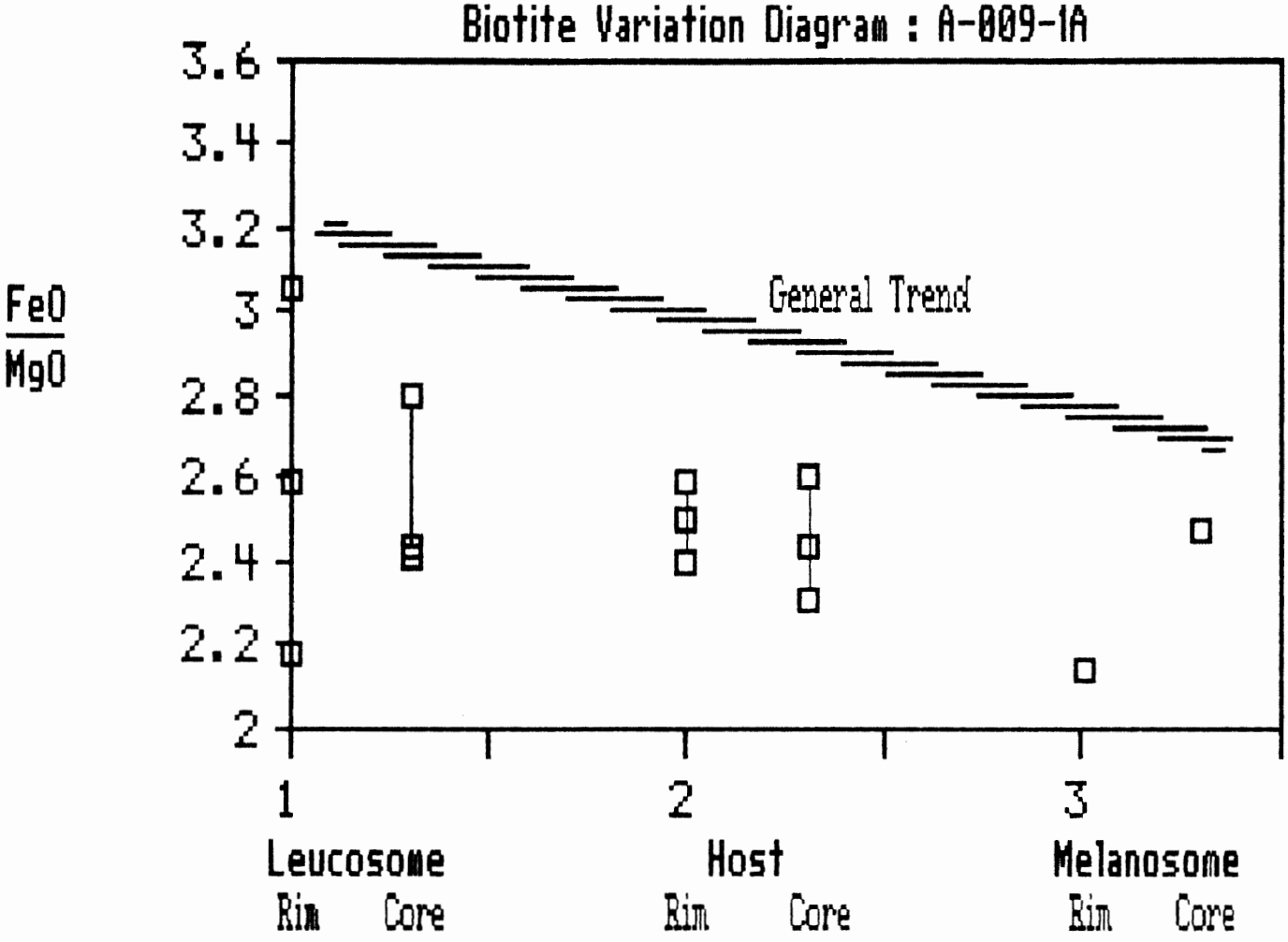
Biotite Variation Diagram : A-009-1A
FeO
MgO
3.6
3.4
3.2
3
2.8
2.6
2.4
2.2
2
General Trend
1
2
3
Leucosome
Rim
Core
Host
Rim
Core
Melanosome
Rim
Core

completely by granitic injection without partial melting, they would again reflect the granite composition. The state of equilibration can be addressed by looking at the two psammite biotite compositions.

Bimodal psammite: Figure 5 shows that the psammite biotites analysed fall into two distinct groups, corresponding well with the granite fields. This bimodal character, however, is only noticeable on the chemical level, there being no obvious mineralogical differences between the types. There are two possibilities that could explain this variation. First, it may be that the original sedimentary rocks had a bimodal nature, i.e. a reflection of different sediment layers (commonly found in the Goldenville Formation). The second possibility is that the psammites equilibrated with the local granite.

All the psammite samples analysed were in contact with granite and the psammite biotite compositions (which express the bimodal nature) reflect those of the immediately adjacent granites. Any variation in relict sedimentary composition should not mimic the granite compositions so closely. This indicates that equilibration has most likely occurred between the biotites of the psammites and granites, at least on the scale of a thin section.

Figure 6 shows that the leucosomes do not reflect the granitic compositions as closely as the psammites. They can be split into two greatly overlapping fields that are similar to those of the granites, but the leucosomes more or less plot

between the granite types. This suggests that the leucosomes are neither completely the result of injection, nor have they entirely equilibrated with the local granite.

Alumino-silicates: According to Johannes (1984) and Thompson (1982), sufficient heating of a rock that is primarily quartzo-feldspathic with biotite and muscovite present will form anatectic melts by dehydration-melting and leave residues containing Al_2SiO_5, garnet, cordierite or hypersthene. However, the melanocratic rims from the study area consistently show high biotite, high to moderate muscovite and none of the other components, with the exception of sillimanite in a few cases (e.g. slide A-002-1).

Figure 14 shows melting and subsolidus relations in the CKNASH system (Johannes, 1984), indicating that below ~7 kbars P_{H_2O}, partial melting can occur with only the components Qz-Or-Ab-An being lost or produced. This seems to best represent the conditions existing in the study area although it does not include biotite. In fact, using the diagram and the statistics in Appendix D for plagioclase An contents, an estimate of leucosome temperature at time of plagioclase formation can be made. The leucosomes produce a good normal distribution around ~34% An content, so depending on the partial pressure of water in the system, the temperature could have ranged between 650 to 700 C.

Figure 11 shows that there is an inverse correlation between FeO and MgO along a relatively straight line. The more

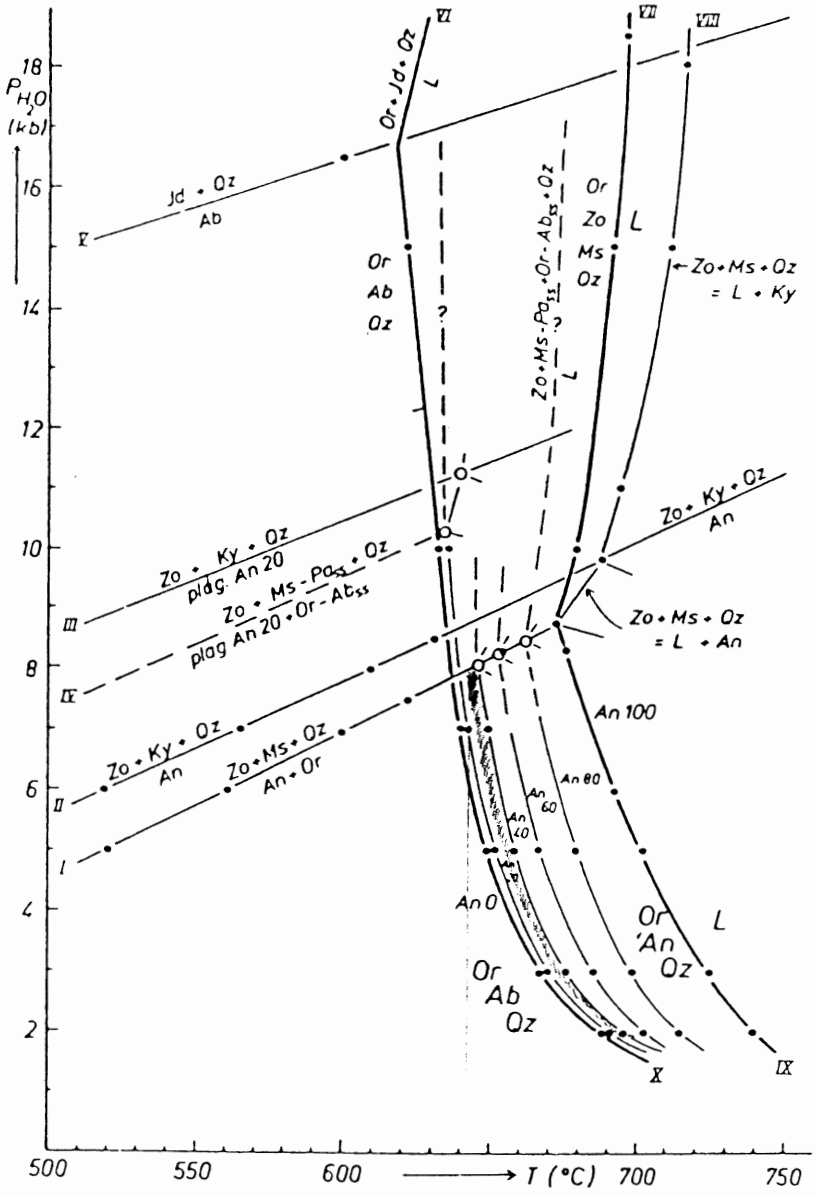

Figure 14 : Melting and subsolidus relations in the CKNASH system, from Johannes (1984).

fractionated a magma is, the greater the FeO % and lower the MgO % will be in the biotites (Deer et al. 1983). This is contradicted, however, in Figure 11 by the position of the aplite, a late-stage extrusive, with respect to the migmatites and related granites. It is clearly separate and plots where a more primitive magma biotite composition would be expected. According to Douma (1986) the pluton is composed of nine different mappable granitoid units. It could be that the aplites, or at least the one analysed, originated from a different, much more primitive unit and is unrelated to the two granite fields found in the study area.

General Discussion: There appears to be a range of migmatites from those resulting entirely from a partial melt (i.e. A-004-5 ([leucosome in pelite near psammite contact] see photo 16) to granitic injections (sample A-005-2 [granite vein in psammite]). Most of the leucosomes fall between these extremes, being locally continuous, often contorted layers usually with a mafic rim. Given that the partial melts (denoted by very low biotite content, coarse and abundant quartz, lens shape not connected to any injections) do not display mafic rims (in the samples available), the biotites of these intermediate leucosomes do not mimic the granitic fields and have muscovite TiO_2 contents suggesting a magmatic origin, they are most likely a combination of both injection and partial melting.

Chapter 6 - Conclusions

The following represents the conclusions that can be made from the available data, with varying degrees of certainty:

1. Granitic injection is common along the semipelitic interbeds, as indicated by field observations.

2. Equilibration of the biotites in the psammites with adjacent granite biotites occurred on the scale of a thin section. This is indicated by Figure 5 (plot of biotite FeO/MgO vs. Al_2O_3 for granite and psammite)

3. Immobility of Ti in muscovite as opposed to more mobile elements (i.e. Fe and Mg), is suggested by analyses across A-004-2B (Figure 9).

4. Hybridization of granitic injections through partial melting of the pelite. This seems indicated since the leucosomes appear to have originated magmatically (muscovite TiO_2, hypidiomorphic zonation in some plagioclases, granitic composition of leucosomes inside a semipelitic schist host) yet do not mimic the granite compositions, nor the texture and mineralogy of the pure partial melts (i.e. <3 % biotite, coarse grained quartzo-feldspathic mineralogy and only occurring in small lenses.

Model for the Port Mouton migmatites: It would appear that the migmatites formed in the following manner (see Figure 15): In Devonian-Carboniferous times a number of granitic units emplaced at a depth of ~10 km (??) into a sequence of fairly high

Figure 15: Simple model for Port Mouton migmatites

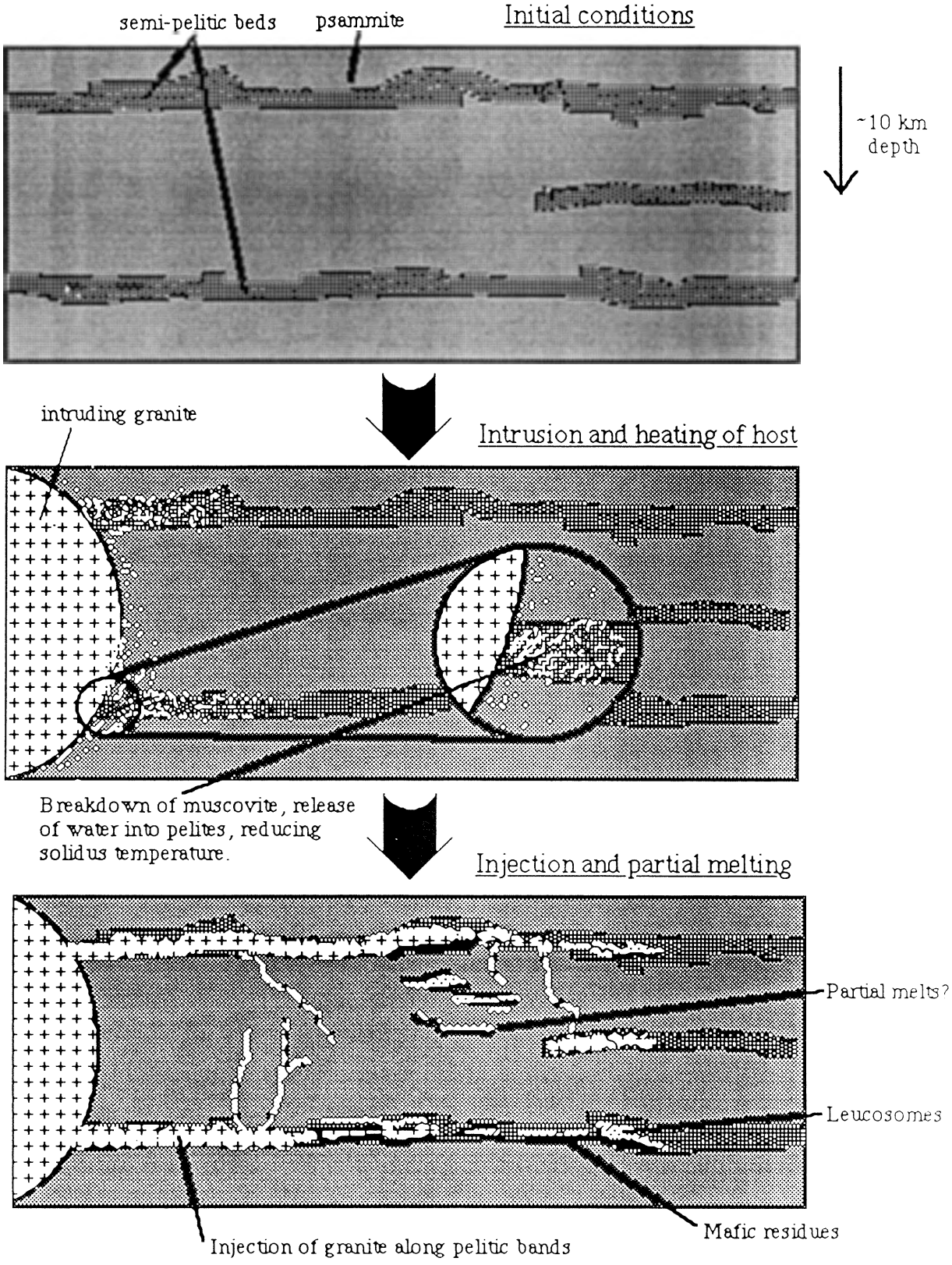

grade (and-staur-cord) metasedimentary rocks. These metasediments were composed mostly of quartzo-feldspathic psammites with interbedded layers of semipelites. As the granite heated the country rock, the muscovites in the semipelites began to break down, releasing water and lowering the local solidus. They melted slightly along grain boundaries, becoming very ductile until finally intrusions from the granite began infiltrating preferentially along these weakened beds. As they penetrated the semipelites, they undoubtedly caused localized melting in places and often may have mixed with 'pods' of melt. There might have been deformation resulting from emplacement that may have displaced neosomes from their original source and caused highly contorted layering within these weaker units. Finally, as the granite cooled and the neosomes solidified, there may have been at least one other period of intrusion of magmatic material (see discussion of outcrop series D, chapter 2), followed by degassing and intrusion of pegmatites and aplites.

Recommendations: Future work on these rocks should include a study of REE's, minor and trace elements. Because of the large degree of equilibration that seems to have taken place, the greater sensitivity of these analyses, plus the more immobile nature of many of those elements would better indicate the processes at work. A more detailed study of the leucosomes found around outcrop C-002 (see Photo 13) and the segregated dykes of outcrop C-001 (Photos 11 and 12) would also prove interesting. A number of samples could be taken along a granite psammite contact

to determine the degree of equilibration between the two units and the granite unit adjacent to the various phases could be studied in more detail. A determination of T, P and water fugacity at time of emplacement would also be very useful, although in felsic igneous rocks these are often difficult to determine.

Bibliography

Albuquerque C. A. R. de, 1977. Geochemistry of the tonalitic and granitic rocks of the Nova Scotia southern plutons. Geochimica et Cosmochimica Acta, v. 41, pp. 1-13

Ashworth J. R., 1985. Introduction. In Ashworth, J.R., (ed.) Migmatites. Glasgow: Blackie, pp. 1-35

Douma, S., 1987. Port Mouton pluton...; unpublished Masters thesis, Dalhousie University, Halifax, Nova Scotia.

Ellis, D.J. and Thompson, A.B., 1985. Subsolidus and partial melting reactions in the $CaO+MgO+Al_2O_3+SiO_2+H_2O$ system under water-excess and water-deficient conditions to 10 kb: Some implications for the origin of peraluminous melts from mafic rocks. Journal of Petrology, v. 27, pp. 91-121

Grant, J.A., Equilibria in low-pressure melting of pelitic rocks. In Atherton, M.P., Gribble, C.D. (eds.), Migmatites, melting and metamorphism. Shiva, Nantwich, pp. 292-293

Green, N.L. and Usdansky, S.I., 1986. Towards a practical plagioclase-muscovite thermometer. American Mineralogist, v. 71, pp. 1109-1117

Halden, N.M., 1983. Development of migmatites in deep levels of a wrench fault zone. In Atherton, M.P., Gribble, C.D. (eds.), Migmatites, Melting and Metamorphism. Shiva, Nantwich, pp. 294-295

Hope, T.L. and Woodend [Douma], S., 1986. Igneous and metamorphic geology: Port Mouton-Port Joli map area.

Hope, T.L., 1987. Contact meta...; unpublished Masters thesis, Acadia University, Wolfville, Nova Scotia.

Hopgood, A.M., et al., 1983. U-Pb and Rb-Sr isotope study of polyphase deformed migmatites in the Svecokarelides, Southern Finland. In Atherton, M.P., Gribble, C.D. (eds.), Migmatites, Melting and Metamorphism. Shiva, Nantwich, pp. 80-92

Jarewicz, S.R. and Watson, E.B., 1985. The distribution of partial melt in a granitic system: The application of liquid phase sintering theory. Geochimica et Cosmochimica Acta, v. 49, pp. 1109-1121

Johannes, W., 1983. On the origin of migmatites. In Atherton, M.P., Gribble, C.D. (eds.), Migmatites, melting and metamorphism. Shiva, Nantwich, pp. 234-248

Johannes, W., 1984. Beginning of melting in the granite system

Qz-Or-Ab-An-H_2O. Contributions to Mineralogy and Petrology, v. 86, pp. 264-273

Johannes W., 1985. The significance of experimental studies for the formation of migmatites. In Ashworth, J.R., (ed.) Migmatites. Blackie, pp. 36-85

Karlsson, G. and Wahlgren, C.H., 1982. A statistical investigation of grain contacts in a migmatite. N. Jb. Miner. Mh., v. 8, pp. 348-360

Kenah, C. and Hollister, L.S., 1983. Anatexis in the Central Gneiss Complex, British Columbia. In Atherton, M.P., Gribble, C.D. (eds.), Migmatites, Melting and Metamorphism. Shiva, Nantwich, pp. 142-161

Manning, D. A. C., and Pichavant, M., 198 . The role of flourine and boron in the generation of granitic melts. In Atherton, M.P., Gribble, C.D. (eds.), Migmatites, Melting and Metamorphism. Shiva, Nantwich, pp. 94-109

McLellan, E.L., 1983. Problems of structural analysis in migmatite terrains. In Atherton, M.P., Gribble, C.D. (eds.), Migmatites, Melting and Metamorphism. Shiva, Nantwich, pp. 299-302

McLellan, E.L., 1983. Contrasting textures in metamorphic and anatectic migmatites: An example from the Scottish Caledonides. Journal of Metamorphic Geology, v. 1, pp. 241-262

McLellan, E., 1984. Deformational behaviour of migmatites and problems of structural analysis in migmatite terrains. Geological Magazine, v. 121(4), pp. 339-345

Miller, C.F., Stoddard, E.F., Bradfish, L.J., and Dollase, W.A., 1981, Composition of plutonic muscovite: Genetic implications. Canadian Mineralogist, v. 19, pp. 25-34

Miller, C.A., 1985. Are strongly peraluminous magmas derived from sedimentary sources? Journal of Geology, v. 93, pp. 673-689

Nockolds S. R., Knox R. W. O'B., Chinner G. A., 1978. Chapter 33 - Metamorphism: deformation and recrystallization. In Nockolds S. R., Knox R. W. O'B., Chinner G. A. In Petrology for Students. Cambridge University Press

Olsen, S.N., 1983. A quantitative approach to local mass balance in migmatites. In Atherton, M.P., Gribble, C.D. (eds.), Migmatites, Melting and Metamorphism. Shiva, Nantwich, pp. 201-233

Park, A.F., 1983. Lit-par-lit migmatite fabrics in a metagabbro anorthosite complex, Sygnefjell, Jotunheim, South Norway. In Atherton, M.P., Gribble, C.D. (eds.), Migmatites, Melting and Metamorphism. Shiva, Nantwich, p. 296

Poole, W. H., 1971. Graptolites, copper and potassium-argon in Goldenville Formation, Nova Scotia. In Report of Activities, Part A. Geological Survey of Canada, Paper 71-1A, pp. 9-11

Sawyer, E.W., in press, The role of partial melting and fractional crystallization in determining discordant migmatite leucosome composition. submitted to Journal of Petrolgoy., 48 pgs.

Sawyer, E.W. and Barnes, S-J, in press. Composition differences between subsolidus and anatectic migmatite leucosomes. submitted to Journal of Metamorphic Geology

Thompson, A. B., 1982. Dehydration melting of pelitic rocks and the generation of H_2O-undersaturated granitic liquids. American Journal of Science, v. 282, pp. 1567-1595

Weber, C., Barbey, P., Cuney, M. and Martin, H., 1985. Trace element behaviour during migmatitization. Evidence for a complex melt-residuum-fluid interaction in the St. Malo migmatitic dome (France). Contributions to Mineralogy and Petrology, v. 90, pp. 52-62

Weber, C. and Barbey, P., 1986. The role of water, mixing processes and metamorphic fabric in the genesis of the Baume migmatites (Ardeche, France). Contributions to Mineralogy and Petrology, v. 92, pp. 481-491

Woodend [Douma], S. and Hope, T.L., 1986. Geological mapping and igneous and metamorphic petrology, Queen's and Shelburne counties, Nova Scotia. In Current Research, Part A, Geological Survey of Canada, Paper 86-1A, pp. 429-433

Zen, E-an, unpublished, Phase relations of peraluminous granitic rocks and their petrogenetic implications.

Appendix A - Sample Descriptions

This appendix will consist basically of the petrography of the different slides augmented by hand-sample descriptions. The samples will be broken into the following groups: Those containing leucosome/melanosome, granite/psammite/pelite, calc-silicate nodules, and aplite/pegmatite. Of the 58 thin sections made, 35 proved useful in describing the characteristics of the area or providing the chemical data via microprobe analysis and are presented below.

Leucosome/melanosome: There are 11 slides in this group. All of them contain leucosomes and many contain co-existing melanosomes. However, not all of them are clearly formed in the same manner and those noted as leucocratic lenses or "fingers" are often vague, with their origin somewhat questionable.

A-002-1: Taken across contact between pelitic material and large (~5 cm) leucocratic bleb, rimmed with mafics. This sample is very heterogeneous with a number of zones blending into one another, with percentage and distribution of the phases varying greatly.

Host (pelitic): Qtz-plag-biot-musc-sill?

	Avg. dia.(mm)	Shape	Alteration	Extinction
Quartz	0.2-0.5	polygonal	-	normal
Plag.	0.2-0.5	polygonal	weak to mod.	some zoning
Biotite	~0.5	tab. to irreg.	some conv. to sill.?	-
Musc.				

Biotite is common and in some places it defines concordant folding. The fold hinges and surrounding area are very fine grained, with needles of muscovite or sillimanite common. The needles can be found as inclusions in muscovite or in the matrix, often closely associated with both biotite and muscovite. Although generally randomly oriented they can also define the folding. Some of the

muscovites display a helicitic structure with respect to their muscovite inclusions (i.e. S_i is concordant with S_e) indicating post-tectonic muscovites. Most of the biotite grains in the folded zone are altering to needles and many of the more altered grains are cut by secondary(?) biotite and/or muscovite. The matrix material is mostly granoblastic quartz and weak to moderately altered plagioclase. Some plagioclase grains display zonation.

There is a biotite-poor zone between the pelitic material and the mafic rim, composed of semi-granoblastic quartz and plagioclase. The rim itself is an aggregate of interlocking biotite and some muscovite grains. There appear to be two groupings of biotite: A) ragged, altered grains with poor cleavage and pleocroism and B) tabular form with strong cleavage and pleochroism. This could be interpreted as primary altered biotite and fresh, secondary biotite co-existing, but aside from the difference in textures there is little evidence to support it. All of the altered biotites and some of the fresh grains have zircon inclusions with pleochroic haloes.

Leucosome: Qtz-plag-biot

	Avg. dia.(mm)	Shape	Alteration	Extinction
Quartz	~0.05-4	irregular	-	v. slightly und.
Plag.	~2-4	~tabular	weak	-
Biotite	0.5	irregular, embayed	-	-

Some very large (~4 mm) quartz and plagioclase grains adjacent to the rim with grain size reducing dramatically (<1/20 mm) toward the next concordantly folded zone (as defined by biotite). The mineralogy is the same as that in the pelite except for a smaller percentage of mica minerals.

A-004-5: Pelite/psammite contact with leucosomes along boundary (photo 19).

Pelite: Qtz-plag-biot-musc

	Avg. dia.(mm)	Shape	Alteration	Extinction
Quartz	0.15-0.5	irreg., rounded	-	norm. to weakly undulose
Plag.	0.15-0.6	irregular	weak-mod.	
Biotite	~0.15 X 0.5	tab. to irreg.	-	simul. extinct.
Musc.	0.25-1	subhedral to irregular	-	-

The pelite composition varies across the thin section from mostly quartzo-feldspathic to mostly mafic minerals. There are both irregular and polygonal associations of quartz-feldspar. Most of the biotites are unaltered except for a few Zr inclusions. Curiously there are a few biotite grains completely altered to chlorite, but none which are intermediate. Even where chloritized biotite grains are adjacent to unaltered ones, the boundary is sharp. The chloritized grains are often oxidized along the cleavage traces. The biotites display a strong foliation parallel to the contact, while the muscovites are randomly oriented. When the stage is rotated under plane polarized light, the biotites display simultaneous extinction, indicating optical as well as spatial orientation.

Psammite: Qtz-plag-biot-musc

	Avg. dia.(mm)	Shape	Alteration	Extinction
Quartz	0.15-0.5	irreg., rounded	-	norm. to slightly und.
Plag.	0.15-0.5	irreg., rounded	weak	-
Biotite	~0.15 X 0.5	tab. to irreg.		
Musc.	~0.5-1	subhedral to irregular	-	-

The muscovites in the psammite appear to be secondary or late-stage crystallizing. The biotites define a foliation parallel to the contact.

Leucosome: Qtz-plag-biot-musc

	Avg. dia.(mm)	Shape	Alteration	Extinction
Quartz	0.5-2	rounded, irregular	-	normal
Plag.	0.5-1	subhedral	weak	
Biotite	~0.5	irreg., rounded	-	-
Musc.	~0.5	irreg., rounded	-	-

The distinction between psammite and pelite is most easily made by grainsize and percentage of biotite. The psammite is finer grained and has less feldspar and biotite than the pelite. The amount and size of the micaceous minerals in the pelite increases toward the contact. The leucosome itself is an aggregate of mostly larger quartz and plagioclase with considerably less biotite and muscovite than present in the two host lithologies. The plagioclase grains in the leucosome are weakly altered with no visible zonation, while the plagioclases in the pelite are midly to moderately altered.

A-008-3A: Injected leucosomes in pelitic host. Two leucosomes are visible in this slide, one microcline bearing and the other not. Leucosome 2 is finer-grained and contains microcline, more biotite and less muscovite than leucosome 1.

Leucosome 1: Qtz-plag-(biot)-(musc)

	Avg. dia.(mm)	Shape	Alteration	Extinction
Quartz	0.25-4 (~1 avg.)	equant to rounded	-	undulose
Plag.	0.5-2	tabular, irreg. edges	weak to mod.	-
Biotite	0.2-0.5	irregular	some chl., oxd.	-
Musc.	0.25-1	tab., subhedral	-	-

The concentration of biotite is <1% and muscovite is ~3% in this leucosome.

Leucosome 2: Qtz-plag-microcline-biot-musc

	Avg. dia.(mm)	Shape	Alteration	Extinction
Quartz	~1	rounded to irregular	-	v. undulose, some subgrains
Plag.	~1	irreg. to subhedral	weak to mod.	-
Biotite	~0.25	~equant	-	-
Musc.	0.25	subhedral	-	-
Microcl.	0.5-1	subhedral	none, some incl.	-

Host: Qtz-feld-biot-musc

	Avg. dia.(mm)	Shape	Alteration	Extinction
Quartz	0.25-1	~equant	-	undulose
Feldspar	0.25-1	~equant	none to weak	und., some vague poly-twins
Biotite	0.25-0.5	tab. (elong.)	some oxid.	simultaneous
Musc.	0.25-0.5	subhedral	-	-

The biotites in the host all extinguish at the same angle.

A-009-1A: Concordantly folded leucosome with thin, well-defined mafic rim.

Leucosome: Qtz-plag-K spar-biot-musc

	Avg. dia.(mm)	Shape	Alteration	Extinction
Quartz	1-6	irreg. to equant	-	undulose
Plag.	1-6	~lath to irreg.	moderate	-
K-spar	~2	equant, irreg. edges	none	normal
Biotite	~0.5	irregular	oxidizing	-
Muscovite				

The leucosome has a distinct mafic rim along its edge composed of an interlocking aggregate of large (>1mm) biotite and muscovite grains. Within the leucosome itself biotite is rare (<3%).

Host: Qtz-plag-biot-musc

	Avg. dia.(mm)	Shape	Alteration	Extinction
Quartz	0.25-0.6	~equant	-	undulose
Plag.	0.25-0.6	blocky	moderate	-
Biotite	0.25-1	irreg. to blocky	some oxidation	-
Muscovite	1-2	tabular	oxid. along cleavages	-

In the host the biotite percentage is fairly high, compared to the leucosome and the grains are generally randomly oriented in a skeletal

framework filled with small quartz grains and some small plagioclase grains. However, sometimes the mica grains are oriented parallel to the contact rather than randomly.

A-009-1B & C: Mineralogically and texturally the same as A-009-1A except that the mafic rim is not as well developed. In C there seems to be a somewhat higher percentage of plagioclase than in the other two. These samples were taken about 5 cm from A-009-1A.

A-009-4A: Leucocratic zone and edge of strongly foliated, micaceous layer.

Foliated micaceous layer: Qtz-plag-biot-(musc)

	Avg. dia.(mm)	Shape	Alteration	Extinction
Quartz	~1/8-1/2	equant, pinned by micas		undulose
Plag.	~1/8-1/2	equant, pinned by micas	mica incl.	
Biotite	~1/4 X 1	Irr., shredded		
Muscovite	~1/16 X 1/4			

The biotites are all elongate, define a strong foliation and extinguish simultaneously, indicating alignment of optical axes. The muscovite is generally very small and closely associated with the biotite. The felsic minerals are all pinned by the mica framework and appear to be recrystallized. The feldspars often have inclusions of biotite or small, shredded and highly birefrigent minerals (muscovite?). The contact between this unit and the next is a semi-continuous sheet of larger, more elongate biotites (note, hand sample broke along the foliation plane defined by this border). These biotite crystals are also aligned optically. On the other side of the contact is a heterogeneous zone of pelite which has been injected and contorted. Zones of coarse (1-2 mm) quartz, plagioclase and mica grains and wholly micaceous layers of very large (2-6mm) muscovite crystals with biotite "stringers" surrounding them.

Heterogeneous zone: Qtz-plag-biot-musc

	Avg. dia.(mm)	Shape	Alteration	Extinction
Quartz	1-4	~equant	-	undulose
Plag.	1-3	~equant	weak-strong musc.(?) incl.	-
Biotite	0.25-1	long stringer or tabular	some oxidation	-
Muscovite	0.25-2	mostly irreg.	-	-

A-009-4B: Very heterogeneous with what appears to be a paired neosome (see figure 5). The leucosome is made up mostly of quartz and plagioclase, both averaging 1/2-1 mm, with rare, poorly formed biotites. The melanosome is composed of large (2 X 4 mm) muscovite crystals with interlocked biotite grains, mostly along the grain boundaries.

Leucosome: Qtz-plag-microcline-biot-musc

	Avg. dia.(mm)	Shape	Alteration	Extinction
Quartz	0.5-2	equant	-	undulose
Plag.	0.5-1	equant, blocky	weak to mod.	-
Microcl.	~1-2	equant(square) to irregular	none	-
Biotite	<0.5	irreg., ragged	chl. and oxid. rims	-
Muscovite	~0.5	irregular	-	-

The leucosome is weakly rimmed with mafics. Biotite and muscovite together make up less than 5% of the components. Some quartz-quartz contacts are sutured and one plagioclase grain was noted to be enclosed by microcline.

A-009-5A: Rimmed leucosome in psammite (see photo 21).

Leucosome: Qtz-plag-biot-musc-K spar

	Avg. dia.(mm)	Shape	Alteration	Extinction
Quartz	~1	~equant	-	undulose, some sub-grains
Plag.	0.25-1	subhdrl laths	mod. interst. alteration	uniform
Biotite	<0.5	rounded	some oxid.	poor pleochroism
Muscovite	0.5-1	irregular	none	
K spar	~1	~equant	weak, mostly conc. along cleavages	

Muscovite occurs both in the leucosome and along plagioclase cleavage planes. The diameter of the quartz grains increases from one side of the leucosome to the other, with the smallest being along the less well defined rim. The leucosome in general shows disequilibrium in terms of feldspar alteration and mineral contacts.

Host: Qtz-feld-biot-musc

	Avg. dia.(mm)	Shape	Alteration	Extinction
Quartz	~0.25-0.5	equant	minor along fractures	undulose, some subgrains
Feldspar	~0.25-0.5	equant	weak	
Biotite	<0.25	blocky to irreg., elongate	some chlorite	
Muscovite	~0.25	irreg, often elongate		

The biotite is mostly concentrated along the leucosome and defines a fabric parallel to the contact. The muscovite appears to be secondary as it is not influenced by the fabric and grows around grain boundaries.

The biotites in the rim itself are mostly elongate and define a fabric, with small, pinned quartz and feldspar crystals growing between grains.

A-009-5B: Psammite with lone leucocratic lenses. The psammite is mostly quartz and biotite with muscovite and some feldspar, particularly plagioclase.

Psammite: Qtz-feld-biot-musc

	Avg. dia.(mm)	Shape	Alteration	Extinction
Quartz	~0.2	polygonal	some incl. of biotite	uniform to undulose
Feld.	~0.2	polygonal	none to weak	
Biotite	~0.33	blocky and elongate	some chlorite	
Muscovite	~0.5	subhedral	none	

As in A-009-5A, the muscovite here appears to be secondary. It is difficult to determine relative proportions of quartz to feldspar in this slide as they both have the same birefringence, grain size and are

mostly unaltered. Also, the polysynthetic twins of the plagioclase crystals are rather vague and are only noticeable under higher magnifications.

The leucocratic lenses appear as vague, commonly aligned "fingers" or zones consisting of relatively large (~0.5mm) quartz and muscovite crystals. The quartz grains show a strong undulose extiction. The leucocratic fingers are defined by larger grain size and lack of biotite.

D-001-2: Leucocratic lenses in psammite

	Leucosome: Qtz-plag-biot-musc			
	Avg. dia.(mm)	Shape	Alteration	Extinction
Quartz	0.5	equant to polygonal	-	normal
Plag.	0.5	equant, ~blocky	none to weak	-
Biotite	~0.25	irreg.	some chl. and rim oxides	-
Muscovite	0.25-1	irregular	-	-

The leucosome is distinguished from the psammite by a slightly larger grain size and substantially lower percentage of biotite (<5% vs. ~20%). Muscovites appear fresh and secondary, many of the quartz-quartz contacts are sutured.

	Psammite: Qtz-plag-biot-musc			
	Avg. dia.(mm)	Shape	Alteration	Extinction
Quartz	0.25	equant to polygonal	-	~undulose
Plag.	0.5	equant to blocky	weak to mod.	-
Biotite	0.25	irreg, elong	some oxididation	-
Muscovite	0.25-1	irregular	-	-

The biotite grains define a foliation and tend to extinguish simultaneously when rotated under PPL. Muscovite grains are often randomly oriented with respect to the foliation and constitute ~5% of the unit.

D-001-3A: Rimmed leucosome in psammite

Leucosome: Qtz-plag-microcline-biot-musc

	Avg. dia.(mm)	Shape	Alteration	Extinction
Quartz	0.5-2.5	equant to polygonal	-	normal
Plag.	0.5	equant	weak to mod.	-
Microcl.	~1	equant	none to weak	-
Feldspar	~1	equant	weak	-

Biotite and muscovite are very minor components (<1%) and appear to be in disequilibrium. Biotite is all converting to chlorite or oxidizing. The muscovites have very irregular outlines.

Psammite: Qtz-plag-biot-musc

	Avg. dia.(mm)	Shape	Alteration	Extinction
Quartz	0.25	equant	-	undulose to sub-grain
Plag.	0.25	equant, blocky	none to weak	-
Biotite	0.1-0.5	irreg, elong.	oxid. rims	-
Muscovite	~0.5	irregular	-	-

Muscovite is rare in the psammite, except along the border of the leucosome. This sample displays the typical recrystallized texture found in most of the psammites.

D-002-2B: Psammite with a rimless leucosome, probably injection.

Psammite: Qtz-plag-biot-musc

	Avg. dia.(mm)	Shape	Alteration	Extinction
Quartz	0.1-1	equant	-	undulose
Plag.	0.1-1	equant, blocky	weak to mod.	-
Biotite	0.25	irreg, elong.	oxid. rims	simult. ext.
Muscovite	~0.5	irregular	-	-

The leucosome is coarse grained (~2-4 mm average), with weak to moderately altered plagioclase (often showing hypidiomorphic zonation). Biotites are concentrated in aggregates, many of the grains strongly oxidized with some chlorite alteration and Zr inclusions.

Granite/psammite/pelite: There are 9 slides in this group, most of which are part of major contacts between the lithologies. However, there are also some granitic veins in host which have been placed here because they could be traced to a plutonic origin.

A-001-1: Granitic vein intruding psammite.

Granite: Qtz-plag-biot

	Avg. dia.(mm)	Shape	Alteration	Extinction
Quartz	~2	equant	-	undulose
Plag.	~2		mod.-strong	zoned
Biotite	0.25-1	irregular	oxid., Zr inclusions	

Some hypidiomorphically zoned plagioclase noted. Scalloped contacts common and muscovite inclusions often found in plagioclase.

Psammite: Qtz-plag-biot

	Avg. dia.(mm)	Shape	Alteration	Extinction
Quartz	~0.5	equant/polygonal	-	undulose
Plag.	~0.15-1	equant/polyg.	weak-mod.	
Biotite	0.15-1	somewhat elongate	some Zr incl.	-

In addition to the usual recrystallized texture this psammite also displays some coarser-grained quartz-plagioclase aggregates.

A-002-2: Contact between psammite and pelite lithologies.

Psammite 1: Qtz-plag-(biot)

	Avg. dia.(mm)	Shape	Alteration	Extinction
Quartz	0.25	equant/polygonal	-	normal
Plag.	0.25	equant/polyg.	weak	-
Biotite	0.15-0.5	irreg.	some oxid.	-

Psammite 2: Qtz-plag-biot

	Avg. dia.(mm)	Shape	Alteration	Extinction
Quartz	~0.5	equant/polygonal	-	normal
Plag.	~0.5	equant/polyg.	none	-
Biotite	~0.25	irreg./blocky	some opaques	-

This appears to be a contact between two slightly different sub-lithologies of the Goldenville psammite unit. Psammite 2 has a somewhat coarser average grain size. The mineralogy of both is mostly quartz and plagioclase, with these felsic minerals occurring in a granoblastic aggregate. Psammite 1 has ~3% biotite while psammite 2 has ~15%.

A-002-4: Contact between psammite and pelite lithologies.

Psammite: Qtz-plag-biot-(musc)

	Avg. dia.(mm)	Shape	Alteration	Extinction
Quartz	~0.33	equant	-	none
Plag.	~0.33	equant	weak	-
Biotite	~0.33	elongate	some oxidation	-
Muscovite	~1	subhedral	-	-

The muscovite is found in close association with biotite, with the biotite defining a foliation. The quartz and plagioclase crystals also tend to have a long axis also oriented in the foliation direction.

Pelite: Qtz-plag-biot-musc

	Avg. dia.(mm)	Shape	Alteration	Extinction
Quartz	~0.5	equant	-	norm. to weakly undulose
Plag.	~0.5	irreg. to subhedral	weak	-
Biotite	0.5-2	irreg./elong.	some oxid.	-
Muscovite	~1	subhedral	mod. along cleav.	-

The contact appears to mark a zone of shearing and recrystallization. There are a number of contact-parallel tufts of very fine-grained and elongate "threads" of biotite (see figure XX). Within these tufts can also be seen aggregates of fine grained, recrystallized quartz and feldspar. Both the biotites in the tufts and those in the pelite have Zr inclusion with pleochroic rims. The feldspar grains within the tufts tend to be strongly altered while those in the pelite show weak alteration and irregular grain shape.

A-004-2A: Contact between granite vein and mafic (pelite?).

Granite: Qtz-plag-biot-musc

	Avg. dia.(mm)	Shape	Alteration	Extinction
Quartz	0.5-2	irregular	-	
Plag.	0.5-2	subhedral		zoned
Biotite		elongate and blocky	minor chl. and oxide	
Muscovite	~0.25	subhedral or needles	-	-

The muscovite is mostly associated with biotite or as secondary

intergrowths along plagioclase cleavage planes. Some highly birefringent needles seen associated with muscovite (sillimanite?).

Mafic: Qtz-plag-biot-musc

	Avg. dia.(mm)	Shape	Alteration	Extinction
Quartz	0.2	~polygonal	-	normal
Plag.	0.2	~polyg/blocky	mod.-strong	-
Biotite	0.2-0.6	irreg. to tabular	Zr inclusions	-
Muscovite	0.2-0.6	irreg. to tabular	-	-

Quartz and plagioclase are mostly recrystallized (polygonal texture) and pinned by the micas, which define a rough foliation parallel to the contact. The size and percentage of biotite grains increases away from the contact.

A-004-2B: Same granite vein as described in A-004-2A with a psammite contact.

Psammite: Qtz-feld-biot-musc

	Avg. dia.(mm)	Shape	Alteration	Extinction
Quartz	0.2	equant	-	normal
Plag.	0.2	equant	clear	some zoning
Biotite	0.25	irreg. to tabular	some oxd., rare chlorite	most simult.
Muscovite	0.2-0.5	irreg. to tabular	-	-

Some indistinct leucocratic "fingers" noted in the psammite, parallel to the contact. Are defined by slightly greater grain size and lack of biotite. This sample of the granite contains some chloritized biotites, not noted in the last.

A-005-2: Psammite host lithology intruded by a granitic vein.

Granite: Qtz-plag-microcline-biot-musc

	Avg. dia.(mm)	Shape	Alteration	Extinction
Quartz	0.5-2	equant with irreg. contact	-	mod. undulose
Plag.	1-2	irregular	strong	-
Microcl.	1-2	blocky, irregular	none to weak	-
Biotite	0.15-0.5	irregular	converting to chl. and musc.	-
Musc.	~0.5	irregular	-	-

Some plagioclase found with highly birefringent interstitial phase (muscovite?) forming very irregular "blebs". The K-feldspar is also strongly altering with some intergrowths of muscovite growing interstitially. Commonly observe a narrow, less birefringent rim around quartz grains (section is thick). Muscovite is strongly embayed to fairly well-formed crystals and is often associated with biotite or plagioclase.

Psammite: Qtz-feld-biot

	Avg. dia.(mm)	Shape	Alteration	Extinction
Quartz	0.2	equant, rounded	-	none to weakly undulose
Feldspar	0.2	equant, rounded	weak	-
Biotite	0.15	blocky to irregular	weak oxd. on rims	most simult.

Quartz is the major felsic component with a seriate texture and often have low birefringent rims. The biotites define a foliation parallel to the contact. Muscovite is very rare and concentrated near the contact and altering (to clays?).

A-008-4A: Pelite with numerous granitic injections and leucosomes.

Granite: Qtz-plag-K-spar-biot-musc

	Avg. dia.(mm)	Shape	Alteration	Extinction
Quartz	~2	irregular	-	strong undulose
Plag.	1-2	irregular	mod.-strong, musc. intergrowth	-
K-spar	2	rounded to irregular	-	-
Biotite	1	irregular	common incipient oxidation	-
Muscovite	0.25-1	tabular to irregular	-	-

The granite is altering and shows a strong disequilibrium fabric. Muscovite occurs as individual porphyroblasts or (more commonly) associated with plagioclase or biotite. Sometimes muscovite also occurs as a fibrous aggregate around crystal contacts.

The border between the granite and the pelitic zone is a solid interwoven biotite aggregate with some porphyroblasts in the aggregate as well as smaller crystals of quartz and feldspar.

Leucosome: Qtz-plag-feld-(biot)-(musc)

	Avg. dia.(mm)	Shape	Alteration	Extinction
Quartz	~2	irregular	-	strong und. to subgrain
Plag.	~1	blocky	mod. along cleavage	-
Feldspar	~1	equant	mod. interstitial	-
Biotite	~1	irreg to bent	Zr incl, mildly oxd. rims	-
Muscovite	~0.5	tabular	-	-

The leucosome occurs as a leucocratic lens in the pelitic material. It can be discriminated from the granite by its generally less-altered appearance and lower percentage of mica. There appears to be some mixing between the pelitic material and the leucosome.

A-009-4D: Contact between the granite and psammite.

Granite: Qtz-plag-microcl-biot-musc

	Avg. dia.(mm)	Shape	Alteration	Extinction
Quartz	1-2	equant/rounded	-	mod. to strongly undulose
Plag.	1-2 X 4	tabular with irreg. contacts	weak to mod.	-
Microcl.	0.5-2	equant/blocky	none, some incl.	-
Biotite	0.5-1	irregular	some chl., Zr and oxd. rims	-
Muscovite	~0.5	long X-cutting to squat, blocky intergrowths	-	-

The quartz and plagioclase occur in a roughly equigranular aggregate with scattered, blocky biotite and rare muscovite. Idiomorphic zonation common found in some plagioclases and exsolution noted in one microcline. Quartz is small (recrystallized) to large grains, often with lobate boundaries. Plagioclase noted with muscovite intergrowths. Microcline observed with interstitial plagioclase that in turn contains interstitial muscovite.

Psammite: Qtz-plag-microcl-biot

	Avg. dia.(mm)	Shape	Alteration	Extinction
Quartz	0.25	equant, rounded	-	weak to strongly undulose
Plag.	0.25	equant/blocky	weak to mod.	-
Microcl.				
Biotite	0.25	elongate/tab.	oxdidation	simult. extinct.

This psammite contains microcline, unlike the other samples. Muscovite very rare and probably secondary, cutting other grains. The phases microcline and plagioclase are approximately 10-15% and 5% respectively. The psammite has a lower percentage of plagioclase and the biotites are roughly aligned parallel to the contact.

C-001-2A: Contact between the granite and pelite lithologies.

Granite: Qtz-plag-biot

	Avg. dia.(mm)	Shape	Alteration	Extinction
Quartz	1-1.5	rounded	-	weakly undulose
Plag.	1-1.5	blocky	cores mod. altered	zoned
Biotite	~1	tab.-irreg.	Zr incl., minor oxd. rims	-

The granite contains idiomophically zoned plagioclase crystals. Some plagioclases also have biotite inclusions and/or muscovite intergrowths. Muscovite is a minor phase, usually tabular and ~0.25 mm in diameter. Some intergranular quartz found at the contact, usually <0.25 mm average diameter.

The contact between the two lithologies is a solid biotite intergrowth which defines a foliation plane. The biotites are peppered with small (~0.001 mm), highly birefringent, blocky grains that do not have pleochroic haloes surrounding them. Into the pelite the muscovite content increases substantially with little quartz or feldspar. The biotites and muscovites tend to be weakly to moderately oxidixed with the muscovite cleavages particularly susceptible.

C-002-1: Contact between granite body and imbedded xenolith.

Granite: Qtz-plag-biot-musc

	Avg. dia.(mm)	Shape	Alteration	Extinction
Quartz	1.5	equant	-	mod. undulose
Plag.	2	blocky/ subhedral	mod. to strong	-
Biotite	0.5-1	irreg/tab.	mod. oxd. along rims and cleavage	-
Muscovite	0.25	tabular/irreg	-	-

The granite phase is very similar to that of C-001-2A. Plagioclase commonly has muscovite intergrowths.

Xenolith: Biot-musc

	Avg. dia.(mm)	Shape	Alteration	Extinction
Biotite	0.5 X 1	elongate/tab.	weak oxd. along cleavage	-
Muscovite	1 X 3	elongate/ ragged	mod. to strong oxd. along cleavages and rim	-

The ratio of biotite to muscovite is about 1:2, with the muscovites occurring as porphyroblasts and the biotites filling the space between grains. Muscovite is commonly oxidized along the cleavages. Except for a couple of inclusions, there is almost no quartz or feldspar in this xenolith.

Calc-silicate nodules: There are 7 slides in this series. Generally their mineralogy consists of some sub-group of the following: quartz-calcite-garnet-biotite-potassium feldspar-amphibole. The only phases that always occur are quartz, feldspar and biotite, with the other phases which ovccur varying from one nodule to another. All the nodules showed a seriate, semi-granoblastic texture and signs of being in disequilibrium.

A-002-6: Quartz grains show a seriate to polygonally recrystallized texture. Biotites are mostly irregular, embayed and oxidizing. Garnets are also strongly embayed, often with only fragments of the original crystal left. Amphibole shows a similar

disequilibrium texture, but to a lesser degree. There is a yellow-brown-orange discolouration visible along many grain boundaries.

Calc-silicate nodule: Qtz-plag-biot-gnt-amph

	Avg. dia.(mm)	Shape	Alteration	Extinction
Quartz	0.05-1	polyg to equant	-	normal
Plag.	0.1	blocky/equant	none to weak	-
Biotite	~0.5 X 1	v. embayed	oxidized	-
Garnet	~0.5-1	v. embayed, relict frag.'s	-	-
Amphibole	~1	embayed, relict fragments	-	-

Biotites are almost all replaced by pennite.

A-004-1:

Calc-silicate nodule: Qtz-feld-pennite-(biot)-gnt

	Avg. dia.(mm)	Shape	Alteration	Extinction
Quartz	0.1-0.5	equant	-	normal
Feldspar	~0.2	equant	none to weak	-
Biotite	0.3	irregular	converting to chlorite	-
Pennite	0.2	irregular	-	-
Garnet	0.2-0.5	rounded, relict	often has qtz inclusions	-

Biotite was ~15-20%, but almost all grains have reverted to pennite. The quartz defines a seriate texture and some muscovite is present as irregular grains. Garnets often encompass small, rounded quartz grains.

A-005-1:

Calc-silicate nodule: Qtz-plag-gnt-chl

	Avg. dia.(mm)	Shape	Alteration	Extinction
Quartz	0.2-0.8	equant	-	normal to weakly und.
Plag.	0.3	irreg/tabular	weak interstitial	-
Garnet	~0.2	round	some narrow, opaque rims	-
Chlorite	~0.5	very irregular	-	-

The chlorite is pennite and appears to have completely replaced the biotite. The quartz grains all display a seriate texture ranging from sub-microscopic to ~1mm in diameter.

A-008-1: The thin section of this nodule is split into two zones, garnet and biotite. The latter has >50% biotite and possibly amphibole occuring as very large crystals (~2 mm) which are pokiloblastic. The biotite are riddled with inclusions and fragmentary with some altering to an opaque phase. Each relict grain of biotite is ~2 mm in diameter. Almost no garnet is found in this zone. Large opaques with sharp boundaries often associated with biotite.

Calc-silicate nodule (bt zone): Biotite-quartz-plag

	Avg. dia.(mm)	Shape	Alteration	Extinction
Biotite	~2	pokiloblastic, very embayed	some oxidation	-
Quartz	0.4	equant	-	none to weakly undulose
Plag.	0.2-0.4	blocky	weak to mod.	-
Opaque(3%)	~0.3	blocky to irregular	-	-

The garnet zone is almost completely devoid of biotite (~3%) and is mostly equant quartz and plagioclase crystals with ~5% irregular garnet grains, often containing inclusions. The garnets average ~0.33 mm in diameter.

Calc-silicate nodule (gnt zone): Qtz-plag-gnt-biot

	Avg. dia.(mm)	Shape	Alteration	Extinction
Quartz	0.1-0.3	equant	-	weakly und.
Plag.	0.05-0.3	blocky	mildly	-
Garnet	0.2-0.3	round	qtz incls, garnets often relict	-
Biotite	0.05 X 0.3	elongate/tab.	some chl., oxd.	-

A-009-6: The quartz and plagioclase in this sample display a seriate texture. No garnet or amphibole were noted in the slide.

Calc-silicate nodule: Qtz-plag-biot

	Avg. dia.(mm)	Shape	Alteration	Extinction
Quartz	~0.25-0.5	equant	-	weak to mod. undulose
Plag.	<1/8	equant	weak-mod.	-
Biotite	<0.5 or >1	blocky-jagged	most xtals oxidized	-

Aplite/Mafic: This phase is mostly discriminated from other, granitic phases by its low biotite content and finer grain-size. It tends to cut all other phases and is often associated with pegmatites.

A-003-1A: Biotite is either completely chloritized or occurs as rare, fresh grains (secondary?).

Aplite: Qtz-plag-(biot)

	Avg. dia.(mm)	Shape	Alteration	Extinction
Quartz	~0.5-2	equant	-	mod. undulose
Plag.	~0.25-0.5	blocky/irreg.	clear-weak	-
Biotite	~0.25	rounded, equant	chloritized	-

Along the contact with the mafic zone there are regions of very fine grained (0.25-0.332mm) quartzo-feldspathic aggregates. Biotite occurs in the mafic zone as either small (<0.5 mm) aggregates of grains and laths to solid, interlocking biotite networks (with average grains 2-3 mm).

Mafic zone: Biot-quartz-plag

	Avg. dia.(mm)	Shape	Alteration	Extinction
Biotite	<0.5,2-3	tabular	oxidizing	-
Quartz	0.03-0.25	equant	-	?
Plag.	0.03-0.25	equant	?	?

The biotites occur either as altered grains, defining a strong foliation, or as fresh grains that are randomly oriented, implying secondary growth of biotite. The zone has a very fine grained (<0.03 mm) matrix of what appears to be quartz and feldspar.

A-003-1B: This aplite similar to last (and located nearby). The average grain size is somewhat smaller (average ~0.33 mm, ranging from 0.06-1 mm). An unusual vein runs perpendicular to the aplite (in outcrop) which petrographic study reveals to be composed almost entirely of very coarse grained (~2-7 mm), deforming (strongly

undulose, showing subgrains) quartz crystals. These quartz crystals commonly contain small (~0.25 mm) plagioclase inclusions.

Aplite: Qtz-plag-biot

	Avg. dia.(mm)	Shape	Alteration	Extinction
Quartz	0.2-1	irreg. to equant	-	none to mod.
Plag.	~0.5	columnar/ blocky	moderate	-
Biotite	0.15	lathlike	reverting to chlorite	-

A-003-2A: Contact between felsic and mafic components of aplite dyke.

Felsic: Qtz-plag-(biot)

	Avg. dia.(mm)	Shape	Alteration	Extinction
Quartz	0.2-1	irreg. to equant	-	none to mod.
Plag.	0.5	blocky, irregular	weak	-
Biotite	~0.33	ragged or blocky with diffuse edges	-	-

A yellowish-orange discolouration permeates the grain boundaries as well as fractures within individual crystals. There is a fairly sharp boundary between the felsic and mafic zones, the grain size in the felsic tending to decrease towards the contact.

Mafic Zone: Biot-qtz-plag

	Avg. dia.(mm)	Shape	Alteration	Extinction
Biotite	0.05 X 0.25 to 0.25 X 2	needles	-	-
Quartz	~0.05	equant	-	normal
Plag.	~0.05	equant	weak?	-

Essentially similar to the mafic zone of A-003-1, except that the biotite aggregates are smaller. A large proportion of the biotite here occurs as needles that are randomly oriented on the scale of the thin section, but when adjacent grains are studied they are noted to be more or less parallel.

D-002-1:

Aplite: Qtz-plag-biot

	Avg. dia.(mm)	Shape	Alteration	Extinction
Quartz	0.1-2	irregular	-	mod. to strongly undulose
Plag.	0.5	blocky/irreg	none to weak	-
Biotite	0.15	irregular	oxd. rims	-

The grain contacts in this slide are generally very irregular. There are obvious signs of deformation (undulose quartz, lobate textures in quartz and feldspars and sutured grain contacts). Minor muscovite is present both as grains and as secondary intergrowths within plagioclase. The mafic zone is similar to A-003-2.

D-002-3:

Aplite: Qtz-plag-microcl-biot-musc

	Avg. dia.(mm)	Shape	Alteration	Extinction
Quartz	0.2-2	equant	-	strongly und.
Plag.	0.2-2	equant/blocky	weak to mod.	-
Microcl.	~0.5	blocky	some musc. intergrowths	-
Biotite	0.25	blocky to irregular	oxidizing	-
Muscovite	0.5	irreg. to subhedral	-	-

This aplite displays a granoblastic texture and an unusually high microcline content. The muscovite percentage is also unusually high, ranging from 3-5%.

Appendix B - Microprobe data

This appendix is broken into two parts, one section where the analyses for each unit on a slide were averaged and then presented by unit, the other with the raw results by slide. For more information on the microprobe in general, see Appendix C.

Biotite Averages

	Granite			Psammite			
Oxide	A-004-2B	A-005-2	C-002-1	A-004-2B	A-005-2	A-002-4	C-002-1
SiO2	35.27	35.16	35.08	35.14	35.07	34.97	35.25
TiO2	2.94	2.94	2.11	3.29	2.71	2.25	2.46
Al2O3	19.25	17.53	19.21	19.01	17.72	19.58	18.99
FeO	19.12	21.89	19.64	19.60	21.86	19.70	18.99
MnO	0.23	0.32	0.20	0.21	0.36	0.27	0.28
MgO	8.73	7.51	8.90	8.26	7.67	8.58	8.69
CaO	0.00	.00	0.00	.00	0.01	.00	0.00
Na2O	0.05	0.06	0.06	0.12	0.08	0.14	0.10
K2O	9.81	9.60	9.44	9.73	9.61	8.94	9.52
Cl	0.04	0.05	0.05	0.04	0.04	0.06	0.03
F	0.78	0.42	0.68	0.56	0.52	0.66	0.65
Total	96.20	95.47	95.36	95.97	95.63	95.14	94.96
FeO/MgO	0.46	0.34	0.45	0.42	0.35	0.44	0.46

Biotite Averages

	Leucosome						Aplite	Melanosome			
Oxide	A-009-1A	A-009-5A	A-8-3A/1	A-8-3A/2	D-001-3A	A-009-1B	A-003-1A	A-009-1A	A-009-5A	D-001-3A	A-009-1B
SiO2	35.39	35.18	35.75	35.54	35.31	34.81	36.42	35.10	35.04	35.28	34.40
TiO2	2.58	3.12	2.72	2.69	3.14	2.75	2.64	2.57	2.65	3.05	2.66
Al2O3	18.55	18.46	17.97	18.39	17.61	18.98	16.90	17.79	18.26	17.98	18.38
FeO	20.98	20.65	21.23	20.79	21.45	19.73	15.49	17.63	21.41	21.52	20.67
MnO	0.37	0.23	0.44	0.42	0.25	0.15	0.28	0.27	0.24	0.17	0.25
MgO	8.19	8.05	8.25	8.16	8.00	7.97	12.31	10.54	8.17	8.09	8.03
CaO	0.01	0.01	0.02	0.01	0.00	0.00	0.00	0.00	0.02	0.00	0.00
Na2O	0.15	0.09	0.19	0.03	0.00	0.02	0.00	0.00	0.12	0.01	0.00
K2O	9.29	9.21	9.29	9.21	9.83	9.78	9.70	9.59	9.43	9.99	9.72
Cl	0.02	.00	0.01	.00	-	0.03	0.05	0.06	0.01	-	0.03
F	0.10	0.00	0.15	0.27	-	0.40	0.62	0.41	0.03	-	0.53
Total	95.64	95.00	96.00	95.51	95.58	94.63	94.39	93.94	95.37	96.08	94.72
FeO/MgO	0.39	0.39	0.39	0.39	0.37	0.40	0.79	0.60	0.38	0.38	0.39

Plagioclase Averages

	Granite			Psammite				
Oxide	A-004-2B	A-005-2	C-002-1	A-008-4A	A-004-2B	A-005-2	A-002-4	D-002-2B
SiO2	61.44	64.69	61.41	63.20	62.70	65.49	63.84	61.64
TiO2	0.00	0.00	0.00	0.00	0.00	0.00	0.00	0.00
Al2O3	23.46	22.49	24.23	22.85	22.94	22.02	23.30	23.69
FeO	0.09	0.13	0.16	0.25	0.10	0.18	0.16	0.26
MnO	0.00	0.00	0.00	0.00	0.00	0.00	0.00	0.00
MgO	0.03	0.02	0.03	0.06	0.03	0.03	0.03	0.06
CaO	5.62	3.16	5.22	4.44	4.95	2.63	4.07	5.41
Na2O	8.70	10.60	9.14	9.35	9.20	10.49	9.82	8.47
K2O	0.17	0.23	0.23	0.17	0.12	0.11	0.10	0.18
Total	99.51	101.32	100.42	100.32	100.04	100.94	101.30	99.71
An content	41	25	38	34	37	22	31	41

Plagioclase Averages

	Leucosome										Aplite	Pelite
Oxide	A-009-1A	A-009-5A	A-8-3A/1	A-8-3A/2	D-001-3A	A-009-1B	A-8-4B/1	A-8-4B/2	D-002-2B	A-004-5	A-003-1A	A-002-4
SiO2	63.35	62.63	62.75	62.45	63.66	62.97	63.33	63.21	61.96	63.23	57.33	63.73
TiO2	0.00	0.00	0.00	0.00	0.00	0.00	0.00	0.00	0.00	0.00	0.00	0.00
Al2O3	22.41	22.75	23.02	23.00	22.04	23.56	22.47	22.58	23.68	22.58	27.57	23.17
FeO	0.12	0.07	0.11	0.12	0.10	0.14	0.21	0.19	0.21	0.19	0.16	0.21
MnO	0.00	0.00	0.00	0.00	0.00	0.00	0.00	0.00	0.00	0.00	0.00	0.00
MgO	0.04	0.02	0.03	0.02	0.02	0.03	0.05	0.06	0.06	0.06	0.03	0.03
CaO	4.16	4.77	4.91	4.58	3.95	4.34	4.01	4.16	5.49	3.83	9.04	3.87
Na2O	9.19	9.23	8.75	9.00	9.44	9.60	9.37	9.42	8.50	9.55	5.93	9.91
K2O	0.25	0.23	0.15	0.29	0.18	0.20	0.18	0.17	0.24	0.15	0.14	0.11
Total	99.51	99.70	99.71	99.45	99.39	100.83	99.62	99.79	100.14	99.59	100.19	101.03
An content	33	36	38	36	31	33	32	33	41	31	62	30

Muscovite Averages

	Granite			Psammite			Leucosome				
Oxide	A-004-2B	A-005-2	C-002-1	A-004-2B	A-002-4	A-005-2	A-009-5A	A-8-3A/1	A-8-3A/2	A-009-1A	A-008-4B
SiO2	44.26	46.31	47.14	46.85	46.68	46.81	47.30	46.92	47.31	47.28	45.84
TiO2	1.32	0.62	0.31	1.31	0.56	1.23	0.90	1.09	1.16	0.72	0.63
Al2O3	32.30	33.02	36.10	36.27	37.17	32.05	34.11	35.50	35.43	36.19	36.18
FeO	6.27	3.30	1.52	1.46	1.21	3.04	1.90	1.39	1.44	1.43	1.55
MnO	0.09	0.02	0.02	0.00	0.02	0.03	0.00	0.00	0.00	0.00	0.00
MgO	2.70	1.28	1.01	0.63	0.61	1.41	1.09	0.73	0.70	0.75	0.68
CaO	0.02	0.01	0.02	0.02	0.01	0.01	0.01	0.02	0.01	0.01	0.01
Na2O	0.58	0.35	0.53	0.68	1.22	0.31	0.41	0.52	0.48	0.56	0.70
K2O	9.10	11.30	10.85	9.94	9.09	11.28	10.65	10.44	10.58	10.11	10.80
Total	96.62	96.20	97.48	97.15	96.56	96.17	96.35	96.60	97.10	97.05	96.40
FeO/MgO	2.3	2.6	1.5	2.3	2.0	2.2	1.7	1.9	2.1	1.9	2.3

Muscovite Averages

	Melanosome			Host				
Oxide	A-009-5A	A-009-1A	A-008-4B	A-008-4B	A-009-1A	A-009-5A	A-008-3A	D-001-3A
SiO2	46.55	46.95	47.08	46.20	46.25	47.08	46.75	46.87
TiO2	1.18	0.85	0.69	0.79	0.92	1.39	1.22	1.42
Al2O3	35.38	36.70	36.56	35.99	36.66	35.50	35.61	35.52
FeO	1.50	1.37	1.50	1.48	1.38	1.48	1.44	2.15
MnO	0.00	0.06	0.02	.00	0.00	0.00	0.00	.00
MgO	0.74	0.70	0.67	0.70	0.70	0.70	0.70	0.75
CaO	0.02	0.02	0.01	.00	0.01	0.01	0.01	0.03
Na2O	0.53	0.60	0.67	0.70	0.58	0.51	0.56	0.49
K2O	10.30	10.07	10.87	11.06	10.05	10.50	10.51	10.91
Total	96.21	97.31	98.06	96.92	96.55	97.17	96.80	98.14
FeO/MgO	2.0	2.0	2.2	2.1	2.0	2.1	2.1	2.9

Slide No.:A-004-2B Analysis: Biotite

	#1 BA		#2 BB		#3 BC		#4 BD	
Oxides	(Psam/Rim)	(Psam/Core)	(Psam/Rim)	(Psam/Core)	(Psam/Rim)	(Psam/Core)	(Psam/Rim)	(Psam/Core)
SiO2	35.48	35.09	35.22	35.38	34.89	34.65	35.27	35.13
TiO2	3.21	3.10	3.67	3.34	3.17	3.27	3.35	3.21
Al2O3	18.80	19.15	18.98	18.71	18.51	19.31	19.63	19.02
Cr2O3	0.00	0.00	0.00	0.00	0.00	0.00	0.00	0.00
FeO	19.98	19.67	19.44	19.51	20.54	19.48	18.38	19.83
NiO	0.00	0.00	0.00	0.00	0.00	0.00	0.00	0.00
MnO	0.16	0.16	0.14	0.21	0.23	0.30	0.21	0.25
MgO	8.28	8.40	7.88	8.35	8.34	8.45	8.30	8.10
CaO	0.00	0.00	0.00	0.00	0.02	0.00	0.00	0.00
Na2O	0.00	0.44	0.00	0.45	0.08	0.00	0.00	0.00
K2O	9.60	9.78	9.82	9.81	9.74	9.58	9.82	9.72
Cl	0.06	0.02	0.03	0.02	0.03	0.05	0.04	0.04
F	1.28	0.80	0.00	0.80	0.80	0.00	0.81	0.00
Total:	96.85	96.61	95.18	96.58	96.35	95.09	95.81	95.30
X-Pos:	49.58	49.51	54.30	54.35	57.84	57.77	61.89	61.86

Slide No.:A-004-2B Analysis: Biotite

	#5 BE		#6 BF		#7 BG		#8 BH	
Oxides	(Gran./Rim)	(Gran./Core)	(Gran./Rim)	(Gran./Core)	(Gran./Rim)	(Gran./Core)	(Gran./Rim)	(Gran./Core)
SiO2	35.14	35.41	35.01	34.89	35.17	35.20	35.71	35.63
TiO2	3.02	2.91	3.02	2.71	2.99	2.86	3.16	2.84
Al2O3	18.83	19.13	18.55	19.23	19.78	18.91	20.07	19.46
Cr2O3	0.00	0.00	0.00	0.00	0.00	0.00	0.00	0.00
FeO	18.91	19.59	19.61	19.34	18.79	19.32	18.04	19.34
NiO	0.00	0.00	0.00	0.00	0.00	0.00	0.00	0.00
MnO	0.21	0.26	0.29	0.28	0.24	0.19	0.19	0.21
MgO	8.75	8.73	8.74	8.83	8.70	9.11	8.25	8.74
CaO	0.00	0.00	0.00	0.00	0.00	0.00	0.00	0.00
Na2O	0.00	0.00	0.00	0.00	0.00	0.00	0.00	0.36
K2O	9.79	9.75	9.75	9.85	10.01	9.91	9.76	9.64
Cl	0.03	0.06	0.02	0.06	0.02	0.00	0.05	0.05
F	0.81	0.80	0.80	1.39	0.80	0.80	0.81	0.00
Total:	95.49	96.64	95.79	96.58	96.50	96.30	96.04	96.27
X-Pos:	66.41	66.14	69.19	69.41	73.76	73.77	77.45	77.21

Slide No.:A-004-2B Analysis: Muscovite

	#1 MA		#2 MB		#3 MC		#4 MD	
Oxides	(Psam/Rim)	(Psam/Core)	(Psam/Rim)	(Psam/Core)	(Psam/Rim)	(Psam/Core)	(Psam/Rim)	(Psam/Core)
SiO2	47.89	46.54	48.42	46.95	46.82	46.68	45.46	46.03
TiO2	1.45	1.33	1.32	1.31	1.57	1.44	1.04	1.01
Al2O3	36.00	36.35	36.19	36.28	36.24	36.10	36.08	36.94
Cr2O3	-	-	-	-	-	-	-	-
FeO	1.34	1.46	1.52	1.45	1.55	1.52	1.41	1.43
NiO	-	-	-	-	-	-	-	-
MnO	-	-	-	-	-	-	-	-
MgO	0.64	0.65	0.69	0.68	0.64	0.66	0.55	0.53

CaO	0.00	0.00	0.00	0.01	0.01	0.04	0.02	0.06
Na2O	0.72	0.66	0.68	0.70	0.59	0.65	0.70	0.70
K2O	9.86	10.03	10.27	10.01	10.18	10.01	9.47	9.68
Total:	97.90	97.02	99.09	97.39	97.60	97.10	94.73	96.38
X-Pos:	2.87	2.87	5.92	5.89	7.59	7.60	17.18	17.19
MgO/FeO:	0.48	0.45	0.45	0.47	0.41	0.43	0.39	0.37

Slide No.:A-004-2B Analysis: Muscovite

	#5 ME		#6 MF		#7 MG		#8 MH Bt. (Excl'd)	
Oxides	(Gran./Rim)	(Gran./Core)	(Gran./Rim)	(Gran./Core)	(Gran./Rim)	(Gran./Core)	(Gran./Rim)	(Gran./Core)
SiO2	48.56	47.26	47.23	45.85	47.69	47.04	34.86	35.57
TiO2	0.57	0.61	1.02	1.05	0.91	0.92	2.86	2.62
Al2O3	36.92	36.84	36.25	36.41	36.20	36.48	19.86	19.44
Cr2O3	-	-	-	-	-	-	-	-
FeO	1.66	1.54	1.56	1.49	1.59	1.44	20.40	20.50
NiO	-	-	-	-	-	-	-	-
MnO	-	-	-	-	-	-	0.31	0.37
MgO	0.63	0.67	0.70	0.65	0.68	0.71	8.62	8.90
CaO	0.00	0.00	0.00	0.06	0.00	0.03	0.00	0.04
Na2O	0.59	0.68	0.74	0.76	0.79	0.76	0.14	0.17
K2O	6.38	6.98	10.07	10.04	10.26	10.09	9.38	9.59
Total:	95.31	94.58	97.57	96.31	98.12	97.47	96.43	97.20
X-Pos:	20.81	20.84	23.34	23.44	28.00	27.93	31.95	31.84
MgO/FeO:	0.38	0.44	0.45	0.44	0.43	0.49	0.42	0.43

Slide No.:A-004-2B
Analysis: Plagioclase

	#1 PA		#2 PF		#3 PG	
Oxides	(Psam/Rim)	(Psam/Core)	(Psam/Rim)	(Psam/Core)	(Psam/Rim)	(Psam/Core)
SiO2	63.00	62.95	62.26	62.38	62.74	62.84
TiO2	0.00	0.00	0.00	0.00	0.00	0.00
Al2O3	22.64	23.01	23.32	23.26	22.71	22.71
Cr2O3	0.00	0.00	0.00	0.00	0.00	0.00
FeO	0.22	0.07	0.02	0.08	0.12	0.11
NiO	0.00	0.00	0.00	0.00	0.00	0.00
MnO	0.00	0.00	0.00	0.00	0.00	0.00
MgO	0.04	0.02	0.02	0.03	0.03	0.03
CaO	4.87	4.83	5.35	4.99	4.76	4.92
Na2O	9.29	9.51	8.74	8.89	9.34	9.41
K2O	0.10	0.14	0.10	0.10	0.13	0.14
Total:	100.16	100.53	99.81	99.73	99.83	100.16
An content	36.52	35.73	40.17	38.11	35.82	36.40
X-Pos	18.31	18.43	22.71	22.68	27.96	27.83

Slide No.:A-004-2B
Analysis: Plagioclase

	#4 PB		#5 PC		#6 PD	
Oxides	(Gran./Rim)	(Gran./Core)	(Gran./Rim)	(Gran./Core)	(Gran./Rim)	(Gran./Core)

SiO2	62.39	61.76	62.77	60.42	63.00	58.28
TiO2	0.00	0.00	0.00	0.00	0.00	0.00
Al2O3	22.75	23.16	22.91	24.00	22.42	25.54
Cr2O3	0.00	0.00	0.00	0.00	0.00	0.00
FeO	0.11	0.09	0.10	0.04	0.07	0.11
NiO	0.00	0.00	0.00	0.00	0.00	0.00
MnO	0.00	0.00	0.00	0.00	0.00	0.00
MgO	0.01	0.03	0.04	0.01	0.05	0.03
CaO	4.74	5.10	4.81	6.23	4.70	8.15
Na2O	9.32	8.95	9.13	8.24	9.34	7.21
K2O	0.21	0.23	0.14	0.16	0.19	0.09
Total:	99.53	99.32	99.90	99.10	99.77	99.41
An content	35.65	38.25	36.57	45.21	35.43	55.34
X-Pos	7.68	7.82	5.07	4.89	10.73	10.92

Slide No.: A-009-5A
Analysis: Biotite

	#1 BG		#2 BH		#3 BI	
Oxides	(Host/Rim)	(Host/Core)	(Host/Rim)	(Host/Core)	(Host/Rim)	(Host/Core)
SiO2	35.69	35.43	35.76	35.20	35.60	34.98
TiO2	3.24	3.31	3.39	3.07	3.29	3.20
Al2O3	19.00	18.42	18.80	18.50	19.16	18.52
Cr2O3	0.00	0.00	0.00	0.00	0.00	0.00
FeO	20.13	20.58	19.48	21.48	20.46	20.69
NiO	0.00	0.00	0.00	0.00	0.00	0.00
MnO	0.09	0.35	0.37	0.31	0.26	0.26
MgO	8.11	7.84	8.13	8.21	8.01	7.85
CaO	0.00	0.04	0.04	0.00	0.02	0.00
Na2O	0.00	0.25	0.00	0.00	0.00	0.00
K2O	9.62	9.68	9.71	9.79	9.40	9.65
Cl	0.01	0.00	0.02	0.00	0.00	0.02
F	0.00	0.00	0.00	0.00	0.20	0.00
----------	2.48	2.63	2.40	2.62	2.55	2.64
Total:	95.89	95.90	95.70	96.56	96.40	95.17

Slide No.: A-009-5A
Analysis: Biotite

	#4 BA		#5 BB		#6 BC	
Oxides	(Leuc./Rim)	(Leuc./Core)	(Leuc./Rim)	(Leuc./Core)	(Leuc./Rim)	(Leuc./Core)
SiO2	34.65	35.46	35.22	35.68	34.73	35.34
TiO2	2.90	3.13	2.84	3.46	3.18	3.22
Al2O3	18.66	18.61	18.25	18.49	18.16	18.61
Cr2O3	0.00	0.00	0.00	0.00	0.00	0.00
FeO	20.32	20.85	20.74	20.39	20.69	20.88
NiO	0.00	0.00	0.00	0.00	0.00	0.00
MnO	0.20	0.28	0.27	0.34	0.16	0.11
MgO	7.99	7.98	8.03	8.06	8.21	8.04
CaO	0.00	0.00	0.04	0.01	0.01	0.01
Na2O	0.12	0.00	0.00	0.09	0.35	0.00
K2O	9.03	9.39	9.15	9.21	9.19	9.26
Cl	0.00	0.00	0.02	0.00	0.00	0.00
F	0.00	0.00	0.00	0.00	0.00	0.00
----------	2.54	2.61	2.58	2.53	2.52	2.60
Total:	93.87	95.70	94.56	95.73	94.68	95.47

Slide No.: A-009-5A
Analysis: Biotite

	#1 BD		#2 BE		#3 BF	
Oxides	(Rim/Rim)	(Rim/Core)	(Rim/Rim)	(Rim/Core)	(Rim/Rim)	(Rim/Core)
SiO2	34.84	34.99	33.92	35.29	35.44	35.73
TiO2	2.42	2.95	2.58	3.05	2.54	2.36
Al2O3	18.24	18.11	17.89	18.58	18.94	17.77
Cr2O3	0.00	0.00	0.00	0.00	0.00	0.00
FeO	22.30	21.71	21.52	21.05	20.70	21.20
NiO	0.00	0.00	0.00	0.00	0.00	0.00
MnO	0.34	0.27	0.06	0.26	0.27	0.24
MgO	7.91	7.90	8.32	8.17	8.21	8.48
CaO	0.04	0.04	0.00	0.04	0.01	0.01
Na2O	0.00	0.12	0.00	0.13	0.24	0.24
K2O	9.37	9.46	9.74	9.43	9.23	9.34
Cl	0.01	0.00	0.02	0.00	0.00	0.02
F	0.20	0.00	0.00	0.00	0.00	0.00
----------	2.82	2.75	2.59	2.58	2.52	2.50
Total:	95.67	95.55	94.05	96.00	95.58	95.39

Slide No.: A-009-5A
Analysis: Muscovite

	#1 ME		#2 MH		#3 MI	
Oxides	(Host/Rim)	(Host/Core)	(Host/Rim)	(Host/Core)	(Host/Rim)	(Host/Core)
SiO2	46.10	47.39	46.87	46.74	47.19	48.20
TiO2	1.40	1.33	1.36	1.43	1.50	1.33
Al2O3	35.51	36.01	35.45	35.30	35.32	35.41
Cr2O3	-	-	-	-	-	-
FeO	1.76	1.42	1.56	1.43	1.29	1.44
NiO	-	-	-	-	-	-
MnO	-	-	-	-	-	-
MgO	0.79	0.65	0.70	0.69	0.72	0.63
CaO	0.01	0.00	0.00	0.00	0.03	0.03
Na2O	0.47	0.65	0.54	0.42	0.47	0.53
K2O	10.31	10.63	10.58	10.30	10.46	10.69
Total:	96.35	98.08	97.06	96.31	96.98	98.26
FeO/MgO	2.23	2.18	2.23	2.07	1.79	2.29

Slide No.: A-009-5A
Analysis: Muscovite

	#4 MA		#5 MB		#6 MC	
Oxides	(Leuc./Rim)	(Leuc./Core)	(Leuc./Rim)	(Leuc./Core)	(Leuc./Rim)	(Leuc./Core)
SiO2	47.31	47.89	46.29	47.10	47.23	47.97
TiO2	0.14	0.04	1.44	1.45	1.10	1.20
Al2O3	31.15	31.54	35.57	35.64	35.40	35.34
Cr2O3	-	-	-	-	-	-
FeO	2.90	2.52	1.37	1.44	1.53	1.61
NiO	-	-	-	-	-	-
MnO	-	-	-	-	-	-
MgO	1.89	1.80	0.64	0.58	0.80	0.82
CaO	0.02	0.00	0.01	0.00	0.00	0.01
Na2O	0.19	0.19	0.48	0.53	0.59	0.50
K2O	10.77	10.74	10.57	10.45	10.71	10.66
Total:	94.37	94.72	96.37	97.19	97.36	98.11
FeO/MgO	1.53	1.40	2.14	2.48	1.91	1.96

Slide No.: A-009-5A
Analysis: Muscovite

	#1 MD		#2 MF		#3 MG	
Oxides	(Rim/Rim)	(Rim/Core)	(Rim/Rim)	(Rim/Core)	(Rim/Rim)	(Rim/Core)
SiO2	46.73	46.76	46.05	46.39	46.25	47.10
TiO2	1.13	0.98	1.31	1.48	0.88	1.30
Al2O3	35.38	35.55	35.48	35.69	35.56	34.63
Cr2O3	-	-	-	-	-	-
FeO	1.54	1.55	1.29	1.38	1.63	1.60
NiO	-	-	-	-	-	-
MnO	-	-	-	-	-	-
MgO	0.80	0.74	0.59	0.62	0.78	0.92
CaO	0.00	0.05	0.08	0.00	0.01	0.00
Na2O	0.52	0.42	0.76	0.59	0.45	0.45
K2O	10.43	10.13	10.08	10.41	10.47	10.30
Total:	96.53	96.18	95.64	96.56	96.03	96.30
FeO/MgO	1.93	2.09	2.19	2.23	2.09	1.74

Slide No.: A-009-5A
Analysis: Plagioclase

	#1 PE		#2 PF		#3 PG	
Oxides	(Host/Rim)	(Host/Core)	(Host/Rim)	(Host/Core)	(Host/Rim)	(Host/Core)
SiO2	62.50	62.58	62.84	62.43	63.43	62.85
TiO2	0.00	0.00	0.00	0.00	0.00	0.00
Al2O3	22.59	22.75	22.80	23.15	22.54	22.83
Cr2O3	0.00	0.00	0.00	0.00	0.00	0.00
FeO	0.06	0.17	0.14	0.06	0.14	0.22
NiO	0.00	0.00	0.00	0.00	0.00	0.00
MnO	0.00	0.00	0.00	0.00	0.00	0.00
MgO	0.04	0.03	0.03	0.01	0.04	0.04
CaO	4.58	4.49	4.53	4.68	4.98	4.69
Na2O	9.25	9.38	9.18	9.04	8.94	9.12
K2O	0.20	0.17	0.11	0.13	0.16	0.18
Total:	99.22	99.57	99.63	99.50	100.23	99.93
An content:	35.05	34.33	35.11	36.18	37.83	35.94

Slide No.: A-009-5A
Analysis: Plagioclase

	#4 PA		#5 PB		#6 PC	
Oxides	(Leuc./Rim)	(Leuc./Core)	(Leuc./Rim)	(Leuc./Core)	(Leuc./Rim)	(Leuc./Core)
SiO2	62.51	62.21	62.59	62.63	63.07	62.75
TiO2	0.00	0.00	0.00	0.00	0.00	0.00
Al2O3	22.84	23.17	22.41	22.79	22.41	22.89
Cr2O3	0.00	0.00	0.00	0.00	0.00	0.00
FeO	0.01	0.11	0.10	0.06	0.04	0.10
NiO	0.00	0.00	0.00	0.00	0.00	0.00
MnO	0.00	0.00	0.00	0.00	0.00	0.00
MgO	0.02	0.03	0.00	0.03	0.04	0.00
CaO	4.45	4.90	4.72	4.79	4.73	5.01
Na2O	9.68	9.02	9.32	9.52	9.09	8.77
K2O	0.18	0.28	0.14	0.22	0.24	0.32
Total:	99.69	99.72	99.28	100.04	99.62	99.84
An content:	33.42	37.04	35.66	35.39	36.11	38.14

Slide No.: A-005-2 Analysis: Biotite

	#1 BA		#2 BB		#3 BC		#4 BD	
Oxides	(Psam/Rim)	(Psam/Core)	(Psam/Rim)	(Psam/Core)	(Psam/Rim)	(Psam/Core)	(Psam/Rim)	(Psam/Core)
SiO2	34.68	34.85	35.06	35.20	35.31	34.92	35.47	35.08
TiO2	2.64	2.79	3.03	2.95	2.38	2.84	2.00	3.01
Al2O3	17.58	17.79	17.87	17.95	17.92	17.74	17.48	17.45
Cr2O3	0.00	0.00	0.00	0.00	0.00	0.00	0.00	0.00
FeO	22.04	22.06	21.06	21.38	21.92	22.40	22.00	22.00
NiO	0.00	0.00	0.00	0.00	0.00	0.00	0.00	0.00
MnO	0.38	0.34	0.38	0.18	0.43	0.41	0.23	0.49
MgO	7.89	7.66	7.78	7.53	7.48	7.57	8.03	7.41
CaO	0.00	0.00	0.00	0.00	0.00	0.00	0.07	0.00
Na2O	0.00	0.00	0.00	0.00	0.00	0.00	0.56	0.05
K2O	9.58	9.49	9.87	9.67	9.92	9.61	9.23	9.53
Cl	0.03	0.05	0.05	0.04	0.05	0.00	0.04	0.04
F	0.79	0.00	0.99	0.00	0.00	0.79	0.79	0.79
Total:	95.61	95.03	96.09	94.90	95.41	96.28	95.90	95.85
X-Pos:	28.10	28.01	23.55	23.62	19.63	19.69	16.17	16.39

Slide No.: A-005-2 Analysis: Biotite

	#5 BE		#6 BF		#7 BG		#8 BH	
Oxides	(Gran./Rim)	(Gran./Core)	(Gran./Rim)	(Gran./Core)	(Gran./Rim)	(Gran./Core)	(Gran./Rim)	(Gran./Core)
SiO2	35.63	35.20	34.95	34.80	35.48	35.69	34.83	34.67
TiO2	2.42	2.58	3.12	3.21	3.16	3.04	3.00	2.96
Al2O3	17.11	17.47	17.43	17.23	17.47	17.82	18.12	17.61
Cr2O3	0.00	0.00	0.00	0.00	0.00	0.00	0.00	0.00
FeO	22.34	22.18	23.03	23.04	21.56	20.84	20.67	21.46
NiO	0.00	0.00	0.00	0.00	0.00	0.00	0.00	0.00
MnO	0.20	0.40	0.40	0.39	0.37	0.33	0.30	0.14
MgO	7.52	7.35	7.33	7.03	7.89	7.66	7.71	7.58
CaO	0.00	0.00	0.00	0.00	0.00	0.00	0.00	0.01
Na2O	0.00	0.00	0.00	0.00	0.20	0.20	0.08	0.00
K2O	9.84	9.42	9.57	9.35	9.85	10.06	9.51	9.17
Cl	0.05	0.06	0.05	0.05	0.05	0.04	0.05	0.07
F	0.00	0.79	0.00	0.00	1.08	0.00	0.70	0.80
Total:	95.11	95.45	95.88	95.10	97.11	95.68	94.97	94.47
X-Pos:	13.63	13.62	11.14	11.01	7.76	7.85	3.17	3.25

Slide No.: A-005-2 Analysis: Muscovite

	#1 MA		#2 MC		#3	
Oxides	(Psam/pt 1)	(Psam/pt 2)	(Psam/pt 1)	(Psam/pt 2)	(Psam/pt 1)	(Psam/pt 2)
SiO2	47.32	47.15	46.81	45.96	47.39	46.22
TiO2	0.66	1.72	0.80	0.69	1.77	1.76
Al2O3	32.34	31.51	33.07	32.03	30.92	32.44
Cr2O3	0.05	0.05	0.05	0.05	0.05	0.05
FeO	3.54	3.06	3.02	2.80	3.12	2.72
NiO	0.00	0.00	0.00	0.00	0.00	0.00
MnO	0.00	0.00	0.00	0.17	0.00	0.00
MgO	1.55	1.58	1.50	1.30	1.39	1.12
CaO	0.02	0.02	0.02	0.00	0.00	0.00
Na2O	0.31	0.25	0.33	0.30	0.28	0.37
K2O	11.12	11.80	11.32	10.45	11.57	11.44
Total:	96.91	97.14	96.92	93.75	96.49	96.12
X-Pos:						

Slide No.: A-005-2 Analysis: Muscovite

Oxides	#4 ME (Gran./pt 1)	#4 ME (Gran./pt 2)	#5 MF (Gran./pt 1)	#5 MF (Gran./pt 2)	#6 MH (Gran./pt 1)	#6 MH (Gran./pt 2)
SiO2	45.80	46.56	45.73	45.67	47.44	46.64
TiO2	0.81	0.36	1.17	0.98	0.24	0.17
Al2O3	32.80	33.06	34.53	35.10	31.73	30.90
Cr2O3	0.05	0.05	0.05	0.05	0.05	0.05
FeO	2.85	2.69	2.76	2.54	4.21	4.72
NiO	0.00	0.00	0.00	0.00	0.00	0.00
MnO	0.00	0.00	0.00	0.00	0.00	0.09
MgO	1.18	1.18	0.79	0.68	1.77	2.07
CaO	0.00	0.00	0.00	0.02	0.01	0.00
Na2O	0.30	0.35	0.52	0.50	0.21	0.24
K2O	11.46	11.67	10.92	11.01	11.37	11.37
Total:	95.25	95.92	96.47	96.55	97.03	96.25
X-Pos:						

Slide No.: A-005-2
Analysis: Plagioclase

Oxides	#1 PD (Psam/Rim)	#1 PD (Psam/Core)	#2 PF (Psam/Rim)	#2 PF (Psam/Core)
SiO2	63.51	61.92	68.96	67.56
TiO2	0.00	0.00	0.00	0.00
Al2O3	23.25	23.73	20.72	20.37
Cr2O3	0.00	0.00	0.00	0.00
FeO	0.16	0.14	0.27	0.16
NiO	0.00	0.00	0.00	0.00
MnO	0.00	0.00	0.00	0.00
MgO	0.03	0.03	0.04	0.02
CaO	4.20	4.39	1.16	0.76
Na2O	9.90	9.73	10.56	11.77
K2O	0.15	0.08	0.10	0.10
Total:	101.20	100.02	101.81	100.74
An content:	31.71	33.15	10.77	6.63
X-Pos	27.63	27.69	18.88	18.86

Slide No.: A-005-2
Analysis: Plagioclase

Oxides	#4 PB (Gran./Rim)	#4 PB (Gran./Core)	#5 PC (Gran./Rim)	#5 PC (Gran./Core)
SiO2	64.92	67.43	63.73	62.69
TiO2	0.00	0.00	0.00	0.00
Al2O3	22.22	21.18	22.83	23.74
Cr2O3	0.00	0.00	0.00	0.00
FeO	0.13	0.11	0.14	0.14
NiO	0.00	0.00	0.00	0.00
MnO	0.00	0.00	0.00	0.00
MgO	0.01	0.01	0.04	0.01
CaO	2.74	1.46	3.80	4.64
Na2O	10.68	11.89	10.10	9.73
K2O	0.18	0.12	0.33	0.28
Total:	100.88	102.20	100.97	101.23
An content:	21.90	11.88	28.93	34.09
X-Pos	6.93	6.86	3.57	3.83

Slide No.: A-003-1A
Analysis: Biotite

	#1 BA		#2 BB		#3 BC	
Oxides	(Apl./Rim)	(Apl./Core)	(Apl./Rim)	(Apl./Core)	(Apl./Rim)	(Apl./Core)
SiO2	36.57	36.50	35.94	36.60	36.39	36.50
TiO2	2.81	2.82	2.52	2.45	2.58	2.64
Al2O3	17.17	16.83	16.74	17.28	16.67	16.68
Cr2O3	0.00	0.00	0.00	0.00	0.00	0.00
FeO	15.26	15.32	15.63	15.23	15.83	15.68
NiO	0.00	0.00	0.00	0.00	0.00	0.00
MnO	0.36	0.32	0.30	0.27	0.16	0.24
MgO	12.59	12.76	11.99	12.29	12.25	11.95
CaO	0.00	0.00	0.00	0.00	0.00	0.00
Na2O	0.00	0.00	0.00	0.00	0.00	0.00
K2O	9.54	9.88	9.57	9.83	9.59	9.77
Cl	0.00	0.07	0.11	0.05	0.02	0.07
F	0.82	0.82	1.23	0.00	0.00	0.82
Total:	95.12	95.32	94.03	94.00	93.49	94.35

Slide No.: A-003-1A
Analysis: Biotite

	#4 BD		#5 BE		#6 BF	
Oxides	(Rim/Rim)	(Rim/Core)	(Rim/Rim)	(Rim/Core)	(Rim/Rim)	(Rim/Core)
SiO2	36.85	37.79	36.84	37.17	37.06	36.81
TiO2	2.27	2.44	2.67	2.76	2.54	2.47
Al2O3	17.12	16.61	16.44	16.60	16.85	16.84
Cr2O3	0.00	0.00	0.00	0.00	0.00	0.00
FeO	15.40	14.98	15.80	15.58	14.71	15.06
NiO	0.00	0.00	0.00	0.00	0.00	0.00
MnO	0.20	0.28	0.16	0.16	0.29	0.33
MgO	12.77	12.86	12.62	12.64	13.01	12.94
CaO	0.00	0.00	0.00	0.00	0.00	0.00
Na2O	0.00	0.00	0.00	0.06	0.00	0.00
K2O	9.77	9.71	9.88	9.41	9.75	9.68
Cl	0.02	0.02	0.02	0.02	0.04	0.02
F	0.92	0.82	0.00	1.72	0.00	0.72
Total:	95.32	95.51	94.43	96.12	94.25	94.87

Slide No.: A-003-1A
Analysis: Biotite

	#1		#2		#3	
Oxides	(Mafic/Rim)	(Mafic/Core)	(Mafic/Rim)	(Mafic/Core)	(Mafic/Rim)	(Mafic/Core)
SiO2	37.58	37.18	37.00	36.77	36.75	36.98
TiO2	2.24	2.19	2.23	2.35	2.16	2.37
Al2O3	16.47	16.83	16.40	16.63	16.71	16.66
Cr2O3	0.00	0.00	0.00	0.00	0.00	0.00
FeO	15.02	15.16	15.08	15.34	14.67	15.02
NiO	0.00	0.00	0.00	0.00	0.00	0.00
MnO	0.10	0.33	0.35	0.33	0.27	0.23
MgO	13.29	13.30	13.02	13.02	13.30	13.54
CaO	0.00	0.00	0.00	0.00	0.00	0.00
Na2O	0.00	0.00	0.08	0.00	0.00	0.00
K2O	9.61	9.53	9.45	9.70	9.60	9.83
Cl	0.03	0.01	0.04	0.03	0.05	0.04
F	0.82	0.00	1.72	0.00	0.00	0.82
Total:	95.16	94.53	95.37	94.17	93.51	95.49

Slide No.: A-003-1A Analysis: Muscovite

Slide No.: A-003-1A

Analysis: Plagioclase

	#1 PA		#2 PB		#3 PC	
Oxides	(Apl./Rim)	(Apl./Core)	(Apl./Rim)	(Apl./Core)	(Apl./Rim)	(Apl./Core)
SiO2	57.53	58.36	56.56	57.30	57.43	56.78
TiO2	0.00	0.00	0.00	0.00	0.00	0.00
Al2O3	27.23	26.93	28.02	27.76	27.29	28.18
Cr2O3	0.00	0.00	0.00	0.00	0.00	0.00
FeO	0.16	0.13	0.16	0.17	0.17	0.18
NiO	0.00	0.00	0.00	0.00	0.00	0.00
MnO	0.00	0.00	0.00	0.00	0.00	0.00
MgO	0.02	0.02	0.03	0.02	0.04	0.04
CaO	8.89	8.38	9.40	9.06	8.90	9.59
Na2O	2.53	5.73	6.80	6.86	6.93	6.73
K2O	0.16	0.15	0.12	0.14	0.11	0.15
Total:	96.52	99.70	101.09	101.31	100.87	101.65
An content:	78.85	61.38	60.16	59.02	58.42	60.82

Slide No.: A-002-4 Analysis: Biotite

Oxides	#1 BA (Psam/Rim)	#1 BA (Psam/Core)	#2 BB (Psam/Rim)	#2 BB (Psam/Core)	#3 BC (Psam/Rim)	#3 BC (Psam/Core)	#4 BD (Psam/Rim)	#4 BD (Psam/Core)
SiO2	34.94	35.09	35.18	35.43	34.92	35.15	33.96	35.07
TiO2	2.32	2.29	2.31	2.25	2.22	2.30	2.11	2.19
Al2O3	19.88	19.45	19.72	19.63	19.53	19.59	18.97	19.90
Cr2O3	-	-	-	-	-	-	-	-
FeO	19.52	20.09	19.68	19.58	19.66	19.64	19.81	19.61
NiO	-	-	-	-	-	-	-	-
MnO	0.19	0.32	0.32	0.30	0.31	0.21	0.09	0.38
MgO	8.56	8.53	8.44	8.55	8.69	8.60	8.76	8.52
CaO	0.00	0.00	0.00	0.00	0.00	0.00	0.02	0.00
Na2O	0.10	0.00	0.20	0.00	0.00	0.48	0.19	0.11
K2O	8.76	8.67	9.15	9.04	9.10	9.10	8.82	8.86
Cl	0.06	0.06	0.06	0.05	0.06	0.09	0.05	0.08
F	1.19	1.29	0.00	0.80	0.00	0.99	1.01	0.00
Total:	95.52	95.79	95.06	95.63	94.49	96.15	93.79	94.72
X-Pos:	50.89	50.81	53.98	53.94	55.76	55.75	59.78	59.71

Slide No.: A-002-4 Analysis: Biotite

Oxides	#5 BE (Pel./Rim)	#5 BE (Pel./Core)	#6 BF (Pel./Rim)	#6 BF (Pel./Core)	#7 BG (Pel./Rim)	#7 BG (Pel./Core)	#8 BH (Pel./Rim)	#8 BH (Pel./Core)
SiO2	34.18	34.92	35.58	34.67	35.26	35.12	35.07	34.93
TiO2	2.00	2.16	1.94	1.99	1.80	1.98	1.85	1.73
Al2O3	19.38	19.66	19.61	19.57	20.32	19.79	19.77	19.37
Cr2O3	-	-	-	-	-	-	-	-
FeO	20.65	19.72	20.31	20.38	19.39	19.70	20.17	20.05
NiO	-	-	-	-	-	-	-	-
MnO	0.38	0.28	0.32	0.36	0.30	0.34	0.28	0.31
MgO	8.72	8.70	8.66	8.69	8.38	8.93	9.01	8.64
CaO	0.00	0.00	0.00	0.00	0.00	0.00	0.00	0.00
Na2O	0.00	0.36	0.37	0.12	0.00	0.63	0.38	0.00
K2O	8.68	9.23	9.26	9.01	9.50	8.81	8.73	8.79
Cl	0.04	0.07	0.07	0.06	0.05	0.04	0.07	0.06
F	0.00	0.00	0.79	0.89	0.00	0.79	0.79	0.80
Total:	94.03	95.10	96.91	95.74	95.00	96.13	96.12	94.68
X-Pos:	64.27	64.31	67.06	67.01	70.29	70.08	73.24	73.21

Slide No.: A-002-4 Analysis: Muscovite

Oxides	#1 MA (Psam/Rim)	#1 MA (Psam/Core)	#2 MB (Psam/Rim)	#2 MB (Psam/Core)	#3 MC (Psam/Rim)	#3 MC (Psam/Core)	#4 MD (Psam/Rim)	#4 MD (Psam/Core)
SiO2	46.85	46.21	46.42	46.44	46.20	46.60	47.68	47.35
TiO2	0.43	0.50	0.62	0.69	0.56	0.66	0.61	0.62
Al2O3	37.56	37.42	37.01	37.20	37.10	37.04	36.87	36.50
Cr2O3	-	-	-	-	-	-	-	-
FeO	1.38	1.31	1.13	1.14	1.00	1.02	1.24	1.17
NiO	-	-	-	-	-	-	-	-
MnO	-	-	0.10	0.03	0.05	-	-	-
MgO	0.64	0.66	0.54	0.54	0.50	0.55	0.65	0.74
CaO	0.00	0.00	0.01	0.00	0.00	0.00	0.00	0.04
Na2O	1.11	1.09	1.27	1.20	1.37	1.37	1.34	1.24
K2O	9.12	9.09	9.02	8.94	8.94	9.17	9.12	9.26
Total:	97.09	96.28	96.12	96.18	95.72	96.41	97.51	96.92
X-Pos:	50.95	51.00	53.95	54.05	57.40	57.43	60.10	60.58
MgO/FeO:	0.46	0.50	0.48	0.47	0.50	0.54	0.52	0.63

Slide No.: A-002-4 Analysis: Muscovite

	#5 ME		#6 MF		#7 MG		#8 MH	
Oxides	(Psam/Rim)	(Psam/Core)	(Pel./Rim)	(Pel./Core)	(Pel./Rim)	(Pel./Core)	(Pel./Rim)	(Pel./Core)
SiO2	46.13	46.00	48.57	46.52	48.43	47.23	47.84	47.29
TiO2	0.61	0.55	0.72	0.80	0.54	0.51	0.55	0.57
Al2O3	37.27	36.83	37.07	36.84	37.13	37.53	37.67	37.52
Cr2O3	-	-	-	-	-	-	-	-
FeO	1.22	1.22	1.41	1.47	1.01	1.38	1.09	0.98
NiO	-	-	-	-	-	-	-	-
MnO	-	-	-	-	-	-	0.06	-
MgO	0.60	0.67	0.66	0.70	0.52	0.71	0.52	0.54
CaO	0.00	0.04	0.00	0.01	0.03	0.00	0.00	0.04
Na2O	1.23	1.17	1.22	1.15	1.35	1.22	1.47	1.26
K2O	9.19	9.16	9.13	9.67	8.90	9.69	8.80	9.11
Total:	96.25	95.64	98.78	97.16	97.91	98.27	98.00	97.31
X-Pos:	65.36	65.37	69.18	69.16	74.21	74.25	77.60	77.61
MgO/FeO:	0.49	0.55	0.47	0.48	0.51	0.51	0.48	0.55

Slide No.: A-002-4
Analysis: Plagioclase

	#1 PA		#2 PC		#3 PB	
Oxides	(Psam/Rim)	(Psam/Core)	(Psam/Rim)	(Psam/Core)	(Psam/Rim)	(Psam/Core)
SiO2		64.76	63.73	64.04	63.61	63.96
TiO2		-	-	-	-	-
Al2O3		23.01	23.34	23.20	23.21	23.43
Cr2O3		-	-	-	-	-
FeO		0.15	0.16	0.13	0.18	0.15
NiO		-	-	-	-	-
MnO		-	-	-	-	-
MgO		0.03	0.03	0.03	0.00	0.04
CaO		3.61	4.00	4.28	3.79	4.20
Na2O		10.24	9.78	9.81	9.92	9.78
K2O		0.10	0.09	0.10	0.10	0.11
Total:	0.00	101.90	101.13	101.59	100.81	101.67
An content:	ERR	27.91	31.00	32.39	29.55	32.03
X-Pos		28.08	31.38	31.34	22.74	22.78

Slide No.: A-002-4
Analysis: Plagioclase

	#4 PD		#5 PF		#6 PG	
Oxides	(Pel./Rim)	(Pel./Core)	(Pel./Rim)	(Pel./Core)	(Pel./Rim)	(Pel./Core)
SiO2	64.70	63.46	64.43	63.12	63.56	63.12
TiO2	-	-	-	-	-	-
Al2O3	23.04	23.17	23.16	23.29	23.13	23.21
Cr2O3	-	-	-	-	-	-
FeO	0.28	0.19	0.22	0.15	0.28	0.15
NiO	-	-	-	-	-	-
MnO	-	-	-	-	-	-
MgO	0.02	0.03	0.03	0.04	0.00	0.05
CaO	3.87	4.12	3.74	4.06	3.82	3.62
Na2O	9.87	9.65	10.16	9.77	10.15	9.83
K2O	0.11	0.16	0.11	0.09	0.08	0.12
Total:	101.89	100.78	101.85	100.52	101.02	100.10
An content:	30.08	31.82	28.77	31.34	29.27	28.76
X-Pos	13.48	13.62	7.66	7.89	4.49	4.46

Slide No.: A-008-3A
Analysis: Biotite

	#1 BA		#2 BB		#3 BC	
Oxides	(Host/Rim)	(Host/Core)	(Host/Rim)	(Host/Core)	(Host/Rim)	(Host/Core)
SiO2	36.12	35.91	33.15	36.40	35.64	35.83
TiO2	3.01	3.07	2.78	3.14	2.96	2.84
Al2O3	17.26	18.37	16.83	18.41	18.79	18.37
Cr2O3	0.00	0.00	0.00	0.00	0.00	0.00
FeO	21.48	21.02	21.21	21.47	20.03	21.38
NiO	0.00	0.00	0.00	0.00	0.00	0.00
MnO	0.20	0.38	0.31	0.47	0.29	0.37
MgO	8.44	8.37	8.64	8.43	8.55	8.40
CaO	0.00	0.02	0.01	0.00	0.00	0.01
Na2O	0.00	0.00	0.22	0.00	0.00	0.00
K2O	9.43	9.21	9.52	9.59	9.64	9.40
Cl	0.00	0.00	0.01	0.01	0.00	0.02
F	0.00	0.80	0.00	0.79	0.00	0.20
----------	2.55	2.51	2.45	2.55	2.34	2.55
Total:	95.94	97.15	92.68	98.71	95.90	96.82

Slide No.: A-008-3A
Analysis: Biotite

	#4 BD		#5 BE	
Oxides	(Lc. 1/Rim)	(Lc. 1/Core)	(Lc. 1/Rim)	(Lc. 1/Core)
SiO2	35.71	36.60	35.42	35.25
TiO2	2.94	2.88	2.91	2.13
Al2O3	17.63	18.12	18.17	17.97
Cr2O3	0.00	0.00	0.00	0.00
FeO	21.22	20.72	21.58	21.39
NiO	0.00	0.00	0.00	0.00
MnO	0.47	0.42	0.50	0.38
MgO	8.58	8.59	7.53	8.29
CaO	0.00	0.00	0.00	0.06
Na2O	0.28	0.24	0.24	0.00
K2O	9.45	9.55	9.30	8.86
Cl	0.02	0.00	0.00	0.00
F	0.00	0.60	0.00	0.00
----------	2.47	2.41	2.87	2.58
Total:	96.30	97.72	95.65	94.33

Slide No.: A-008-3A
Analysis: Biotite

	#1 BF		#2 BG		#3 BH	
Oxides	(Lc. 2/Rim)	(Lc. 2/Core)	(Lc. 2/Rim)	(Lc. 2/Core)	(Lc. 2/Rim)	(Lc. 2/Core)
SiO2	34.63	36.06	34.73	36.60	35.67	35.53
TiO2	2.56	2.66	2.58	2.56	2.91	2.86
Al2O3	17.73	18.42	18.62	18.59	18.03	18.94
Cr2O3	0.00	0.00	0.00	0.00	0.00	0.00
FeO	20.55	20.25	20.80	20.54	21.90	20.68
NiO	0.00	0.00	0.00	0.00	0.00	0.00
MnO	0.34	0.47	0.43	0.39	0.47	0.44
MgO	8.59	8.46	8.35	8.22	7.61	7.75
CaO	0.00	0.00	0.04	0.00	0.01	0.03
Na2O	0.11	0.07	0.00	0.00	0.00	0.00
K2O	9.79	9.47	8.12	9.11	9.46	9.30
Cl	0.01	0.00	0.00	0.00	0.00	0.00
F	0.00	0.00	0.81	0.00	0.80	0.00
----------	2.39	2.39	2.49	2.50	2.88	2.67
Total:	94.31	95.86	94.48	96.01	96.86	95.53

Slide No.: A-008-3A
Analysis: Muscovite

	#1 MD		#2 ME		#3 MF	
Oxides	(Host/Rim)	(Host/Core)	(Host/Rim)	(Host/Core)	(Host/Rim)	(Host/Core)
SiO2	44.64	47.44	46.11	46.33	47.47	48.53
TiO2	1.23	1.20	1.25	1.24	1.19	1.18
Al2O3	35.62	35.86	35.52	35.59	35.69	35.38
Cr2O3	-	-	-	-	-	-
FeO	1.38	1.46	1.50	1.48	1.46	1.38
NiO	-	-	-	-	-	-
MnO	-	-	-	-	-	-
MgO	0.71	0.65	0.68	0.69	0.71	0.75
CaO	0.04	0.03	0.00	0.00	0.00	0.00
Na2O	0.59	0.50	0.55	0.62	0.54	0.53
K2O	10.56	10.62	10.14	10.27	10.75	10.71
Total:	94.77	97.76	95.75	96.22	97.81	98.46
FeO/MgO	1.94	2.25	2.21	2.14	2.06	1.84

Slide No.: A-008-3A
Analysis: Muscovite

	#4 MA		#5 MB		#6 MC	
Oxides	(Lc. 1/Rim)	(Lc. 1/Core)	(Lc. 1/Rim)	(Lc. 1/Core)	(Lc. 1/Rim)	(Lc. 1/Core)
SiO2	47.28	47.08	45.93	45.41	47.17	48.62
TiO2	1.15	1.24	1.03	1.04	1.05	1.03
Al2O3	35.55	35.07	35.51	35.76	35.60	35.51
Cr2O3	-	-	-	-	-	-
FeO	1.41	1.36	1.41	1.35	1.51	1.30
NiO	-	-	-	-	-	-
MnO	-	-	-	-	-	-
MgO	0.75	0.68	0.72	0.72	0.77	0.73
CaO	0.00	0.08	0.00	0.00	0.02	0.00
Na2O	0.55	0.58	0.51	0.55	0.49	0.43
K2O	10.24	10.66	10.33	10.22	10.62	10.55
Total:	96.93	96.75	95.44	95.05	97.23	98.17
FeO/MgO	1.88	2.00	1.96	1.88	1.96	1.78

Slide No.: A-008-3A
Analysis: Muscovite

	#1 MG		#2 MH		#3 MI	
Oxides	(Lc. 2/Rim)	(Lc. 2/Core)	(Lc. 2/Rim)	(Lc. 2/Core)	(Lc. 2/Rim)	(Lc. 2/Core)
SiO2	46.97	47.96	46.27	47.24	47.52	47.89
TiO2	1.24	1.22	1.25	1.23	1.00	1.01
Al2O3	35.41	35.46	35.06	35.30	35.92	35.42
Cr2O3	-	-	-	-	-	-
FeO	1.37	1.39	1.48	1.39	1.52	1.49
NiO	-	-	-	-	-	-
MnO	-	-	-	-	-	-
MgO	0.75	0.72	0.66	0.67	0.70	0.71
CaO	0.00	0.00	0.00	0.01	0.05	0.02
Na2O	0.43	0.48	0.43	0.40	0.50	0.63
K2O	10.64	10.72	10.36	10.27	10.85	10.61
Total:	96.81	97.95	95.51	96.51	98.06	97.78
FeO/MgO	1.83	1.93	2.24	2.07	2.17	2.10

Slide No.: A-008-3A
Analysis: Plagioclase

Oxides	#1 (Lc. 2/Rim)	#1 (Lc. 2/Core)	#2 PB (Lc. 2/Rim)	#2 PB (Lc. 2/Core)	#3 PC (Lc. 2/Rim)	#3 PC (Lc. 2/Core)
SiO2			63.31	62.76	61.69	63.22
TiO2			0.00	0.00	0.00	0.00
Al2O3			22.56	23.03	23.64	22.83
Cr2O3			0.00	0.00	0.00	0.00
FeO			0.11	0.05	0.13	0.13
NiO			0.00	0.00	0.00	0.00
MnO			0.00	0.00	0.00	0.00
MgO			0.04	0.01	0.03	0.03
CaO			4.34	4.97	5.60	4.74
Na2O			9.13	8.75	8.48	8.65
K2O			0.12	0.08	0.14	0.26
Total:	0.00	0.00	99.61	99.65	99.71	99.86
An content:	ERR	ERR	34.25	38.42	41.93	37.26

Slide No.: A-008-3A
Analysis: Plagioclase

Oxides	#4 PD (Lc. 1/Rim)	#4 PD (Lc. 1/Core)	#5 PE (Lc. 1/Rim)	#5 PE (Lc. 1/Core)
SiO2	63.22	62.83	63.54	60.21
TiO2	0.00	0.00	0.00	0.00
Al2O3	22.83	23.12	22.95	23.08
Cr2O3	0.00	0.00	0.00	0.00
FeO	0.13	0.03	0.13	0.17
NiO	0.00	0.00	0.00	0.00
MnO	0.00	0.00	0.00	0.00
MgO	0.03	0.04	0.00	0.00
CaO	4.74	4.63	4.50	4.46
Na2O	8.65	8.99	9.30	9.07
K2O	0.26	0.26	0.24	0.40
Total:	99.86	99.90	100.66	97.39
An content:	37.26	35.84	34.46	34.56

Slide No.: A-008-4B
Analysis: Muscovite

	#1 MA		#2 MB		#3 MC	
Oxides	(Host/pt 1)	(Host/pt 2)	(Host/pt 1)	(Host/pt 2)	(Host/pt 1)	(Host/pt 2)
SiO2	43.57	46.67	47.35	46.59	46.49	46.50
TiO2	0.67	0.76	0.81	0.78	0.96	0.75
Al2O3	36.22	35.64	36.09	36.36	35.73	35.89
Cr2O3	0.05	0.05	0.05	0.05	0.05	0.05
FeO	1.32	1.46	1.57	1.55	1.51	1.48
NiO	0.00	0.00	0.00	0.00	0.00	0.00
MnO	0.00	0.00	0.00	0.00	0.02	0.00
MgO	0.64	0.66	0.75	0.71	0.68	0.75
CaO	0.00	0.00	0.00	0.00	0.00	0.02
Na2O	0.57	0.60	0.83	0.72	0.77	0.72
K2O	11.37	11.21	10.94	10.90	10.80	11.14
Total:	94.41	97.05	98.39	97.66	97.01	97.30
FeO/MgO	2.06	2.21	2.09	2.18	2.22	1.97

Slide No.: A-008-4B
Analysis: Muscovite

	#4 MD		#5 MH		#6 MI	
Oxides	(Leuc./pt 1)	(Leuc./pt 2)	(Leuc./pt 1)	(Leuc./pt 2)	(Leuc./pt 1)	(Leuc./pt 2)
SiO2	46.58	46.83	46.70	42.60	45.90	46.44
TiO2	0.76	0.65	0.58	0.51	0.75	0.55
Al2O3	36.28	35.86	36.04	36.42	36.10	36.39
Cr2O3	0.05	0.05	0.05	0.05	0.05	0.05
FeO	1.59	1.56	1.66	1.41	1.56	1.54
NiO	0.00	0.00	0.00	0.00	0.00	0.00
MnO	0.00	0.00	0.00	0.00	0.00	0.00
MgO	0.72	0.69	0.64	0.67	0.70	0.63
CaO	0.00	0.00	0.00	0.02	0.05	0.01
Na2O	0.63	0.70	0.57	0.74	0.75	0.78
K2O	11.08	10.81	10.93	10.72	10.89	10.39
Total:	97.69	97.15	97.17	93.14	96.75	96.78
FeO/MgO	2.21	2.26	2.59	2.10	2.23	2.44

Slide No.: A-008-4B
Analysis: Muscovite

	#1 MG		#2 MH		#3 MI	
Oxides	(Rim/pt 1)	(Rim/pt 2)	(Rim/pt 1)	(Rim/pt 2)	(Rim/pt 1)	(Rim/pt 2)
SiO2	46.79	46.72	46.76	47.31	47.52	47.40
TiO2	0.81	0.72	0.56	0.64	0.70	0.69
Al2O3	36.48	36.75	36.74	36.47	36.67	36.27
Cr2O3	0.05	0.05	0.05	0.05	0.05	0.05
FeO	1.51	1.44	1.45	1.54	1.53	1.51
NiO	0.00	0.00	0.00	0.00	0.00	0.00
MnO	0.00	0.05	0.00	0.03	0.01	0.00
MgO	0.61	0.64	0.72	0.66	0.69	0.72
CaO	0.00	0.00	0.02	0.03	0.00	0.00
Na2O	0.64	0.65	0.64	0.69	0.67	0.72
K2O	10.96	10.99	10.97	10.83	10.83	10.62
Total:	97.85	98.01	97.91	98.25	98.67	97.98
FeO/MgO	2.48	2.25	2.01	2.33	2.22	2.10

Slide No.: A-008-4B
Analysis: Plagioclase

	#1 PD		#2 PE		#3 PF	
Oxides	(Host/Rim)	(Host/Core)	(Host/Rim)	(Host/Core)	(Host/Rim)	(Host/Core)
SiO2	63.49	62.89	63.80	62.00	63.94	62.22
TiO2	0.00	0.00	0.00	0.00	0.00	0.00
Al2O3	22.11	22.64	22.42	22.77	22.01	23.20
Cr2O3	0.00	0.00	0.00	0.00	0.00	0.00
FeO	0.19	0.22	0.22	0.18	0.20	0.16
NiO	0.00	0.00	0.00	0.00	0.00	0.00
MnO	0.00	0.00	0.00	0.00	0.00	0.00
MgO	0.05	0.06	0.05	0.06	0.05	0.05
CaO	3.86	4.44	3.82	4.56	3.64	4.89
Na2O	9.76	9.17	9.90	9.08	9.74	9.02
K2O	0.11	0.12	0.07	0.12	0.18	0.11
Total:	99.57	99.54	100.28	98.77	99.76	99.65
An content:	30.26	34.67	29.80	35.50	28.98	37.28

Slide No.: A-008-4B
Analysis: Plagioclase

	#4 PA		#5 PB		#6 PC	
Oxides	(Leuc 1/Rim)	(Leuc 1/Core	(Leuc 1/Rim)	(Leuc 1/Core	(Leuc 1/Rim)	(Leuc 1/Core)
SiO2	64.27	63.84	62.49	63.27	63.49	62.60
TiO2	0.00	0.00	0.00	0.00	0.00	0.00
Al2O3	22.22	22.26	22.75	22.59	22.26	22.75
Cr2O3	0.00	0.00	0.00	0.00	0.00	0.00
FeO	0.23	0.15	0.19	0.20	0.24	0.22
NiO	0.00	0.00	0.00	0.00	0.00	0.00
MnO	0.00	0.00	0.00	0.00	0.00	0.00
MgO	0.05	0.07	0.04	0.05	0.05	0.05
CaO	3.55	4.09	4.25	4.21	3.63	4.35
Na2O	9.99	9.05	9.33	9.45	9.38	9.01
K2O	0.11	0.13	0.25	0.20	0.24	0.14
Total:	100.42	99.59	99.30	99.97	99.29	99.12
An content:	28.05	33.10	33.10	32.69	29.61	34.56

Slide No.: A-008-4B
Analysis: Plagioclase

	#1		#2		#3	
Oxides	(Leuc 2/Rim)	(Leuc 2/Core	(Leuc 2/Rim)	(Leuc 2/Core	(Leuc 2/Rim)	(Leuc 2/Core)
SiO2	63.39	63.24	63.55	63.36	63.14	62.59
TiO2	0.00	0.00	0.00	0.00	0.00	0.00
Al2O3	22.35	22.56	22.34	22.61	22.73	22.89
Cr2O3	0.00	0.00	0.00	0.00	0.00	0.00
FeO	0.22	0.19	0.18	0.22	0.17	0.18
NiO	0.00	0.00	0.00	0.00	0.00	0.00
MnO	0.00	0.00	0.00	0.00	0.00	0.00
MgO	0.05	0.05	0.07	0.07	0.06	0.04
CaO	3.71	4.03	3.85	4.36	4.52	4.51
Na2O	9.85	9.41	9.41	9.43	9.30	9.09
K2O	0.21	0.17	0.14	0.15	0.13	0.19
Total:	99.78	99.65	99.54	100.20	100.05	99.49
An content:	29.10	31.87	30.93	33.59	34.74	35.10

Slide No.: C-002-1 Analysis: Biotite

Oxides	#1 BA (Psam/Rim)	#1 BA (Psam/Core)	#2 BB (Psam/Rim)	#2 BB (Psam/Core)	#3 BC (Psam/Rim)	#3 BC (Psam/Core)
SiO2	35.33	35.06	35.27	35.34	35.26	35.25
TiO2	1.94	2.57	2.57	2.59	2.49	2.58
Al2O3	18.25	19.48	18.86	19.03	19.03	19.29
Cr2O3	0.00	0.00	0.00	0.00	0.00	0.00
FeO	18.79	18.80	18.77	19.15	19.15	19.26
NiO	0.00	0.00	0.00	0.00	0.00	0.00
MnO	0.30	0.29	0.26	0.22	0.33	0.26
MgO	9.34	8.73	8.73	8.45	8.54	8.36
CaO	0.00	0.00	0.00	0.00	0.00	0.00
Na2O	0.00	0.12	0.00	0.00	0.50	0.00
K2O	9.25	9.52	9.77	9.33	9.63	9.60
Cl	0.05	0.00	0.03	0.00	0.06	0.06
F	0.00	0.81	1.10	1.20	0.00	0.80
Total:	93.25	95.38	95.36	95.31	94.99	95.46
X-Pos:	53.57	53.55	55.66	55.43	58.65	58.32

Slide No.: C-002-1 Analysis: Biotite

Oxides	#4 BE (Gran./Rim)	#4 BE (Gran./Core)	#5 BF (Gran./Rim)	#5 BF (Gran./Core)	#6 BG (Gran./Rim)	#6 BG (Gran./Core)
SiO2	34.63	35.64	34.82	35.35	34.64	35.39
TiO2	2.08	2.05	2.13	2.09	2.20	2.08
Al2O3	19.19	19.42	18.98	19.30	19.16	19.19
Cr2O3	0.00	0.00	0.00	0.00	0.00	0.00
FeO	19.52	19.61	19.39	19.40	20.09	19.82
NiO	0.00	0.00	0.00	0.00	0.00	0.00
MnO	0.15	0.24	0.27	0.20	0.28	0.06
MgO	9.01	8.83	9.11	8.87	8.69	8.88
CaO	0.00	0.00	0.00	0.00	0.00	0.00
Na2O	0.35	0.00	0.00	0.00	0.00	0.00
K2O	9.32	9.44	9.52	9.53	9.36	9.48
Cl	0.07	0.03	0.04	0.03	0.06	0.07
F	0.80	0.00	0.80	0.80	0.90	0.79
Total:	95.12	95.26	95.06	95.57	95.38	95.76
X-Pos:	67.77	67.60	71.34	71.23	73.88	74.14

Slide No.: C-002-1 Analysis: Muscovite

Oxides	#1 MA (Xeno./pt 1)	#1 MA (Xeno.pt 2)	#2 MB (Xeno.pt 1)	#2 MB (Xeno.pt 2)	#3 MC (Xeno.pt 1)	#3 MC (Xeno.pt 2)
SiO2	43.27	46.67	46.58	46.60	47.16	45.57
TiO2	0.63	0.85	0.56	0.55	0.90	0.95
Al2O3	37.30	36.92	37.21	37.62	38.12	37.72
Cr2O3	0.05	0.05	0.05	0.05	0.05	0.05
FeO	1.62	1.09	1.19	1.00	1.05	0.97
NiO	0.00	0.00	0.00	0.00	0.00	0.00
MnO	0.00	0.00	0.01	0.00	0.00	0.00
MgO	0.66	0.68	0.69	0.60	0.60	0.63
CaO	0.02	0.00	0.02	0.00	0.01	0.01
Na2O	0.72	0.76	0.56	0.69	0.68	0.69
K2O	10.73	10.77	10.88	10.84	10.63	10.73
Total:	95.00	97.79	97.75	97.95	99.20	97.32
X-Pos:	50.07	50.02	55.10	55.21	58.45	58.48

Slide No.: C-002-1 Analysis: Muscovite

Oxides	#4 MD (Xeno./pt 1)	#4 MD (Xeno./pt 2)	#5 ME (Gran./pt 1)	#5 ME (Gran./pt 2)	#6 MF (Gran./pt 1)	#6 MF (Gran./pt 2)
SiO2	46.96	46.92	47.83	47.83	46.31	46.58
TiO2	0.75	0.88	0.14	0.14	0.46	0.48
Al2O3	37.97	37.53	35.00	35.00	36.86	37.54
Cr2O3	0.05	0.05	0.05	0.05	0.05	0.05
FeO	0.90	0.80	1.89	1.89	1.08	1.20
NiO	0.00	0.00	0.00	0.00	0.00	0.00
MnO	0.00	0.00	0.00	0.00	0.06	0.00
MgO	0.55	0.53	1.31	1.31	0.71	0.70
CaO	0.03	0.01	0.03	0.03	0.02	0.00
Na2O	0.63	0.72	0.39	0.39	0.58	0.75
K2O	10.70	10.95	11.05	11.05	10.59	10.70
Total:	98.54	98.39	97.69	97.69	96.72	98.00
X-Pos:	62.06	62.05	67.39	67.39	69.68	69.70
			inclusion in plag.		inclusion in plag.	

Slide No.: C-002-1
Analysis: Plagioclase

Oxides	#1 PB (Gran/Rim)	#1 PB (Gran/Core)	#2 PA (Gran/Rim)	#2 PA (Gran/Core)	#3 PC (Gran/Rim)	#3 PC (Gran/Core)
SiO2	62.97	60.47	62.55	60.95	63.14	58.38
TiO2	0.00	0.00	0.00	0.00	0.00	0.00
Al2O3	23.58	24.23	23.55	24.17	23.41	26.45
Cr2O3	0.00	0.00	0.00	0.00	0.00	0.00
FeO	0.17	0.15	0.23	0.14	0.13	0.14
NiO	0.00	0.00	0.00	0.00	0.00	0.00
MnO	0.00	0.00	0.00	0.00	0.00	0.00
MgO	0.06	0.04	0.03	0.01	0.00	0.05
CaO	4.34	5.53	4.36	5.07	4.24	7.80
Na2O	9.79	9.14	9.71	9.08	9.51	7.62
K2O	0.19	0.25	0.20	0.27	0.23	0.21
Total:	101.10	99.81	100.63	99.69	100.66	100.65
An content:	32.60	39.65	32.87	37.71	32.66	52.63
X-Pos	12.89	13.24	9.31	10.45	11.29	10.62

Slide No.: A-009-1A
Analysis: Biotite

	#1 BA		#2 BB		#3 BC	
Oxides	(Host/Rim)	(Host/Core)	(Host/Rim)	(Host/Core)	(Host/Rim)	(Host/Core)
SiO2	34.87	35.78	35.74	35.75	35.45	35.69
TiO2	2.39	2.59	2.47	2.50	2.64	2.67
Al2O3	18.64	19.25	18.57	18.58	19.11	19.19
Cr2O3	0.00	0.00	0.00	0.00	0.00	0.00
FeO	21.03	20.78	21.32	21.10	20.42	20.21
NiO	0.00	0.00	0.00	0.00	0.00	0.00
MnO	0.09	0.25	0.14	0.34	0.18	0.30
MgO	8.42	8.54	8.24	8.11	8.52	8.77
CaO	0.00	0.01	0.00	0.00	0.00	0.07
Na2O	0.00	0.12	0.00	0.36	0.18	0.00
K2O	9.53	9.75	9.31	9.13	9.28	9.16
Cl	0.00	0.00	0.01	0.00	0.01	0.00
F	0.00	0.00	0.00	0.00	0.80	0.00
Total:	94.97	97.07	95.80	95.87	96.59	96.06

Slide No.: A-009-1A
Analysis: Biotite

	#4 BD		#5 BE		#6 BG	
Oxides	(Leuc./Rim)	(Leuc./Core)	(Leuc./Rim)	(Leuc./Core)	(Leuc./Rim)	(Leuc./Core)
SiO2	35.66	36.03	36.31	33.55	35.20	35.59
TiO2	2.18	2.72	2.65	2.58	2.60	2.76
Al2O3	17.70	19.00	19.03	17.98	18.35	19.24
Cr2O3	0.00	0.00	0.00	0.00	0.00	0.00
FeO	22.15	21.71	19.47	20.07	22.42	20.08
NiO	0.00	0.00	0.00	0.00	0.00	0.00
MnO	0.41	0.37	0.38	0.27	0.46	0.35
MgO	8.56	7.76	8.93	8.34	7.33	8.24
CaO	0.01	0.01	0.00	0.00	0.05	0.00
Na2O	0.00	0.00	0.35	0.33	0.24	0.00
K2O	8.87	9.28	9.64	9.17	9.13	9.62
Cl	0.05	0.04	0.02	0.00	0.00	0.00
F	0.00	0.00	0.00	0.62	0.00	0.00
Total:	95.59	96.92	96.78	92.91	95.78	95.88

Slide No.: A-009-1A
Analysis: Biotite

	#1 BF	
Oxides	(Rim/Rim)	(Rim/Core)
SiO2	33.70	35.35
TiO2	2.50	2.72
Al2O3	18.89	19.08
Cr2O3	0.00	0.00
FeO	19.58	21.02
NiO	0.00	0.00
MnO	0.30	0.11
MgO	9.12	8.50
CaO	0.00	0.02
Na2O	0.00	0.00
K2O	9.40	9.22
Cl	0.04	0.00
F	0.00	0.00
Total:	93.53	96.02

Slide No.: A-009-1A
Analysis: Muscovite

	#1 MG		#2 MH		#3 MI	
Oxides	(Host/1)	(Host/2)	(Host/1)	(Host/2)	(Host/1)	(Host/2)
SiO2	46.99	46.69	46.81	46.62	43.53	46.87
TiO2	0.99	0.95	1.04	0.98	0.76	0.82
Al2O3	36.89	36.55	36.37	37.02	36.67	36.46
Cr2O3	-	-	-	-	-	-
FeO	1.49	1.34	1.33	1.35	1.30	1.47
NiO	-	-	-	-	-	-
MnO	-	-	-	-	-	-
MgO	0.67	0.70	0.69	0.72	0.61	0.81
CaO	0.03	0.00	0.00	0.00	0.00	0.00
Na2O	0.57	0.59	0.59	0.57	0.57	0.58
K2O	10.16	10.03	10.15	9.96	9.96	10.04
Total:	97.79	96.85	96.98	97.22	93.40	97.05
MgO/FeO:	0.45	0.52	0.52	0.53	0.47	0.55

Slide No.: A-009-1A
Analysis: Muscovite

	#4 MA		#5 MB		#6 MC	
Oxides	(Leuc./1)	(Leuc./2)	(Leuc./1)	(Leuc./2)	(Leuc./1)	(Leuc./2)
SiO2	47.60	47.26	46.29	47.07	48.06	47.39
TiO2	0.93	0.90	0.87	0.77	0.30	0.56
Al2O3	36.49	36.69	35.90	36.73	35.34	36.00
Cr2O3	-	-	-	-	-	-
FeO	1.24	1.21	1.27	1.32	1.92	1.63
NiO	-	-	-	-	-	-
MnO	-	-	-	-	-	-
MgO	0.64	0.72	0.63	0.65	0.98	0.90
CaO	0.00	0.00	0.00	0.02	0.03	0.00
Na2O	0.61	0.57	0.50	0.53	0.49	0.66
K2O	10.32	10.29	9.55	10.31	10.01	10.17
Total:	97.83	97.64	95.01	97.40	97.13	97.31
MgO/FeO:	0.52	0.60	0.50	0.49	0.51	0.55

Slide No.: A-009-1A
Analysis: Muscovite

	#1 MD		#2 ME		#3 MF	
Oxides	(Rim/1)	(Rim/2)	(Rim/1)	(Rim/2)	(Rim/1)	(Rim/2)
SiO2	46.90	47.69	47.22	46.48	46.33	47.09
TiO2	0.99	0.92	0.91	0.73	0.81	0.76
Al2O3	36.01	37.05	36.55	36.91	36.95	36.72
Cr2O3	-	-	-	-	-	-
FeO	1.39	1.31	1.40	1.35	1.43	1.32
NiO	-	-	-	-	-	-
MnO	-	-	-	0.16	-	0.18
MgO	0.68	0.66	0.71	0.69	0.71	0.72
CaO	0.06	0.00	0.00	0.03	0.00	0.00
Na2O	0.57	0.52	0.72	0.59	0.59	0.59
K2O	9.59	10.05	10.07	9.97	10.34	10.42
Total:	96.19	98.20	97.58	96.91	97.16	97.80
MgO/FeO:	0.49	0.50	0.51	0.51	0.50	0.55

Slide No.: A-009-1A
Analysis: Plagioclase

	#1 PA	
Oxides	(Host/Rim)	(Host/Core)
SiO2	62.79	60.51
TiO2	0.00	0.00
Al2O3	22.47	23.98
Cr2O3	0.00	0.00
FeO	0.12	0.10
NiO	0.00	0.00
MnO	0.00	0.00
MgO	0.02	0.02
CaO	4.24	6.15
Na2O	9.22	8.37
K2O	0.21	0.24
Total:	99.07	99.37
An content:	33.37	44.35

Slide No.: A-009-1A
Analysis: Plagioclase

	#4 PB		#5 PC		#6 PD	
Oxides	(Leuc./Rim)	(Leuc./Core)	(Leuc./Rim)	(Leuc./Core)	(Leuc./Rim)	(Leuc./Core)
SiO2	63.11	62.78	63.34	62.78	64.20	63.87
TiO2	0.00	0.00	0.00	0.00	0.00	0.00
Al2O3	22.47	22.65	22.52	22.01	22.33	22.47
Cr2O3	0.00	0.00	0.00	0.00	0.00	0.00
FeO	0.11	0.02	0.14	0.14	0.16	0.15
NiO	0.00	0.00	0.00	0.00	0.00	0.00
MnO	0.00	0.00	0.00	0.00	0.00	0.00
MgO	0.04	0.04	0.04	0.05	0.02	0.02
CaO	4.34	4.32	4.18	4.08	4.01	4.05
Na2O	9.45	8.88	9.40	8.80	9.40	9.22
K2O	0.16	0.31	0.27	0.23	0.18	0.33
Total:	99.68	99.00	99.89	98.09	100.30	100.11
An content:	33.42	34.45	32.54	33.50	31.77	32.17

Slide No.: D-001-3A
Analysis: Biotite

	#1		#2		#3	
Oxides	(Host/Rim)	(Host/Core)	(Host/Rim)	(Host/Core)	(Host/Rim)	(Host/Core)
SiO2	35.46	35.09	35.00	35.36	34.93	34.86
TiO2	3.56	3.53	3.09	3.19	3.18	3.36
Al2O3	18.51	18.55	19.05	19.49	18.70	18.07
Cr2O3	0.00	0.00	0.00	0.00	0.00	0.00
FeO	20.90	21.29	21.32	20.70	21.49	21.49
NiO	0.00	0.00	0.00	0.00	0.00	0.00
MnO	0.11	0.09	0.13	0.16	0.11	0.18
MgO	7.61	7.54	7.96	7.68	8.13	8.18
CaO	0.00	0.00	0.00	0.00	0.00	0.00
Na2O	0.00	0.00	0.00	0.00	0.00	0.00
K2O	9.87	9.86	10.01	10.02	9.52	9.97
Cl						
F						
Total:	96.02	95.95	96.56	96.60	96.06	96.11

Slide No.: D-001-3A
Analysis: Biotite

	#4 BA		#5 BB		#6 BC	
Oxides	(Leuc./Rim)	(Leuc./Core)	(Leuc./Rim)	(Leuc./Core)	(Leuc./Rim)	(Leuc./Core)
SiO2	35.39	35.46	36.53	34.77	34.81	34.90
TiO2	3.28	3.14	2.89	3.09	2.90	3.51
Al2O3	17.91	17.18	16.21	18.01	18.28	18.06
Cr2O3	0.00	0.00	0.00	0.00	0.00	0.00
FeO	20.90	21.40	21.14	21.72	21.73	21.80
NiO	0.00	0.00	0.00	0.00	0.00	0.00
MnO	0.24	0.29	0.26	0.22	0.26	0.24
MgO	8.28	7.70	8.77	7.88	7.93	7.41
CaO	0.00	0.00	0.00	0.00	0.00	0.00
Na2O	0.00	0.00	0.00	0.00	0.00	0.00
K2O	10.07	9.77	9.85	9.93	9.60	9.77
Cl						
F						
Total:	96.07	94.94	95.65	95.62	95.51	95.69

Slide No.: D-001-3A
Analysis: Biotite

	#1 BD		#2 BE		#3 BF	
Oxides	(Rim/Rim)	(Rim/Core)	(Rim/Rim)	(Rim/Core)	(Rim/Rim)	(Rim/Core)
SiO2	35.18	35.47	34.98	35.42	35.36	35.26
TiO2	2.88	3.27	2.78	2.92	3.37	3.07
Al2O3	18.13	18.16	17.85	17.28	17.98	18.46
Cr2O3	0.00	0.00	0.00	0.00	0.00	0.00
FeO	22.22	21.23	21.32	21.25	21.43	21.69
NiO	0.00	0.00	0.00	0.00	0.00	0.00
MnO	0.04	0.22	0.24	0.13	0.15	0.24
MgO	7.87	8.22	8.22	8.51	7.84	7.85
CaO	0.00	0.00	0.00	0.00	0.00	0.00
Na2O	0.00	0.00	0.00	0.00	0.03	0.00
K2O	10.48	10.06	9.92	9.94	9.71	9.83
Cl						
F						
Total:	96.80	96.63	95.31	95.45	95.87	96.40

Slide No.: D-001-3A
Analysis: Muscovite

	#1 MA		#2 MB		#3 MC	
Oxides	(Host/pt 1)	(Host/pt 2)	(Host/pt 1)	(Host/pt 2)	(Host/pt 1)	(Host/pt 2)
SiO2	47.23	47.00	46.75	46.48	46.87	46.89
TiO2	0.95	1.33	1.49	1.76	1.74	1.22
Al2O3	36.01	35.45	35.09	34.89	35.77	35.88
Cr2O3	-	-	-	-	-	-
FeO	2.11	2.27	2.13	2.13	2.15	2.13
NiO	-	-	-	-	-	-
MnO	0.00	0.02	0.00	0.00	0.00	0.00
MgO	0.65	0.82	0.75	0.79	0.74	0.73
CaO	0.02	0.00	0.05	0.08	0.00	0.05
Na2O	0.58	0.54	0.37	0.46	0.49	0.50
K2O	10.70	10.76	11.11	11.07	11.07	10.75
Total:	98.25	98.19	97.74	97.66	98.83	98.15

Slide No.: D-001-3A
Analysis: Muscovite

	#4 MG		#5 MH	
Oxides	(Leuc./pt 1)	(Leuc./pt 2)	(Leuc./pt 1)	(Leuc./pt 2)
SiO2	46.55	46.51	47.10	46.98
TiO2	1.18	1.05	1.18	1.28
Al2O3	35.53	35.67	36.12	35.72
Cr2O3	-	-	-	-
FeO	2.29	2.12	2.07	1.98
NiO	-	-	-	-
MnO	0.07	0.00	0.00	0.07
MgO	0.72	0.76	0.68	0.65
CaO	0.09	0.06	0.09	0.02
Na2O	0.56	0.63	0.60	0.61
K2O	10.84	10.33	10.83	10.88
Total:	97.83	97.13	98.67	98.19

Slide No.: D-001-3A
Analysis: Muscovite

	#6 MD		#7 ME		#8 MF	
Oxides	(Rim/pt 1)	(Rim/pt 2)	(Rim/pt 1)	(Rim/pt 2)	(Rim/pt 1)	(Rim/pt 2)
SiO2	46.22	46.34	46.95	46.70	45.85	47.01
TiO2	1.67	1.68	1.63	1.51	1.47	1.23
Al2O3	35.39	34.85	35.08	35.03	35.33	36.03
Cr2O3	-	-	-	-	-	-
FeO	2.20	2.14	2.14	1.95	2.13	2.16
NiO	-	-	-	-	-	-
MnO	0.00	0.00	0.00	0.16	0.00	0.02
MgO	0.73	0.66	0.77	0.74	0.70	0.60
CaO	0.00	0.00	0.03	0.00	0.00	0.00
Na2O	0.52	0.59	0.52	0.58	0.55	0.52
K2O	10.78	10.84	10.91	10.87	10.88	11.03
Total:	97.51	97.10	98.03	97.54	96.91	98.60

Slide No.: D-001-3A
Analysis: Plagioclase

	#1 PC		#2 PG	
Oxides	(Host/Rim)	(Host/Core)	(Host/Rim)	(Host/Core)
SiO2	63.51	63.43	64.77	63.53
TiO2	0.00	0.00	0.00	0.00
Al2O3	22.48	22.49	21.91	22.52
Cr2O3	0.00	0.00	0.00	0.00
FeO	0.08	0.12	0.13	0.10
NiO	0.00	0.00	0.00	0.00
MnO	0.00	0.00	0.00	0.00
MgO	0.04	0.04	0.01	0.01
CaO	4.24	4.71	3.99	4.59
Na2O	9.19	9.08	9.84	8.49
K2O	0.16	0.25	0.13	0.24
Total:	99.70	100.12	100.78	99.48
An content:	33.52	36.03	30.76	36.97

Slide No.: D-001-3A
Analysis: Plagioclase

	#4 PA		#5 PB	
Oxides	(Leuc 1/Rim)	(Leuc 1/Core	(Leuc 1/Rim)	(Leuc 1/Core)
SiO2	63.67	63.37	64.70	62.91
TiO2	0.00	0.00	0.00	0.00
Al2O3	21.86	22.30	21.50	22.50
Cr2O3	0.00	0.00	0.00	0.00
FeO	0.12	0.05	0.11	0.10
NiO	0.00	0.00	0.00	0.00
MnO	0.00	0.00	0.00	0.00
MgO	0.02	0.02	0.03	0.02
CaO	3.90	4.20	3.35	4.36
Na2O	9.46	9.27	9.72	9.30
K2O	0.18	0.26	0.09	0.20
Total:	99.21	99.47	99.50	99.39
An content:	31.04	32.96	27.46	33.82

Slide No.: D-002-2B
Analysis: Plagioclase

	#1 PC		#2 PD		#3 PE	
Oxides	(Psam/Rim)	(Psam/Core)	(Psam/Rim)	(Psam/Core)	(Psam/Rim)	(Psam/Core)
SiO2	61.97	60.31	61.86	62.01	61.66	62.02
TiO2	0.00	0.00	0.00	0.00	0.00	0.00
Al2O3	23.53	24.24	23.43	23.87	23.40	23.69
Cr2O3	0.00	0.00	0.00	0.00	0.00	0.00
FeO	0.34	0.20	0.40	0.24	0.19	0.18
NiO	0.00	0.00	0.00	0.00	0.00	0.00
MnO	0.00	0.00	0.00	0.00	0.00	0.00
MgO	0.05	0.06	0.06	0.06	0.07	0.06
CaO	5.14	6.27	5.18	5.68	4.96	5.23
Na2O	8.40	8.29	8.39	8.38	8.48	8.87
K2O	0.18	0.19	0.16	0.27	0.12	0.15
Total:	99.61	99.56	99.48	100.51	98.88	100.20
An content:	40.01	45.16	40.26	42.32	39.04	39.19
X-Pos	9.53	9.58	8.10	8.03	5.88	5.74

Slide No.: D-002-2B
Analysis: Plagioclase

	#4 PA		#5 PB		#6 PF	
Oxides	(Luec./Rim)	(Luec./Core)	(Luec./Rim)	(Luec./Core)	(Luec./Rim)	(Luec./Core)
SiO2	63.93	60.95	61.30	61.78	61.62	62.19
TiO2	0.00	0.00	0.00	0.00	0.00	0.00
Al2O3	22.87	24.36	23.67	23.73	23.74	23.73
Cr2O3	0.00	0.00	0.00	0.00	0.00	0.00
FeO	0.20	0.21	0.21	0.24	0.21	0.20
NiO	0.00	0.00	0.00	0.00	0.00	0.00
MnO	0.00	0.00	0.00	0.00	0.00	0.00
MgO	0.05	0.06	0.06	0.06	0.05	0.06
CaO	4.61	6.26	5.41	5.44	5.45	5.75
Na2O	8.95	7.84	8.63	8.48	8.61	8.47
K2O	0.34	0.21	0.21	0.21	0.19	0.29
Total:	100.95	99.89	99.49	99.94	99.87	100.69
An content:	35.71	46.44	40.54	41.10	40.81	42.32
X-Pos	24.28	24.15	16.73	16.41	19.92	20.30

Slide No.: A-008-4A
Analysis: Plagioclase

Oxides	#1 PB (Gran./Rim)	#1 PB (Gran./Core)	#2 PC (Gran./Rim)	#2 PC (Gran./Core)
SiO2	63.94	61.35	64.41	63.10
TiO2	0.00	0.00	0.00	0.00
Al2O3	22.11	23.93	22.24	23.13
Cr2O3	0.00	0.00	0.00	0.00
FeO	0.19	0.21	0.35	0.23
NiO	0.00	0.00	0.00	0.00
MnO	0.00	0.00	0.00	0.00
MgO	0.06	0.06	0.05	0.07
CaO	3.71	5.88	3.60	4.55
Na2O	9.88	8.56	9.84	9.13
K2O	0.18	0.17	0.16	0.17
Total:	100.07	100.16	100.65	100.38
An content:	29.08	42.84	28.58	35.24

Slide No.: A-004-5
Analysis: Plagioclase

	#1 PA		#2 PB		#3 PC	
Oxides	(Leuc./Rim)	(Leuc./Core)	(Leuc./Rim)	(Leuc./Core)	(Leuc./Rim)	(Leuc./Core)
SiO2	63.71	63.33	63.43	63.90	62.73	62.27
TiO2	0.00	0.00	0.00	0.00	0.00	0.00
Al2O3	22.39	22.52	22.46	22.26	22.82	23.04
Cr2O3	0.00	0.00	0.00	0.00	0.00	0.00
FeO	0.18	0.18	0.24	0.14	0.21	0.20
NiO	0.00	0.00	0.00	0.00	0.00	0.00
MnO	0.00	0.00	0.00	0.00	0.00	0.00
MgO	0.06	0.05	0.05	0.06	0.06	0.06
CaO	3.57	3.70	3.84	3.37	4.27	4.25
Na2O	9.28	9.91	9.50	9.97	9.20	9.44
K2O	0.18	0.16	0.15	0.10	0.12	0.18
Total:	99.37	99.85	99.67	99.80	99.41	99.44
An content:	29.57	28.99	30.66	27.07	33.71	32.95
X-Pos	62.72	62.54	60.63	60.99	63.69	63.71

Slide No.: A-004-5
Analysis: Plagioclase

	#4 PD	
Oxides	(Host/Rim)	(Host/Core)
SiO2	62.95	63.23
TiO2	0.00	0.00
Al2O3	22.99	22.42
Cr2O3	0.00	0.00
FeO	0.27	0.18
NiO	0.00	0.00
MnO	0.00	0.00
MgO	0.06	0.08
CaO	4.07	4.01
Na2O	9.33	9.68
K2O	0.17	0.15
Total:	99.84	99.75
An content:	32.27	31.19
X-Pos	58.66	58.57

Slide No.: A-009-1B
Analysis: Biotite

	#1 BE		#2 BF		#3 BG	
Oxides	(Host/Rim)	(Host/Core)	(Host/Rim)	(Host/Core)	(Host/Rim)	(Host/Core)
SiO2	34.23	34.44	34.53	34.72	34.39	34.68
TiO2	2.49	2.57	2.55	2.65	2.67	2.77
Al2O3	18.51	18.90	18.40	18.76	18.95	18.36
Cr2O3	0.00	0.00	0.00	0.00	0.00	0.00
FeO	20.16	20.82	22.01	20.00	20.61	21.12
NiO	0.00	0.00	0.00	0.00	0.00	0.00
MnO	0.36	0.30	0.38	0.32	0.22	0.31
MgO	7.93	7.59	7.54	7.82	7.55	7.74
CaO	0.00	0.00	0.00	0.00	0.00	0.00
Na2O	0.39	0.00	0.00	0.00	0.00	0.00
K2O	9.52	9.52	9.57	9.90	9.45	9.71
Cl	0.06	0.04	0.06	0.04	0.00	0.05
F	0.81	0.80	0.79	0.80	0.80	0.90
Total:	94.46	94.98	95.83	95.01	94.64	95.64

Slide No.: A-009-1B
Analysis: Biotite

	#4 BA		#5 BB		#6 BC	
Oxides	(Leuc./Rim)	(Leuc./Core)	(Leuc./Rim)	(Leuc./Core)	(Leuc./Rim)	(Leuc./Core)
SiO2	34.46	34.78	34.69	34.47	34.91	35.57
TiO2	2.85	2.65	2.75	2.78	2.67	2.79
Al2O3	18.28	19.06	19.13	18.69	19.37	19.34
Cr2O3	0.00	0.00	0.00	0.00	0.00	0.00
FeO	20.35	19.97	19.70	19.58	19.53	19.25
NiO	0.00	0.00	0.00	0.00	0.00	0.00
MnO	0.00	0.10	0.27	0.15	0.15	0.24
MgO	8.08	8.15	8.05	7.85	7.64	8.07
CaO	0.00	0.00	0.00	0.00	0.00	0.00
Na2O	0.00	0.11	0.00	0.00	0.00	0.00
K2O	9.97	9.94	9.90	9.72	9.48	9.65
Cl	0.04	0.01	0.05	0.04	0.05	0.01
F	0.00	0.00	0.00	0.81	0.71	0.90
Total:	94.03	94.77	94.54	94.09	94.51	95.82

Slide No.: A-009-1B
Analysis: Biotite

	#1 BD		#2 BH		#3	
Oxides	(Rim/Rim)	(Rim/Core)	(Rim/Rim)	(Rim/Core)	(Rim/Rim)	(Rim/Core)
SiO2	34.90	34.87	34.37	33.69		
TiO2	2.71	2.56	2.61	2.74		
Al2O3	18.72	18.60	18.20	18.01		
Cr2O3	0.00	0.00	0.00	0.00		
FeO	20.47	20.63	21.10	20.46		
NiO	0.00	0.00	0.00	0.00		
MnO	0.25	0.19	0.29	0.27		
MgO	8.11	7.90	7.72	8.40		
CaO	0.00	0.00	0.00	0.00		
Na2O	0.00	0.00	0.00	0.00		
K2O	9.68	9.88	9.73	9.59		
Cl	0.04	0.05	0.00	0.03		
F	0.80	0.50	0.00	0.81		
Total:	95.68	95.18	94.02	94.00	0.00	0.00

Slide No.: A-009-1B

Slide No.: A-009-1B
Analysis: Plagioclase

	#1 PC	
Oxides	(Host/Rim)	(Host/Core)
SiO2	62.42	63.54
TiO2	0.00	0.00
Al2O3	23.29	23.35
Cr2O3	0.00	0.00
FeO	0.15	0.00
NiO	0.00	0.00
MnO	0.00	0.00
MgO	0.02	0.03
CaO	4.22	4.13
Na2O	9.97	9.91
K2O	0.15	0.11
Total:	100.22	101.07
An content:	31.66	31.38

Slide No.: A-009-1B
Analysis: Plagioclase

	#4 PA		#5 PB		#6 PD	
Oxides	(Leuc./Rim)	(Leuc./Core)	(Leuc./Rim)	(Leuc./Core)	(Leuc./Rim)	(Leuc./Core)
SiO2	63.22	62.71	62.58	62.68	63.54	63.08
TiO2	0.00	0.00	0.00	0.00	0.00	0.00
Al2O3	23.35	23.51	23.54	23.97	23.22	23.78
Cr2O3	0.00	0.00	0.00	0.00	0.00	0.00
FeO	0.11	0.15	0.11	0.11	0.16	0.18
NiO	0.00	0.00	0.00	0.00	0.00	0.00
MnO	0.00	0.00	0.00	0.00	0.00	0.00
MgO	0.02	0.03	0.03	0.03	0.02	0.03
CaO	4.09	4.45	4.24	4.61	3.97	4.70
Na2O	9.92	9.71	9.49	9.30	9.73	9.44
K2O	0.15	0.17	0.23	0.18	0.23	0.21
Total:	100.86	100.73	100.22	100.88	100.87	101.42
An content:	31.09	33.37	32.71	35.11	30.75	35.16

Slide No.: A-008-2A
Analysis: Plagioclase

	#1 PD		#2 PE	
Oxides	(Host/Rim)	(Host/Core)	(Host/Rim)	(Host/Core)
SiO2	63.38	60.47	62.91	62.45
TiO2	0.00	0.00	0.00	0.00
Al2O3	22.24	24.23	22.56	22.92
Cr2O3	0.00	0.00	0.00	0.00
FeO	0.19	0.20	0.22	0.31
NiO	0.00	0.00	0.00	0.00
MnO	0.00	0.00	0.00	0.00
MgO	0.07	0.06	0.06	0.06
CaO	3.81	5.88	3.85	4.47
Na2O	8.85	8.10	9.29	9.31
K2O	0.25	0.21	0.11	0.15
Total:	98.79	99.15	99.00	99.67
An content:	31.84	44.10	31.25	34.43

Slide No.: A-008-2A
Analysis: Plagioclase

	#4 PA		#5 PB		#6 PC	
Oxides	(Inj./Rim)	(Inj./Core)	(Inj./Rim)	(Inj./Core)	(Inj./Rim)	(Inj./Core)
SiO2	62.52	63.17	63.63	62.59	62.39	62.95
TiO2	0.00	0.00	0.00	0.00	0.00	0.00
Al2O3	22.41	22.35	22.44	22.84	22.50	22.47
Cr2O3	0.00	0.00	0.00	0.00	0.00	0.00
FeO	0.23	0.18	0.20	0.22	0.26	0.19
NiO	0.00	0.00	0.00	0.00	0.00	0.00
MnO	0.00	0.00	0.00	0.00	0.00	0.00
MgO	0.07	0.06	0.05	0.05	0.04	0.04
CaO	4.17	3.64	3.90	4.32	3.89	3.76
Na2O	9.51	9.58	9.42	9.01	9.30	9.41
K2O	0.19	0.27	0.18	0.29	0.14	0.22
Total:	99.10	99.25	99.82	99.32	98.52	99.04
An content:	32.36	29.19	31.12	34.16	31.40	30.31

Appendix C - Analytical Techniques

Microprobe: The analytical work was done on a Jeol 733 electron microprobe, run at 15 KeV and 5 nanoamps using the Tracor Northern ZAF lattice correction scheme and mineral standards for calibration.

Microprobe Error Analysis: In order to determine the range of analytical error for the microprobe a session was set up in which three grains of each phase, muscovite, biotite and plagioclase, were probed repeatedly. One grain of muscovite and biotite from the host, melanosome and leucosome and one grain of plagioclase from the host and leucosome of A-009-5A were probed fifteen times each. The results of these analyses are at the end of this appendix. The probe results (minus the first two plagioclase analyses) were averaged with the standard deviation taken as the error of analysis (the standard deviation represents the field into which 75% of the analyses occur) and are listed in Table C.1. The results indicate highly variable results depending on not only the phase probed but the element being analysed. With the biotite and muscovite error runs care was taken to ensure the exact spot was not probed repeatedly, as certain oxides, particularly Na_2O, are depleted by exposure to the X-ray beam, as indicated by Figure A.1, for a plagioclase grain in which the same point was repeatedly probed. While the other elements remained fairly constant, Na displayed a continuous decrease in concentration with each probing. So the points were moved 5-10 microns for each analysis (beam width = ~3 microns) in order to ensure undepleted grain was probed while minimizing any possible heterogeneities in the chemical composition of the grain.

Table C.1 - Variation in 15 analyses of three grains per phase, with the error expressed as +/- one standard deviation

Plagioclase		Biotite		Muscovite	
Oxide	$\bar{X}$(sigma)	Oxide	$\bar{X}$(sigma)	Oxide	$\bar{X}$(sigma)
SiO2	0.41	SiO2	0.60	SiO2	0.64
Al2O3	0.22	TiO2	0.22	TiO2	0.06
FeO	0.04	Al2O3	0.36	Al2O3	0.26
MgO	0.01	FeO	0.47	FeO	0.09
CaO	0.08	MnO	0.09	MnO	0.01
Na2O	0.22	MgO	0.19	MgO	0.04
K2O	0.02	CaO	0.03	CaO	0.02
An %	0.88	Na2O	0.09	Na2O	0.04
		K2O	0.50	K2O	0.39
		Cl	0.02	FeO/MgO	0.10
		F	1.02		
		FeO/MgO	0.06		

General Probing: When probing any phases, two analyses would be done per grain. In the case of large grains (>50 microns) and plagioclase, it was always done as rim and core. On some of the smaller grains, particularly in the muscovites, two analyses would be done in unaltered areas, often the crystal not being large enough for a distinct core and rim. Checks against the standard were performed regularly at intervals of approximately 20-30 analyses and re-calibration was performed if the analysis exceeded +/- 0.5 weight percent of those oxides in concentrations of greater than 10 weight percent. Those oxides under 10 percent were recalibrated when the difference was greater than +/- 0.3 weight percent. The totals were checked and the grain re-run if the muscovite or biotite total fell below 94 weight percent or above 97 weight percent. The plagioclase totals range was 98 to 101 weight percent with those outside being re-run.

Appendix D - Statistics

Plagioclase - An content

THE FOLLOWING RESULTS ARE FOR:
PHASE$ = APLITE

BAR GRAPH OF VARIABLE AN , N = 6

VALUE	COUNT	PERCENT	
58.000	2	33.33	##########
60.000	3	50.00	################
62.000	0	.00	
64.000	0	.00	
66.000	0	.00	
68.000	0	.00	
70.000	0	.00	
72.000	0	.00	
74.000	0	.00	
76.000	0	.00	
78.000	1	16.67	#####

THE FOLLOWING RESULTS ARE FOR:
PHASE$ = GRANITE

BAR GRAPH OF VARIABLE AN , N = 19

VALUE	COUNT	PERCENT	
20.000	1	5.26	#####
22.000	0	.00	
24.000	0	.00	
26.000	0	.00	
28.000	3	15.79	###############
30.000	0	.00	
32.000	3	15.79	###############
34.000	4	21.05	####################
36.000	2	10.53	##########
38.000	2	10.53	##########
40.000	0	.00	
42.000	1	5.26	#####
44.000	1	5.26	#####
46.000	0	.00	
48.000	0	.00	
50.000	0	.00	
52.000	1	5.26	#####
54.000	1	5.26	#####

```
THE FOLLOWING RESULTS ARE FOR:
            PHASE$     = HOST

BAR GRAPH OF VARIABLE       AN     , N =     24

    VALUE        COUNT  PERCENT
       20.000        1     2.44
       22.000        0      .00
       24.000        0      .00
       26.000        0      .00
       28.000        5    12.20 ##
       30.000        7    17.07 ###
       32.000        5    12.20 ##
       34.000       11    26.83 #####
       36.000        7    17.07 ###
       38.000        2     4.88 #
       40.000        0      .00
       42.000        1     2.44
       44.000        2     4.88 #

THE FOLLOWING RESULTS ARE FOR:
            PHASE$     = LEUCOSOME

BAR GRAPH OF VARIABLE       AN     , N =     54

    VALUE        COUNT  PERCENT
       20.000        1     1.05
       22.000        0      .00
       24.000        0      .00
       26.000        2     2.11 #
       28.000       10    10.53 #####
       30.000       14    14.74 ########
       32.000       20    21.05 ##########
       34.000       24    25.26 ############
       36.000       11    11.58 ######
       38.000        4     4.21 ##
       40.000        4     4.21 ##
       42.000        2     2.11 #
       44.000        2     2.11 #
       46.000        1     1.05

THE FOLLOWING RESULTS ARE FOR:
            PHASE$     = PELITE

BAR GRAPH OF VARIABLE       AN     , N =      6

    VALUE        COUNT  PERCENT
       20.000        1     3.03
       22.000        0      .00
       24.000        0      .00
       26.000        2     6.06 #
       28.000       13    39.39 ######
       30.000       17    51.52 #########
```

THE FOLLOWING RESULTS ARE FOR:
PHASE$ = PSAMMITE

BAR GRAPH OF VARIABLE AN , N = 18

VALUE	COUNT	PERCENT	
20.000	1	.85	
22.000	0	.00	
24.000	0	.00	
26.000	2	1.69	#
28.000	14	11.86	########
30.000	19	16.10	##########
32.000	23	19.49	############
34.000	26	22.03	##############
36.000	13	11.02	#######
38.000	7	5.93	###
40.000	7	5.93	###
42.000	3	2.54	#
44.000	3	2.54	#

Biotite - FeO/MgO

THE FOLLOWING RESULTS ARE FOR:
PHASE$ = APLITE

BAR GRAPH OF VARIABLE FEMG , N = 6

VALUE	COUNT	PERCENT	
1.200	4	66.67	########################
1.300	2	33.33	############

THE FOLLOWING RESULTS ARE FOR:
PHASE$ = GRANITE

BAR GRAPH OF VARIABLE FEMG , N = 22

VALUE	COUNT	PERCENT	
1.200	4	14.29	########################
1.300	2	7.14	############
1.400	0	.00	
1.500	0	.00	
1.600	0	.00	
1.700	0	.00	
1.800	0	.00	
1.900	0	.00	
2.000	0	.00	
2.100	8	28.57	##
2.200	5	17.86	##############################
2.300	1	3.57	######
2.400	0	.00	
2.500	0	.00	
2.600	1	3.57	######
2.700	2	7.14	############
2.800	1	3.57	######
2.900	1	3.57	######
3.000	1	3.57	######
3.100	1	3.57	######
3.200	1	3.57	######

THE FOLLOWING RESULTS ARE FOR:
PHASE$ = HOST

BAR GRAPH OF VARIABLE FEMG , N = 30

VALUE	COUNT	PERCENT	
1.200	4	7.27	######################
1.300	2	3.64	##########
1.400	0	.00	
1.500	0	.00	
1.600	0	.00	
1.700	0	.00	
1.800	0	.00	
1.900	0	.00	
2.000	0	.00	
2.100	8	14.55	##
2.200	5	9.09	##########################
2.300	5	9.09	##########################
2.400	4	7.27	######################
2.500	8	14.55	##
2.600	9	16.36	###
2.700	6	10.91	################################
2.800	2	3.64	##########
2.900	2	3.64	##########

THE FOLLOWING RESULTS ARE FOR:
PHASE$ = LEUCOSOME

BAR GRAPH OF VARIABLE FEMG , N = 34

VALUE	COUNT	PERCENT	
1.200	4	4.44	##
1.300	2	2.22	#
1.400	0	.00	
1.500	0	.00	
1.600	0	.00	
1.700	0	.00	
1.800	0	.00	
1.900	0	.00	
2.000	0	.00	
2.100	9	10.00	####
2.200	5	5.56	##
2.300	8	8.89	####
2.400	14	15.56	########
2.500	18	20.00	##########
2.600	11	12.22	######
2.700	10	11.11	######
2.800	4	4.44	##
2.900	3	3.33	#
3.000	2	2.22	#

THE FOLLOWING RESULTS ARE FOR:
PHASE$ = PSAMMITE

BAR GRAPH OF VARIABLE FEMG , N = 30

VALUE	COUNT	PERCENT	
1.200	4	3.39	##
1.300	2	1.69	#
1.400	0	.00	
1.500	0	.00	
1.600	0	.00	
1.700	0	.00	
1.800	0	.00	
1.900	0	.00	
2.000	1	.85	
2.100	11	9.32	#####
2.200	13	11.02	######
2.300	15	12.71	########
2.400	18	15.25	##########
2.500	18	15.25	##########
2.600	11	9.32	#####
2.700	13	11.02	######
2.800	6	5.08	###
2.900	6	5.08	###

THE FOLLOWING RESULTS ARE FOR:
PHASE$ = RIM

BAR GRAPH OF VARIABLE FEMG , N = 18

VALUE	COUNT	PERCENT	
1.200	4	3.08	##
1.300	2	1.54	#
1.400	0	.00	
1.500	0	.00	
1.600	0	.00	
1.700	0	.00	
1.800	0	.00	
1.900	0	.00	
2.000	1	.77	
2.100	12	9.23	######
2.200	13	10.00	######
2.300	15	11.54	########
2.400	22	16.92	###########
2.500	24	18.46	############
2.600	12	9.23	######
2.700	17	13.08	#########
2.800	8	6.15	####

Muscovite - FeO/MgO

THE FOLLOWING RESULTS ARE FOR:
PHASE$ = GRANITE

BAR GRAPH OF VARIABLE FEMG , N = 16

VALUE	COUNT	PERCENT	
1.400	2	12.50	##########
1.500	1	6.25	######
1.600	0	.00	
1.700	1	6.25	######
1.800	0	.00	
1.900	0	.00	
2.000	1	6.25	######
2.100	0	.00	
2.200	5	31.25	##############################
2.300	2	12.50	##########
2.400	1	6.25	######
2.500	0	.00	
2.600	1	6.25	######
2.700	0	.00	
2.800	0	.00	
2.900	0	.00	
3.000	0	.00	
3.100	0	.00	
3.200	0	.00	
3.300	0	.00	
3.400	1	6.25	######
3.500	0	.00	
3.600	0	.00	
3.700	1	6.25	######

THE FOLLOWING RESULTS ARE FOR:
PHASE$ = HOST

BAR GRAPH OF VARIABLE FEMG , N = 30

VALUE	COUNT	PERCENT	
1.400	2	4.55	#
1.500	1	2.27	
1.600	0	.00	
1.700	2	4.55	#
1.800	3	6.82	#
1.900	4	9.09	##
2.000	5	11.36	##
2.100	4	9.09	##
2.200	13	29.55	######
2.300	2	4.55	#
2.400	1	2.27	
2.500	0	.00	
2.600	2	4.55	#
2.700	1	2.27	
2.800	1	2.27	
2.900	2	4.55	#
3.000	0	.00	
3.100	0	.00	
3.200	1	2.27	

THE FOLLOWING RESULTS ARE FOR:
PHASE$ = LEUCOSOME

BAR GRAPH OF VARIABLE FEMG , N = 30

VALUE	COUNT	PERCENT	
1.300	1	1.49	
1.400	2	2.99	#
1.500	2	2.99	#
1.600	1	1.49	
1.700	3	4.48	#
1.800	7	10.45	###
1.900	12	17.91	######
2.000	9	13.43	####
2.100	7	10.45	###
2.200	17	25.37	#########
2.300	2	2.99	#
2.400	3	4.48	#
2.500	1	1.49	

THE FOLLOWING RESULTS ARE FOR:
PHASE$ = PSAMMITE

BAR GRAPH OF VARIABLE FEMG , N = 24

VALUE	COUNT	PERCENT	
1.300	1	1.08	
1.400	2	2.15	#
1.500	3	3.23	#
1.600	1	1.08	
1.700	3	3.23	#
1.800	8	8.60	####
1.900	17	18.28	#########
2.000	12	12.90	#######
2.100	12	12.90	#######
2.200	21	22.58	###########
2.300	3	3.23	#
2.400	5	5.38	##
2.500	2	2.15	#
2.600	3	3.23	#

THE FOLLOWING RESULTS ARE FOR:
PHASE$ = RIM

BAR GRAPH OF VARIABLE FEMG , N = 18

VALUE	COUNT	PERCENT	
1.300	1	.94	
1.400	2	1.89	#
1.500	3	2.83	#
1.600	1	.94	
1.700	4	3.77	##
1.800	9	8.49	####
1.900	21	19.81	##########
2.000	18	16.98	##########
2.100	13	12.26	#######
2.200	24	22.64	###########
2.300	4	3.77	##
2.400	6	5.66	###

Muscovite - TiO_2

THE FOLLOWING RESULTS ARE FOR:
PHASE$ = GRANITE

BAR GRAPH OF VARIABLE TIO2 , N = 16

VALUE	COUNT	PERCENT
0.000	0	.00
0.100	3	18.75
0.200	1	6.25
0.300	1	6.25
0.400	2	12.50
0.500	1	6.25
0.600	1	6.25
0.700	0	.00
0.800	1	6.25
0.900	3	18.75
1.000	2	12.50
1.100	1	6.25

THE FOLLOWING RESULTS ARE FOR:
PHASE$ = HOST

BAR GRAPH OF VARIABLE TIO2 , N = 30

VALUE	COUNT	PERCENT
0.000	0	.00
0.100	3	6.52
0.200	1	2.17
0.300	1	2.17
0.400	2	4.35
0.500	1	2.17
0.600	2	4.35
0.700	4	8.70
0.800	3	6.52
0.900	8	17.39
1.000	3	6.52
1.100	4	8.70
1.200	4	8.70
1.300	5	10.87
1.400	3	6.52
1.500	0	.00
1.600	0	.00
1.700	2	4.35

THE FOLLOWING RESULTS ARE FOR:
PHASE$ = LEUCOSOME

BAR GRAPH OF VARIABLE TIO2 , N = 30

VALUE	COUNT	PERCENT	
0.000	1	1.35	
0.100	4	5.41	
0.200	2	2.70	
0.300	1	1.35	
0.400	2	2.70	
0.500	5	6.76	
0.600	3	4.05	
0.700	7	9.46	
0.800	5	6.76	
0.900	10	13.51	
1.000	8	10.81	
1.100	7	9.46	
1.200	9	12.16	
1.300	5	6.76	
1.400	5	6.76	

THE FOLLOWING RESULTS ARE FOR:
PHASE$ = PSAMMITE

BAR GRAPH OF VARIABLE TIO2 , N = 24

VALUE	COUNT	PERCENT	
0.000	1	1.00	
0.100	4	4.00	
0.200	2	2.00	
0.300	1	1.00	
0.400	6	6.00	
0.500	6	6.00	
0.600	10	10.00	
0.700	7	7.00	
0.800	6	6.00	
0.900	10	10.00	
1.000	10	10.00	
1.100	7	7.00	
1.200	9	9.00	
1.300	8	8.00	
1.400	7	7.00	
1.500	1	1.00	
1.600	0	.00	
1.700	5	5.00	

Secondary

Primary

THE FOLLOWING RESULTS ARE FOR:
PHASE$ = RIM

BAR GRAPH OF VARIABLE TIO2 , N = 18

VALUE	COUNT	PERCENT	
0.000	1	.89	
0.100	4	3.57	
0.200	2	1.79	
0.300	1	.89	
0.400	6	5.36	
0.500	7	6.25	
0.600	13	11.61	
0.700	10	8.93	
0.800	9	8.04	
0.900	14	12.50	
1.000	10	8.93	
1.100	8	7.14	
1.200	10	8.93	
1.300	9	8.04	
1.400	8	7.14	